Aus dem Fachbereich Medizin

der Johann Wolfgang Goethe-Universität

Frankfurt am Main

Institut für Biochemie I – Pathobiochemie

und dem Fachbereich Biologie

der Technischen Universität Kaiserslautern

Institut für Zellbiologie

# Generation of sphingosine-1-phosphate by apoptotic cells and its impact on macrophage polarization in cancer development

Dissertation

zur Erlangung des Doktorgrades der theoretischen Medizin

des Fachbereiches Medizin der Johann Wolfgang Goethe-Universität

Frankfurt am Main

vorgelegt von

Andreas Weigert

Worms

Frankfurt am Main 2007

Was man in der Natur Geheimnisvolles pries,

das wagen wir verständig zu probieren,

und was sie sonst organisieren ließ,

das lassen wir kristallisieren.


Johann Wolfgang von Goethe, Faust II

# Index

## List of Figures

## List of Tables

## Abbreviations

| | |
|---|---|
| AC | Apoptotic cells |
| A | Alanine |
| AA | Arachidonic acid |
| ABC | ATP binding cassette ABC1 |
| AC | Adenylyl cyclase |
| ACAMPs | Apoptotic cell-associated molecular patterns |
| ACM | Apoptotic cell conditioned medium |
| ANOVA | Analysis of variance |
| AP-1 | Activating protein-1 |
| APAF-1 | Apoptotic protease activating factor 1 |
| APS | Ammonium persulfate |
| Asp | Aspartic acid |
| ATP | Adenosine triphosphate |
| BH | Bcl-2 homology domains |
| BSA | Bovine serum albumin |
| $Ca^{2+}$ | Calcium |
| CD | Cluster of differentiation |
| CDase | Ceramidases |
| CDSyn | Ceramide synthase |
| CHX | Cycloheximide |
| COX | Cyclooxygenase |
| Cyt c | Cytochrome c |
| D | Aspartate |
| DAPI | 4´,6-diamidino-2-phenylindol |
| $DiOC_6$ | 3,3'-Dihexyloxacarbocyanine iodide |
| DISC | Death-induced signaling complex |
| DMEM | Dulbecco's modified eagle medium |
| DMS | N,n-dimethylsphingosine |
| DMSO | Dimethylsulfoxide |
| DNA | Deoxyribonucleic acid |
| DTT | Dithiothreitole |
| EDTA | Ethylene diamine tetra acetate |
| EGTA | Ethylene glycol tetra acetate |
| EMAP II | Endothelial monocytes-activating polypeptide II |
| EMEM | Minimal essential medium |
| ER | Endoplasmatic reticulum |
| ERK1/2 | Extracellular signal-regulated kinase 1/2 |
| FADD | Fas-associated death domain |

| | |
|---|---|
| FCS | Fetal calf serum |
| FITC | Fluoreszeinisothiocyanat |
| GEF | Guanine nucleotide exchange factor |
| GM-CSF | Granulocyte macrophage-colony stimulating factor |
| GSK3 | Glycogen synthase kinase 3 |
| HA | Hemagglutinin |
| HIV | Human immunodeficiency virus |
| IFN | Interferon |
| IL | Interleukin |
| IL-1ra | IL-1 receptor antagonist |
| IL-1RL | IL-1 receptor ligand |
| iNOS | Inducible NO-Synthase |
| $iPLA_2$ | Cytosolic calcium-independent phospholipase $A_2$ |
| JC-1 | 5,5',6,6'-tetrachloro-1,1',3,3'-tetraethyl-benzimidazolylcarbocyanine chloride |
| JNK | Jun N-terminal kinase |
| KCl | Potassium chloride |
| $KH_2PO_4$ | Potassium hydrogen phosphate |
| $KHCO_3$ | Potassium hydrogen carbonate |
| LC-MS/MS | Liquid chromatography-tandem mass spectrometry |
| LLOQ | Lower limit of quantification |
| LOX1 | Oxidized low-density lipoprotein receptor 1 |
| LPA | Lysophosphatidic acid |
| LPC | Lysophosphatidylcholine |
| LPS | Lipopolysacharide |
| MAPK | Mitogen-activated protein kinases |
| M-CSF | Macrophage-colony stimulating factor |
| MFG-E8 | Milk-fat globule epidermal growth factor 8 |
| $MgCl_2$ | Magnesium chloride |
| $MgSO_4$ | Magnesium sulfate |
| MHC | Major histocompatibility complex |
| MOMP | Mitochondrial outer membrane permeabilization |
| MR | Mannose receptor |
| $Na_2HPO_4$ | Sodium hydrogen phosphate |
| NaCl | Sodium chloride |
| NaF | Sodium fluoride |
| NBD-Sphingosine | Omega(7-nitro-2-1,3-benzoxadiazol-4-yl)-D-*erythro*-Sphingosine |
| NC | Necrotic cells |
| NES | Nuclear export signal |

| | |
|---|---|
| NF | Nuclear factor |
| NH$_4$Cl | Ammonium chloride |
| NLS | Nuclear localization signal |
| NO | Nitric oxide |
| O$_2^-$ | Superoxide |
| oxLDL | Oxidized lipoproteins |
| PAF | Platelet-activating factor |
| PBMCs | Peripheral blood mononuclear cells |
| PBS | Phosphate buffered saline |
| PC | Phosphatidylcholine |
| PE | Phycoerythrin |
| PFA | Paraformaldehyde |
| PG | Prostaglandin |
| PI | Propidium iodide |
| PI3K | Phosphatidylinositol-3 kinase |
| PK | Protein kinase |
| PL | Phospholipase |
| PMSF | Phenylmethylsulphonylfluoride |
| PPAR | Peroxisome proliferator-activated receptor |
| PS | Phosphatidylserine |
| PSR | PS receptor |
| ROS | Reactive oxygen species |
| RPMI | Roswell park memorial institute |
| S1P | Sphingosine-1-phosphate |
| S1PR | S1P receptor |
| SD | Standard deviation |
| SDS | Sodium dodecyl sulfate |
| SEM | Standard error of the mean |
| SHIP | Src homology2-containing inositol-5'-phosphatase |
| SMase | Sphingomyelinase |
| SMSyn | Sphingomyelin synthase |
| SphK | Sphingosine kinase |
| SPL | S1P lyase |
| SPP | S1P phosphohydrolase |
| SRA | Scavenger receptor A |
| STAT | Signal transducer and activator of transcription |
| Sts | Staurosporine |
| T | Threonine |
| TAM | Tumor-associated macrophages |
| TEMED | Tetraethylendiamine |

| | |
|---|---|
| TGF | Transforming growth factor |
| TLR | Toll-like receptor |
| TLRL | Toll-like receptor ligand |
| TNF | Tumor necrosis factor |
| TPA | 12-Tetradecanoyl-phorbol-13-acetate |
| VC | Viable cells |
| VEGF | Vascular endothelial growth factor |
| VnR | Vitronectin receptor |

# 1    Summary

The removal of apoptotic cells (AC) can be regarded as an integral component of the program to terminate inflammation. Clearance of AC by professional phagocytes such as macrophages induces an anti-inflammatory phenotype in the latter ones. Anti-inflammatory or M2 polarization is also observed in macrophages infiltrating certain human tumors. These tumor-associated macrophages (TAM) contribute actively to tumor progression by promoting immune evasion, angiogenesis and tumor cell survival. The aim of my Ph.D. thesis was to approach the mechanisms as well as the characteristics of macrophage phenotype alterations induced by AC, and to elucidate a possible connection between tumor cell apoptosis and TAM generation.

In the first part of my studies, I investigated the impact of AC on macrophage viability. I could show that macrophage survival against pro-apoptotic agents increased after the interaction with AC. Protection of macrophages against cell death required activation of phosphatidylinositol-3 kinase (PI3K), extracellular signal-regulated kinase 1/2 (ERK1/2) and $Ca^{2+}$ signaling, and correlated with Bcl-$X_L$ and Bcl-2 up-regulation as well as Ser136-Bad phosphorylation. Unexpectedly, neither phagocytosis nor binding of apoptotic debris to the phagocyte was necessary to induce protection. AC released the bioactive lipid sphingosine-1-phosphate (S1P), dependent on sphingosine kinase (SphK) 2, as a survival messenger. These data indicated an active role of AC in preventing cell destruction in their neighborhood.

My next aim was to elucidate the mechanism of S1P production by AC. During cell death, SphK 2 was cleaved at its N-terminus by caspase-1. Thereupon, the truncated but enzymatically active fragment of SphK 2 was released from cells. This release was coupled to phosphatidylserine exposure, a hallmark of apoptosis and a crucial signal for the phagocyte/apoptotic cell interaction. Thus, I observed a link between common signaling events during apoptosis and the extracellular production of S1P, which is known to affect immune cell attraction and polarization as well as angiogenesis in cancer.

In the next part of my studies, I asked for a correlation between tumor cell apoptosis and TAM polarization. During co-culture of human macrophages with human breast cancer carcinoma cells (MCF-7), the latter ones were killed, while macrophages acquired an alternatively activated phenotype. This was characterized by decreased tumor necrosis factor (TNF)-α and interleukin (IL)-12-p70 production, but increased formation of IL-8 and IL-10. Alternative macrophage activation required tumor cell death, because a co-culture with apoptosis-resistant colon carcinoma cells (RKO) or Bcl-2-overexpressing MCF-7 cells failed to induce phenotype alterations. These phenotype alterations were also achieved with conditioned media from apoptotic tumor cells, which again argued for a soluble factor being involved. Knock-down of SphK2, but not SphK1, to attenuate S1P formation in MCF-7 cells, repressed the otherwise observed alternative macrophage polarization during co-culture. Furthermore, macrophage polarization achieved by tumor cell apoptosis or substitution of authentic S1P was characterized by suppression of pro-inflammatory nuclear factor (NF)-κB DNA binding. These findings suggested that tumor cell apoptosis-derived S1P contributes to the macrophage polarization present in human tumors.

To validate these *in vitro* data, I used an *in vivo* tumor model to clarify the relevance of SphK2 and S1P in tumor development. The growth of, as well as blood vessel infiltration into SphK2 knock-down MCF-7 (MCF-7-siSphK2) xenografts in nude mice was markedly decreased in comparison to control MCF-7 xenografts. In contrast, macrophage infiltration was similar or even more pronounced. These data provided a first hint for an *in vivo* role of SphK2-derived S1P in macrophage polarization associated with tumor promotion.

In summary, these data indicate a new mechanism how AC themselves shape macrophage polarization, which results in the termination of inflammatory responses and macrophage survival. Furthermore, my studies present evidence that human tumors may utilize this mechanism to foster growth via increased angiogenesis.

## 2    Zusammenfassung

Die Phagozytose apoptotischer Zellen (AZ) kann als ein integraler Bestandteil des Mechanismus zur Beendigung von Entzündungsreaktionen angesehen werden. Die Beseitigung von AZ induziert einen anti-inflammatorischen Phänotyp in Makrophagen. Ein ähnlicher Phänotyp (M2) ist auch für Makrophagen beschrieben, die in humane Tumore infiltrieren. Diese Tumor- assoziierten Makrophagen (TAM) tragen aktiv zur Tumorprogression bei, indem sie die Gefäßbildung und das Überleben von Tumorzellen fördern, aber auch das körpereigene Immunsystem ausschalten. Das Ziel meiner Doktorarbeit war es, die Mechanismen und Charakteristika der Makrophagenpolarisierung durch AZ besser zu verstehen, und eine mögliche Verbindung von Tumorzell-Apoptose und der Ausprägung des TAM- Phänotyps aufzuzeigen.

Im ersten Teil meiner Studien untersuchte ich den Einfluss von AZ auf die Überlebensfähigkeit von Makrophagen. Diese war nach der Interaktion mit AZ erhöht. Der Schutz vor Zelltod benötigte die Aktivierung der Phosphatidylinositol-3 Kinase (PI3K), der Mitogen-aktivierten Proteinkinasen ERK1/2, sowie Calcium-Signale, und korrelierte mit vermehrter Expression von Bcl-2 und Bcl-$X_L$, sowie mit Phosphorylierung von Bad an Ser136. Interessanterweise war der Schutzeffekt unabhängig von Phagozytose oder direkter Interaktion zwischen Makrophagen und AZ, sondern vielmehr von der Freisetzung des bioaktiven Lipids Sphingosin-1-Phosphat (S1P) aus AZ, generiert durch die Sphingosinkinase (SphK) 2.

Mein nächstes Ziel war es den dafür verantwortlichen Mechanismus aufzuzeigen. Während des Zelltods fand eine Spaltung der SphK2 durch die Caspase-1 an deren N-Terminus statt, woraufhin ein enzymatisch aktives Fragment aus den AZ freigesetzt wurde. Diese Freisetzung war eng an die Exposition von Phosphatidylserin gekoppelt, welche ein Kennzeichen von Apoptose, und ein wichtiges Signal bei der Interaktion von Makrophagen und AZ ist. Somit konnte ich eine Verknüpfung zwischen allgemeinen Signalwegen der Apoptose und der extrazellulären Produktion von S1P nachweisen. Von letzterem ist bekannt, dass es sowohl die Polarisierung und das Anlocken von Immunzellen, als auch die Gefäßbildung im Tumor beeinflussen kann.

Im nachfolgenden Teil meiner Studien untersuchte ich eine mögliche Verbindung zwischen Tumorzell-Apoptose und der TAM- Polarisierung. In einer Ko-Kultur von menschlichen Makrophagen mit MCF-7 Brustkrebszellen wurden letztere getötet, woraufhin die Makrophagen einen alternativ aktivierten Phänotyp annahmen. Dieser war durch verminderte Produktion des Tumor-Nekrose- Faktors (TNF)-α und des Interleukins (IL)-12p70 sowie durch erhöhte Freisetzung der Interleukine 8 und 10 charakterisiert. Die alternative Aktivierung der Makrophagen in den Ko-Kulturen war Tumorzelltod- abhängig, da Apoptose-resistente Darmkrebszellen (RKO) oder Bcl-2 überexprimierende MCF-7 Zellen diese nicht auslösten. Dies war jedoch mit Zellkulturüberständen von apoptotischen Tumorzellen der Fall, was wiederum auf einen löslichen Faktor hindeutete. Das Ausschalten der SphK2, nicht jedoch der SphK1, was die S1P- Freisetzung von MCF-7 Zellen unterband, verhinderte die alternative Aktivierung von Makrophagen in den Ko-Kulturen. Ein weiteres Charakteristikum der Makrophagenpolarisierung durch apoptotische Tumorzellen und S1P war die Hemmung der DNA-Bindung des entzündungsfördernden Transkriptionsfaktors NF-κB.

Um die Relevanz der SphK2 und von S1P in der Tumorentwicklung genauer zu untersuchen, führte ich ein *in vivo* Tumormodell durch. Tumorzell-Implantate von SphK2-defizienten MCF-7 Zellen in Nacktmäusen wiesen sowohl deutlich reduziertes Wachstum, als auch Blutgefäßbildung, im Vergleich zu Kontrollimplantaten (MCF-7) auf. Die Einwanderung von Makrophagen war jedoch nicht vermindert, sondern eher erhöht. Diese Daten lieferten einen ersten Hinweis auf eine Rolle von SphK2-abhängig freigesetztem S1P in der Makrophagenpolarisierung, in Verbindung mit einer Förderung der Tumorentwicklung.

Zusammengefasst deuten meine Daten auf einen neuen Mechanismus hin, wie AZ die Makrophagenpolarisierung gestalten. Dieser Prozess resultiert letztlich in der Beendigung von Entzündungsreaktionen und erhöhter Überlebensfähigkeit von Makrophagen. Weiterhin weisen meine Studien darauf hin, dass Tumore eventuell diesen Mechanismus nutzen, um ihr Wachstum durch vermehrte Gefäßbildung zu sichern.

# 3    Introduction

## 3.1  Cell death

Two principle control mechanisms ensuring tissue homeostasis were developed by metazoans. Besides the production of 'new' cells through activation of the cell cycle of progenitor cells, followed by differentiation into specialists, death of redundant cells is a major regulator. Different modes of physiological cell death with varying morphological characteristics are known, including mitotic catastrophe (1), programmed necrosis (2) and autophagy (3). However, the major mode found in multicellular organisms is apoptosis.

Naturally occurring cell death was first described by Carl Vogt in 1842 as a unique process accompanied by typical morphological changes, followed by more than a hundred reports already in the nineteenth century (4). After a long period of neglect due to its 'invisibility', the process was rediscovered and named programmed cell death by Lockshin and Williams in 1965 (5). The term apoptosis, the Greek word for the fall of leaves in autumn, was first used by Kerr, Wyllie and Currie seven years later (6). In this and following studies, they identified certain morphological criteria to discriminate between physiological (apoptosis) and non-physiological cellular demise (necrosis).

Apoptosis is characterized by nuclear condensation and fragmentation, cell shrinkage and controlled cell disintegration through formation of membrane vesicles, so-called 'apoptotic bodies', whose membrane integrity is maintained (6, 7). It is energy-dependent and tightly regulated concerning its initiation, execution and termination, the latter ensuring its 'immunological silence' by providing signals for rapid clearance of apoptotic debris by professional phagocytes *in vivo* (8, 9). Furthermore, aside from being simply removed, apoptotic cells (AC) directly influence the phenotype of their 'captors' to shut down inflammation (10). Thus, suppression of inflammation is an intrinsic feature of apoptotic cell death.

In contrast, necrosis is usually induced by external force like heat, irradiation, mechanical stress or toxins, which leads to uncontrolled cell swelling and

rupture due to loss of cell membrane integrity. The consequence is leakage of cytosolic components into the interstitial space, which may cause severe inflammation (9). Membrane disintegration is also observed when phagocytosis of apoptotic material is defective, a process which is termed secondary necrosis. It occurs *in vivo* when the number of AC outstrips the phagocytic capacity by far (10).

## 3.1.1  Roads to apoptosis

The key players in classical apoptotic cell death are a family of cystein proteases, which cleave their substrates after aspartic acid (Asp) residues and were therefore named caspases (<u>c</u>ysteinyl <u>asp</u>artate protein<u>ases</u>) (11). More than a dozen caspase isoforms have been identified in mammals (12). They are highly conserved throughout evolution, even down to low complexity organisms like hydra (13).

Most caspase isoforms function as major executioners of apoptosis via cleavage of specific targets ensuring efficient physiological cell fragmentation. Nevertheless, additional properties have been attributed to caspase-dependent protein cleavage. The most prominent example is the role of caspase-1 in inflammation. Its activation in response to pathogens initiates the release of pro-inflammatory cytokines like interleukin (IL)-1β or IL-18 from immune cells (14). Thus caspase-1, together with other isoforms, whose specific substrates are yet unidentified, forms the subfamily of inflammatory caspases (15).

Caspases are synthesized as enzymatically inert zymogens (pro-caspases), which are activated via proteolytic processing at cleavage sites containing Asp-X residues as well (16). Therefore, the most efficient way to activate a pro-caspase is to expose it to another active caspase, an activation strategy termed the 'caspase cascade' (17). Apoptotic caspases are further subdivided into initiator and effector caspases, the latter being activated by the first (18). The main initiator caspases are caspase-8 and -9. Their respective activation is the sensitive step in apoptosis induction. It is coupled to two principally different pathways (Figure 1).

Briefly, caspase-8 is activated in the extrinsic cell death pathway upon binding of tumor necrosis factor (TNF) family members, the death ligands, to their specific death receptors on the cell surface. After receptor ligation, pro-caspase-8 is recruited to the death-induced signaling complex (DISC) by the adaptor protein FADD (Fas-associated death domain) (19). The formation of this complex results in caspase-8 activation, subsequent processing of effector caspase-3, -6 and -7, which thereupon execute cell death (20).

In contrast, caspase-9 is activated via the intrinsic pathway, which is initiated by the release of cytochrome c from the mitochondria in response to reactive oxygen and/or nitrogen species, growth factor withdrawal or DNA damage (21). Leakage of pro-apoptotic cytochrome c from mitochondria is tightly regulated by members of the Bcl-2 protein family. This family subsumes proteins with pro- as well as anti-apoptotic properties, which share up to four Bcl-2 homology domains (BH1-BH4). The anti-apoptotic members, like Bcl-2, Bcl-$x_L$ or Mcl-1 share all four domains, whereas the pro-apoptotic ones share three (BH1-BH3), like Bax and Bak, or possess only the BH3 domain, like Bad, Bid or Bim (22). Bcl-2 family proteins regulate apoptosis mainly through formation of heterodimers between pro- and anti-apoptotic members. Thus, their function may simply be neutralization of each other. A shift of this balance in either direction would then determine the cell's fate (17). However, reality seems to be much more complex. Although oversimplified, one may subsume that BH3-only proteins are activated by intrinsic death stimuli, thereupon inhibit anti-apoptotic or activate pro-apoptotic Bcl-2 family members with high specificity, which equally results in permeabilization of the outer mitochondrial membrane (MOMP) (23). Cytochrome c is released, induces ATP-dependent heptamerization of usually monomeric APAF-1 (apoptotic protease activating factor 1), which is then called the apoptosome. Caspase-9 is recruited to the apoptosome and activated by dimerization, whereupon it activates effector caspases (24). Importantly, the intrinsic pathway can also be induced by death ligands via caspase-8 dependent cleavage of the BH3-only protein Bid, which then induces MOMP (17).
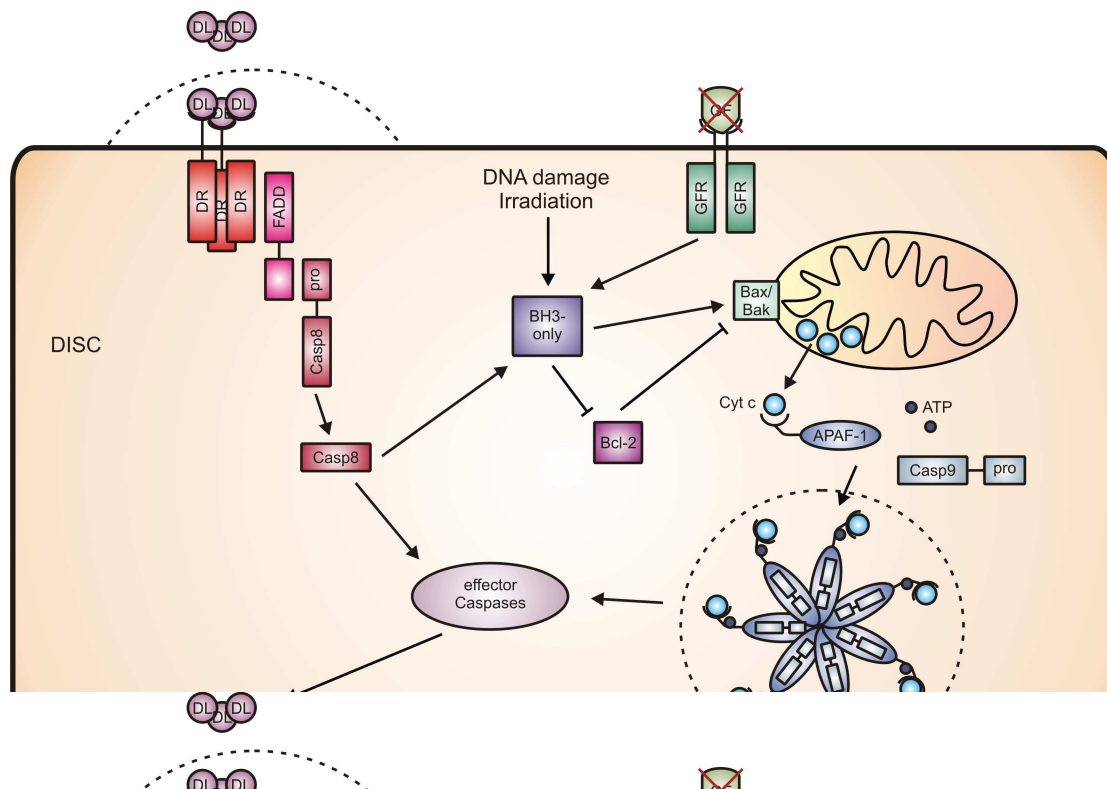
Figure 1: Signaling towards apoptosis. The extrinsic pathway is triggered by binding of death ligands (DL) to their specific death receptors (DR). Upon activation DRs recruit FADD (Fas-associated death domain), which binds the pro-form of capase-8 (Casp8) to form the death-induced signaling complex (DISC). Active caspase-8 may cross-activate the intrinsic pathway, which is usually activated by defective growth factor (GF) binding to their receptors (GFR), DNA damage or irradiation. Thereby, BH3-only proteins activate pro-apoptotic (Bax/Bak) or inhibit anti-apoptotic (Bcl-2) Bcl-2 family members. Cytochrome c is released from the mitochondria, binds to APAF-1 (apoptotic protease activating factor-1), which ATP-dependently forms the apoptosome. The holoenzyme of Caspase-9 (Casp9) is recruited to the apoptosome and activated. Caspase-9 and -8 again activate the effector caspases which execute apoptosis.

### 3.1.2  Death in disease

Apoptosis and disruption of its regulatory mechanisms play an essential role for the onset or progression of a large number of human pathologies. Since apoptosis serves to maintain tissue homeostasis, its control will be defective in diseases where the balance between production of 'new' cells and removal of dispensable cells is disturbed. The connection to cancer development is obvious. Any mutation in pathways towards apoptosis leading to protein

malfunction will be beneficial for tumor growth and metastasis, since cancer cells have to survive in a potentially hostile environment. Therefore, it is not surprising that indeed overexpression of anti-apoptotic proteins of the Bcl-2 family is found for instance in most human lymphomas (25) and is associated with poor prognosis in several solid tumors (26). A mutation that occurs in more than half of human tumors, is inactivation of p53, the so-called 'guardian of the genome' (27). p53 senses DNA-damage, and as a result it up-regulates and/or activates a number of pro-apoptotic proteins, including Bax (28).

Disease may also arise from excessive depletion of particular cell types. Maybe the most dramatic case is depletion of $CD4^+$ T cells by the human immunodeficiency virus (HIV), which results in impaired immune functions and death due to minor infections (29). Neurodegenerative diseases like Parkinson's disease, amyotrophic lateral sclerosis and Huntington's disease also originate at least in part from unusual degeneration of certain neuronal subsets (30).

Another example linking apoptosis to pathology is the maintenance of immune tolerance. Autoimmune diseases arise on the one hand from defective elimination of autoimmune T or B cells. Recognition of pathogens by the immune system induces rapid amplification of lymphocyte populations. Once the pathogen is destroyed, tissue homeostasis must be restored. Defects in apoptosis induction may then lead to autoimmunity (31). On the other hand, impaired clearance of AC, which represents a malfunction in the termination of cell death, will also result in an enhanced immune response against the body's own tissues, since AC may then function as autoantigens (32). Furthermore, efficient interaction of AC with phagocytes is a prerequisite for the resolution of inflammation (33). Its disruption may have implications in the development of pathologies associated with chronic inflammation, such as atherosclerosis (34). To understand the impact of interaction between AC and phagocytes in diseases, one has to take a closer look at the underlying molecular mechanisms.

## 3.2   Phagocytosis of apoptotic cells

Clearance of AC is the last step in the apoptotic machinery and is as neatly regulated as its initiation or execution. It can be subdivided into three steps:

I) Attraction of phagocytes to the site of tissue damage.

II) Specific recognition of AC by the phagocytes

III) Engulfment of AC or their fragments by the phagocytes

These steps will be explained in detail in the following paragraphs regarding their mechanistic principles (Figure 2).

### 3.2.1   Attraction

AC must be removed in order to avoid secondary necrosis. Obviously, a problem arises, since professional phagocytes such as macrophages are usually not found in close proximity to the dying cells. Therefore it is rational to assume that AC provide molecular signals to direct the phagocyte towards its 'meal'. Indeed, two different groups observed the release of chemoattractants factors from AC (35, 36).

Aminoacyl-tRNA synthetase, an enzyme critical for decoding genetic information in translation, is split in two fragments during apoptosis. One of them, the endothelial monocytes-activating polypeptide II (EMAP II), is able to bind to IL-8 receptors upon release from cells (36). IL-8 is an important mediator of leukocyte infiltration into inflamed tissues. Its action is mimicked by EMAP II.

The most detailed study concerning macrophage migration towards AC provided a direct connection between the apoptotic machinery and the release of a chemotactic lipid agent. A cytosolic calcium-independent phospholipase $A_2$ (iPLA$_2$) is activated during apoptosis via cleavage of ankyrin repeats by caspase-3.   iPLA$_2$   then   generates   arachidonic   acid   (AA)   and lysophosphatidylcholine (LPC) by hydrolysis of the membrane phospholipid

phosphatidylcholine (PC). Both lipids are released from AC (35, 37), but only the latter induces macrophage migration *in vitro* and *in vivo*. Thus, LPC exerts some anti-inflammatory property by ensuring efficient AC clearance through phagocyte attraction (38). However, its direct impact on macrophages is usually considered as pro-inflammatory and linked to inflammatory diseases such as atherosclerosis (39). Since interaction of AC and phagocytes induces anti-inflammatory signaling in the latter ones, we have to proceed and look closer at the next step, the specific recognition of AC.


### 3.2.2 Recognition

Phagocytes have to discriminate if the target they encounter is a pathogen, a necrotic cell or an apoptotic cell in order to respond properly concerning the immunological outcome. Therefore, they have to 'feel' their way towards specific recognition. The most efficient way to distinguish AC from necrotic or viable cells is sensing molecular changes at their plasma membranes. These apoptotic cell-associated molecular patterns (ACAMPs) are also called 'eat me' signals. In a complex network, they are recognized by phagocyte receptors, often coupled to bridging molecules, which serve to strengthen their recognition (40).

A critical hallmark of apoptosis-associated cell surface alterations is externalization of the membrane phospholipid phosphatidylserine (PS) (41, 42). In viable cells, PS is restricted to the inner leaflet of the plasma membrane. This feature of phospholipid asymmetry is secured by aminophospholipid translocase, which 'flips' PS back to its proper place when it appears at the outer leaflet. During apoptosis, activity of aminophospholipid translocase is disrupted, which prevents retraction of PS from the cell surface (43). Additionally, PS exposure is enhanced by caspase-3-dependent activation of scramblase, an enzyme that promotes energy-independent, bidirectional scrambling of all classes of phospholipids across the membrane (44). More recent studies indicate PS oxidation through oxidized cytochrome c prior to exposure as a prerequisite for recognition by phagocytes (45).
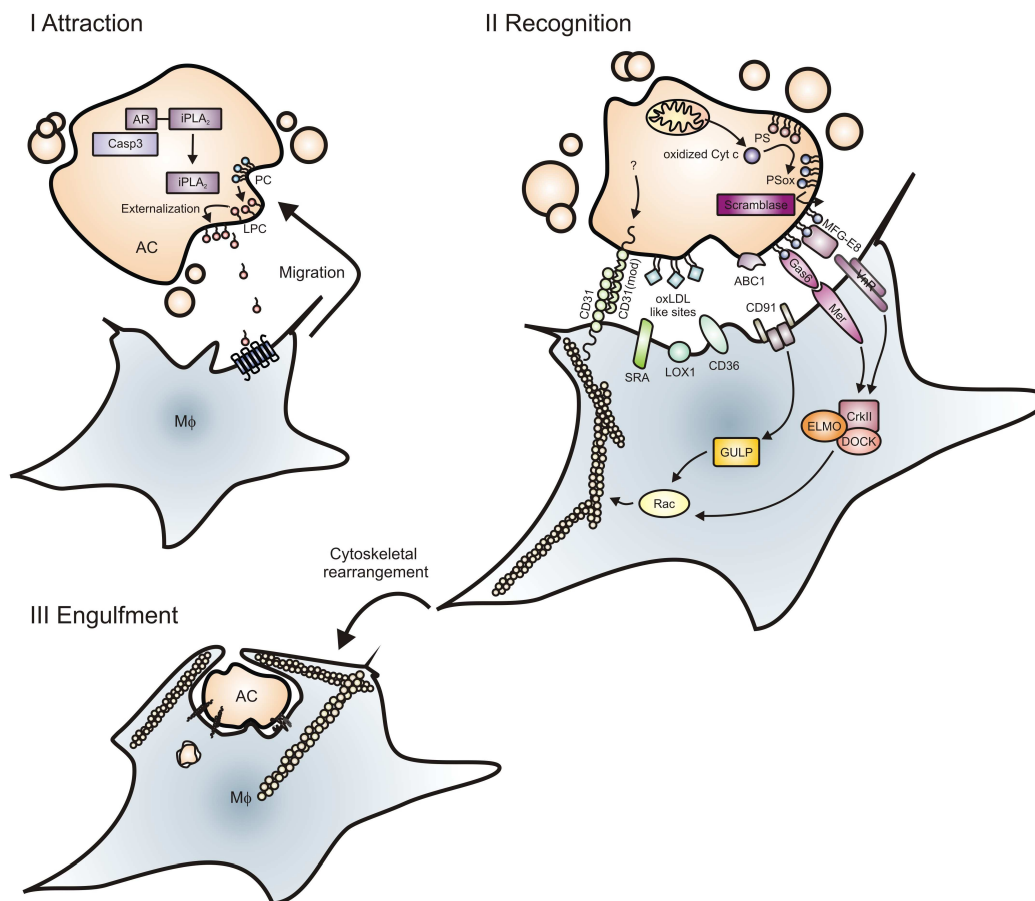
Figure 2: Phagocytosis of AC. I) During apoptosis, a calcium-independent phospholipase $A_2$ ($iPLA_2$) is activated via cleavage of ankyrin repeats (AR) by caspase-3 (Casp3), hydrolyses phosphatidylcholine (PC) to produce lysoPC (LPC), which is then released and serves as an attraction signal for macrophages. II) Oxidized cytochrome c (Cyt c) is released from mitochondria in AC, oxidizes phosphatidylserine (PS), which is externalized via scramblase. The bridging molecules Gas6 and milk-fat globule epidermal growth factor 8 (MFG-E8) connect PS to the phagocytic receptors Mer and vitronectin receptor (VnR), respectively. AC also exhibit other oxidized phospholipids (oxLDL like sites) on their surface that are recognized by macrophage scavenger receptors (SRA, LOX1, CD36). Furthermore, CD31 is modified during apoptosis, which binds to CD31 on the macrophage surface, serving as another recognition signal. Downstream of Mer and/or VnR, the ELMO/DOCK/CrkII complex is assembled, which activates the G-protein Rac to induce cytoskeletal rearrangement. Rac may also be activated via interaction of ATP binding cassette transporter 1 (ABC1) on AC with CD91 on the macrophage. III) After specific tethering, the macrophage's cytoskeleton is rearranged and AC are engulfed via a zipper-like mechanism.

Albeit the exact mechanism of PS exposure during apoptosis is still under investigation, it may not be limited to AC. Necrotic cell death, induced by death ligands, also induces PS externalization in some cell types (46). These necrotic cells are then engulfed by macrophages, but do not induce inflammation. Since necrosis may also be 'physiological' under these special conditions, PS may be a more general marker of physiological cell death associated with anti-inflammatory signaling.

Phagocytic receptors bind PS on AC usually via specific bridging molecules that may be ubiquitous or secreted from AC. The plasma factor $\beta_2$-glycoprotein I binds to its specific receptor upon interacting with PS (47). Mer kinase receptor recognition of PS is mediated via ambilateral GAS6 binding and the milk-fat globule epidermal growth factor 8 (MGF-E8) connects PS to the vitronectin receptor (VnR) (48). Much attention was given to a receptor specific for PS without requisition of a bridging molecule (49). Nevertheless, recent work suggests that this putative PS receptor is dispensable for interaction of phagocytes with AC (50).

Numerous other receptors on macrophages participate in AC recognition. Most are known from other conditions when the macrophages dinner is served, which are engulfment of pathogens or recognition of oxidized lipoproteins (oxLDL). Among them are the scavenger receptors CD36 (51), scavenger receptor A (SRA) (52) or oxidized low-density lipoprotein receptor 1 (LOX1) (53), which recognize oxidized phospholipids, so-called oxLDL like sites on AC. Furthermore, receptors necessary for pathogen recognition, like integrin receptors, complement receptors or Fc receptors are involved (40).

Another interesting alteration of surface structures on AC is modification of CD31. Its expression on viable cells serves as a detachment or 'don't eat me' signal via homophilic interaction with macrophage CD31 (54). Disruption of this interaction marks cells as suitable targets for phagocytosis.

### 3.2.3  Removal

Naturally, signaling pathways towards engulfment should emerge from the 'eat me' signal/macrophage receptor interactions mentioned above. They induce rearrangement of the phagocyte's cytoskeleton resulting in a 'zipper-

like' ingestion process. Therefore, phagocytic receptors must be linked mechanistically to the phagocyte's actin filaments. Unfortunately, no direct connection could be uncovered by now.

Two distinct signaling modules mediating engulfment were identified by genetic studies of phagocytosis defective mutants in the worm *C. elegans* (55). The proteins forming these complexes have mammalian homologues, whose functional properties in phagocytosis of AC were confirmed lately (56).

One complex consisting of CrkII, ELMO and DOCK180 is recruited to the plasma membrane in nascent phagosomes, serving as a guanine nucleotide exchange factor (GEF) for the G-protein Rac1, which then induces changes in the phagocytes cytoskeleton (48). The Crk-ELMO-DOCK180 complex is possibly activated downstream of VnR (57) or Mer (48) interactions with PS on AC, but the exact mechanisms in the context of AC removal remain to be elucidated.

Rac1 activation can also be achieved via activation of GULP, which possibly transmits signals downstream of the interaction between ABC1 on AC and CD91 on the phagocyte's membrane (56). However, definite mechanistic studies are still outstanding. This may be partially described to the numerous observations relating most of the immunomodulatory effects of AC to ligation of 'eat me' signals with phagocytic receptors, rather then to the uptake process *per se*. To understand the impact of AC on the macrophage's behavior regarding inflammation, we first have to scrutinize the principles of macrophage polarization.

## 3.3   Macrophage polarization

Macrophages are part of the body's innate immune system, the first defense line against invading pathogens. They originate from myeloid progenitor cells in the bone marrow, which differentiate into monocytes dependent on lineage-determining cytokines like GM-CSF (granulocyte macrophage-colony stimulating factor).

Monocytes are able to surpass the border separating the bone marrow from the blood stream and enter into the latter one. Allured by an appropriate stimulus, they migrate into different tissues, where they differentiate into tissue macrophages under the influence of growth factors like GM-CSF or M-CSF (macrophage-colony stimulating factor). There, by changing their morphology and metabolism, they acquire special features, depending on the micro-environment of the respective tissue (58).

### 3.3.1   Macrophage phenotypes

Macrophages exhibit high plasticity in their functional responses, which means they express different phenotypes in response to micro-environmental signals. Their major task is modulation of inflammation, both regarding its initiation and its resolution.

In 1794, the surgeon John Hunter defined inflammation as a salutary operation proximate to violence or disease. This crucial insight implicates that inflammation, rather than being a disease in itself, usually serves to eliminate the sources of disease, followed by implicit resolution and tissue repair (33).

Inflammation is characterized by the rapid influx of inflammatory cells, such as neutrophils, lymphocytes and monocytes.

The monocytes mature into inflammatory macrophages triggered by microbial cell wall components like lipopolysacharide (LPS) and T helper 1 ($T_H1$) lymphocyte-derived interferon (IFN)-γ. Such 'classically activated' macrophages produce cytotoxic mediators like nitric oxide (NO), superoxide ($O_2^-$) and TNF-α, as well as a variety of pro-inflammatory cytokines and chemokines (59), which mediate killing of pathogens, but also of surrounding
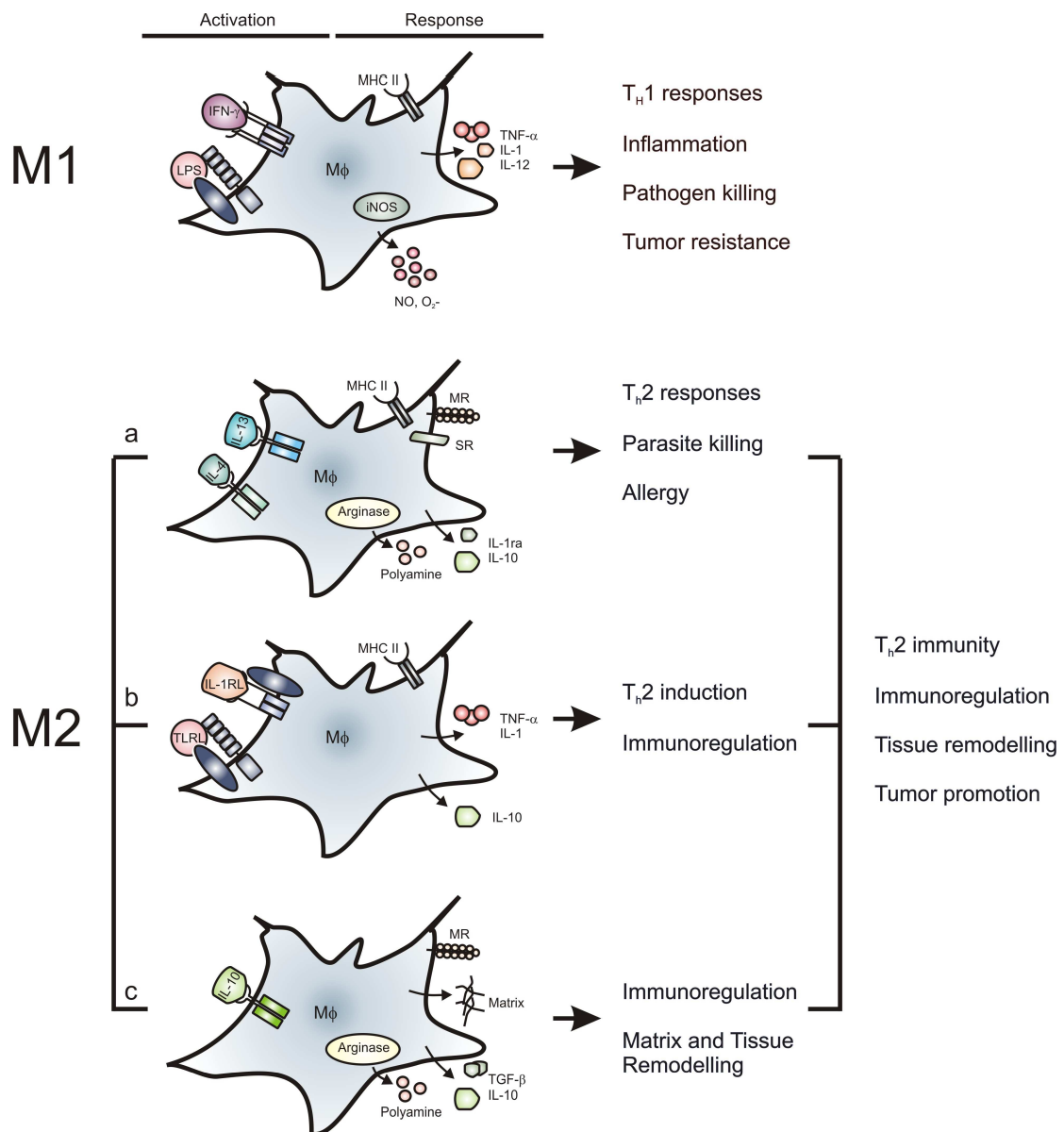
Figure 3: The M-Phenotypes. M1 polarization is induced via lipopolysacharide (LPS) and interferon (IFN)-γ. M1 macrophages produce tumor necrosis factor (TNF)-α, interleukins (IL)-1 and -12, as well as cytotoxic nitric oxide (NO) via inducible NO-Synthase (iNOS) and superoxide ($O_2^-$). They present antigens via major histocompatibility complex II (MHC II). Three distinct M2 phenotypes are known. M2a is induced by interleukins (IL)-4 and -13, characterized by up-regulation of the arginase pathway with concomitant polyamine production, release of IL-1 receptor antagonist (IL-1ra) and IL-10 and exhibition of MHC II, the mannose receptor (MR) and scavenger receptors (SR). M2b polarization is mediated by toll-like receptor ligands (TLRL) and IL-1 receptor ligands (IL-1RL), accompanied with TNF-α, IL-1 and IL-10 release as well as MHC II expression. The M2c phenotype is induced by IL-10, characterized by arginase induction, IL-10 and transforming growth factor (TGF)-β release, production of extracellular matrix components as well as MR expression.

resident tissue cells and other immune cells. Although excess resident cell destruction may end in failure of organ function (60), induction of apoptosis during inflammation usually determines its end.

First, pro-inflammatory reactions are terminated by death of immune cells like neutrophils and lymphocytes, and second by recognition and removal of the apoptotic debris by macrophages. After AC recognition the previous 'killer' macrophages actively contribute to healing by releasing growth factors, anti-inflammatory cytokines like IL-10 and TGF-β, pro-angiogenic and matrix-remodeling factors, and suppress $O_2^-$ as well as NO formation (61). These 'healer' macrophages were often classified as 'de-activated', which is apparently inexact. It may be owed to the fact that the term 'alternatively activated' macrophage was given away earlier (62). Usually, alternative activation is defined as T helper 2 ($T_H2$) lymphocyte mediated stimulation of macrophages with IL-4, IL-10 or IL-13, which occurs during i.e. allergic responses, and dampens $O_2^-$ release, blocks NO production via arginase expression, enhances IL-10 generation and induces expression of scavenger receptors (59).

Since several macrophage phenotypes apart from the 'classically activated' are known, which could all be termed 'alternatively activated', I prefer to use the classification introduced by Alberto Mantovani, who denominated 'classically activated' macrophages as M1 and otherwise polarized macrophages as M2 (63). An overview of the different faces of macrophage activation is given in Figure 3, especially regarding the distinct M2 phenotypes.

### 3.3.2  Macrophage polarization by apoptotic cells

During the last decade, plenty of evidence was provided that AC modulate innate immune responses aside from simply being removed (Figure 4). One of the first studies reported down-regulation of TNF-α and IL-1β, as well as up-regulation of IL-10 in co-cultures of human monocytes with AC after stimulation with LPS (64). Later, an AC-mediated anti-inflammatory phenotype was confirmed for human macrophages. This phenotype was characterized by production of transforming growth factor (TGF)-β, prostaglandin (PG) $E_2$ or

platelet-activating factor (PAF), which again prevented LPS-induced pro-inflammatory cytokine production (65). Strong supporting argumentation emerged from studies in CD14 knockout mice (66). In this model, phagocytosis of AC was blocked, but neither TGF-β production nor down-regulation of TNF-α was affected. Although AC remained persistent, the resolution of inflammation was unimpaired, unlinking it from the process of clearance. However, mechanistic details how AC modulate the macrophage phenotype are ill defined.

Since recognition of externalized PS is a prominent feature of macrophage/AC interaction, many studies investigated its impact in immunomodulation, unfortunately with special emphasis on the role of the putative PS receptor (PSR). PS recognition by PSR was mechanistically connected with TGF-β production (49). Additionally, a pro-inflammatory phenotype was observed in PSR knock-out mice (67, 68). Recent reports disagreed with the assumption that the putative PSR participates in AC-mediated immune regulation (50, 69, 70), therefore this topic remains contradictory. However, other macrophage receptors recognizing PS, such as VnR or Mer might be relevant.

Studies in Mer-deficient mice revealed its importance in AC clearance (71, 72). Indeed, Mer deficiency in macrophages revealed a pronounced pro-inflammatory phenotype, although in a model unrelated to AC recognition (73). More evidence is given for the VnR. A mutant form of MGF-E8, the bridging molecule that links PS to VnR, inhibited IL-10 production by macrophages (74). Along that line, inhibition of VnR on murine macrophages reduced TGF-β and $PGE_2$ production in response to AC (75). $PGE_2$ production was diminished by pharmacological inhibition of cyclooxygenase (COX)-2, the rate limiting enzyme in $PGE_2$ production (65). Therefore one may suggest COX-2 induction by AC via VnR. The authors went on and linked VnR-dependent TGF-β production to reduced NO generation in LPS-stimulated macrophages, thus providing evidence that AC interfere with macrophage cytotoxicity. Unfortunately, in another study, PS-enriched Jurkat cells did not show prevention of LPS-induced NO generation, although apoptotic Jurkat cells actively did. Therefore, one must conclude that PS exposure alone is insufficient in down-regulating NO production (76). Taking further into consideration that PS-enriched Jurkat cells upregulated TGF-β,

one must suggest that factors other than TGF-β account for inhibition of macrophage NO-production.

Beside NO, macrophages produce reactive oxygen species (ROS) to kill pathogens. ROS generation was inhibited by PS-enriched Jurkat cells (76) as well as AC in LPS-stimulated murine macrophages (77). In macrophages, AC provoked rapid activation of the immunoregulatory transcription factor peroxisome proliferator-activated receptor (PPAR)-γ. PPAR-γ prevented protein kinase C (PKC)-α-mediated activation of NADPH-oxidase, a protein complex, which is crucial for ROS induction (77). Although a potential role of PS in affecting PPAR-γ remains unclear, it is intriguing to speculate on the involvement of PPAR-γ in AC-mediated immunomodulation (78).

Recently, the group of Ucker showed that LPS-induced nuclear factor (NF)-κB activation was impaired in macrophages that had recognized AC (79). NF-κB inhibition partly is a rational explanation for macrophage polarization by AC, since it is the most prominent pro-inflammatory transcription factor in macrophages (80). However, considering that contact of macrophages with AC provokes active anti-inflammatory signaling rather than de-activation, NF-κB inhibition alone is insufficient to explain their phenotype transition. Indeed, anti-inflammatory signaling *per se* was unrelated to NF-κB, thus arguing for additional transcriptional modulator systems under the control of AC (81). As an explanation for NF-κB inhibition, depletion of transcriptional co-activators was suggested (79). Interestingly, this is an established function of PPARs (82), thus putting PPAR-γ into focus once more.

The direct interaction between macrophages and AC appears multifaceted and yet another level of complexity is added by findings that AC secrete soluble, potentially immunomodulatory factors. Chen et al. observed TGF-β release from apoptotic T-cells, which repressed LPS-mediated TNF-α production in murine macrophages (83). This is interesting, since most studies did not identify the origin of TGF-β production, with their approach of discriminating whether binding and/or phagocytosis of AC was necessary for TGF-β release. In addition, evidence emerged that IL-10 and IL-4 are released from AC (84, 85).
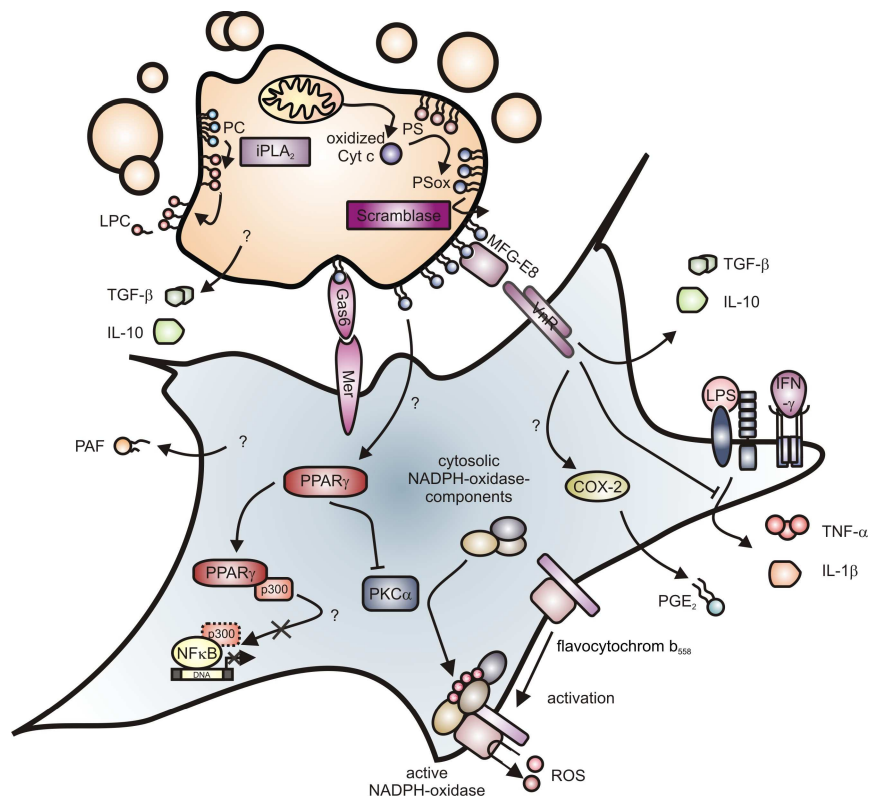
Figure 4: Macrophage polarization by AC. AC release lysophosphatidylcholine (LPC), transforming growth factor (TGF)-β and interleukin (IL)-10 and express phosphatidylserine (PS) on their surface. Bridging of PS to the vitronectin receptor (VnR) via milk-fat globule epidermal growth factor 8 (MFG-E8) is associated with TGF-β and IL-10 release from macrophages, suppression of lipopolysacharide (LPS)/interferon (IFN)-γ induced tumor necrosis factor (TNF)-α and IL-1β production and shedding of prostaglandin (PG) $E_2$, possibly via cyclooxygenase (COX)-2 induction. PS externalization may also activate the peroxisome proliferator-activated receptor (PPAR)-γ, which inhibits protein kinase (PK) Cα induced NADPH-oxidase assembly and subsequent reactive oxygen species (ROS) production. PPAR-γ is able to inhibit nuclear factor (NF)-κB DNA transcriptional activity by scavenging its cofactor p300, which may also occur in macrophages after AC-interaction. Moreover, macrophages release platelet activating factor (PAF) after encounter of AC, although mechanistic details are unclear. Mer kinase, coupled to PS via Gas6, may further be capable of suppressing pro-inflammatory responses. The same is true for TGF-β and IL-10, which may bind to their specific receptors on the macrophage surface. Speculative mechanisms are marked with '?'.

Besides IL-10 and TGF-β as protein factors, also lipid mediators are secreted during apoptosis. As mentioned under paragraph 3.2.1, LPC and AA are generated by caspase-3 dependent cleavage. Discussing a putative role of LPC in macrophage polarization, it is interesting that immunosuppressive properties of AC rather are caspase-3 independent, since caspase-3 deficient MCF-7 breast cancer cells effectively acted immunosuppressive (86).

Although an immune regulatory function of AC is now generally accepted, the discussion of underlying molecular pathways remains heterogeneous. A precise definition of the type of macrophage/AC interaction that affects the anti-inflammatory responses elicited during cell demise is needed to understand, and finally interfere with, its contribution to human diseases. However, there might be no single molecular switch that controls the pro- vs. anti-inflammatory phenotype, because physiological cell death obviously provides a variety of signaling patterns that can be recognized by macrophages.

### 3.3.3   Macrophages in cancer development

In the 19th century, Rudolf Virchow, the founder of cellular pathology, observed the presence of leukocytes in human tumors using the newly discovered technique of microscopy. He connected the infiltration of immune cells with cancer progression, suggesting that cancer emerged from chronic irritation. Although this observation sank into oblivion for about a century, the consequences of immune cell infiltration into tumors were put into perspective again in recent years.

Macrophages are a major cellular constituent of the leukocyte infiltrate of tumors (87). In breast cancer, TAM may even comprise up to 50% of the tumor mass (88). The presence of tumor-associated macrophages (TAM) correlates with a poor survival prognosis for patients with solid human tumors, especially in breast, prostate, ovarian and cervical cancer (89). TAM acquire complex functions in their interactions with neoplastic cells and multiple evidence suggests that they are part of the program that promotes tumor growth and progression (90).

TAM display a polarized M2 phenotype (91). In contrast to M1 macrophages,

they show reduced capacity in the production of anti-tumor molecules like TNF-α or NO. Contrarily, TAM support tumor survival, growth, metastasis and seem to play a major role in tumor angiogenesis and immune evasion (90-92). Especially in breast cancer development, the pro-angiogenic property of TAM was highlighted. When macrophage infiltration into breast tumors was abolished in a mouse model, tumor development was delayed due to inaccurate vascular development, which usually is a prerequisite for tumor malignancy (93). Furthermore, macrophage infiltration was positively correlated with high tumor blood vessel density, and the presence of pro-angiogenic cytokines like vascular endothelial growth factor (VEGF), IL-8 and TGF-α (94).

TAM polarization seems to represent the composition of the surrounding tumor microenvironment. Tumor-derived molecules such as IL-4, IL-10, TGF-β, $PGE_2$ and chemokines, as well as tumor hypoxia are held responsible for TAM generation (87, 90, 95). Recently, another concept of tumor-induced macrophage polarization was introduced. Administration of apoptotic tumor cells reduced macrophage cytotoxicity against vital tumor cells (96). Furthermore, disruption of AC recognition by macrophages or dendritic cells *in vivo* induced tumor regression (97). Interestingly, TAM share several activation patterns with AC-stimulated macrophages. They express low of amounts of the pro-inflammatory cytokines TNF-α, IL-12p70, IL-1β and IL-6 when stimulated with LPS, probably due to defective NF-κB signaling, but high amounts of IL-10 or TGF-β (98). Therefore it is tempting to speculate, that tumors utilize the physiological role of macrophages in the resolution of inflammation associated with tissue repair and angiogenesis, by providing signals comparable to AC.

## 3.4  Sphingosine-1-phosphate

Sphingosine-1-phosphate (S1P) is a bioactive lipid mediator, i.e. a lipid that plays a role in cellular signaling rather than being simply a component of cellular membranes or a means to store energy. Its intracellular concentrations are always low, whereas in plasma it can reach concentrations of 0.2 to 0.9 µM, usually bound to lipoproteins.

S1P is found far downstream in the pathway of sphingolipid metabolism (Figure 5). De novo synthesis of sphingolipids occurs by condensation of serine and palmitoyl-CoA to form 3-ketosphinganine which is then converted into ceramide via multiple catalytical steps. Ceramide can also be released via hydrolysis of membrane sphingomyelin by sphingomyelinases, and is subsequently deacylated by ceramidases to sphingosine. Sphingosine and other sphingoid bases can be phosphorylated by sphingosine kinases (SphKs) to form S1P. Turnover of S1P is mediated either by reversible dephosphorylation to sphingosine by specific S1P phosphohydrolases (SPPs) or by irreversible cleavage by S1P lyase (SPL) (99).

S1P was originally defined as a second messenger with intracellular activity. Although no direct intracellular target for S1P was identified up to date, this view is still supported by several studies. The cellular balance between pro-apoptotic ceramide/sphingosine and anti-apoptotic S1P seems to be critical to determine cell viability. Furthermore, S1P is activated by growth factors like VEGF and mediates intracellular signaling via mitogen-activated protein kinases (MAPK) or calcium ($Ca^{2+}$) currents (100). In a similar fashion, TNF-α induces S1P, which in turn activates NF-κB (101).

New roads were opened by the identification of a family of five G protein-coupled receptors specific for S1P (S1PR1-5) in higher organisms. S1P binds to its receptors with affinities ranging from 2 nM to 63 nM (102). Coupling of S1P to its specific receptors is important for the growth of new blood vessels, vascular maturation, cardiac development, directed cell movement and immunity (103). Its importance was supported by S1PR knock-out studies, which revealed severe developmental vascular defects, resulting in prenatal death of the mouse embryos in S1PR1 knock-out mice (104). The pathways

activated downstream of S1PRs read like the 'who-is-who' in cellular signaling (Figure 5).
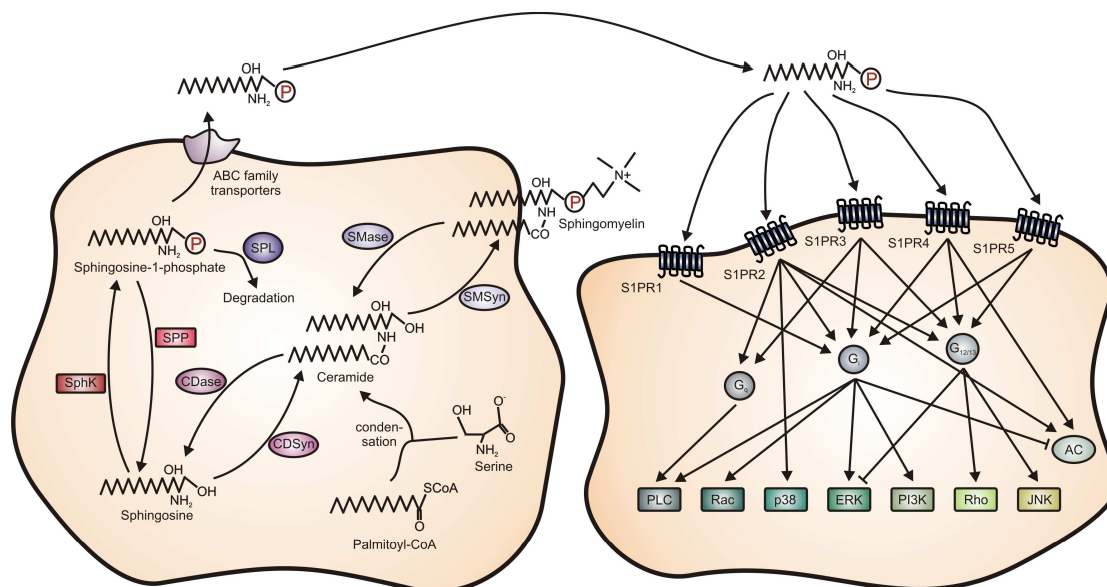


Figure 5: Production and actions of sphingosine-1-phosphate. S1P may be synthesized *de novo* via condensation of serine and palmitoyl-CoA, or by sphingomyelinase (SMase)-mediated hydrolysis of sphingomyelin to ceramide. Ceramide can be reconverted to sphingomyelin by sphingomyelin synthase (SMSyn). Ceramidases (CDase) convert ceramide into sphingosine, whereas the reverse reaction is catalyzed by ceramide synthase (CDSyn). Sphingosine is phosphorylated by sphingosine kinases (SphK) to S1P. S1P degradation occurs via reconversion to sphingosine by S1P phosphohydrolase (SPP) or irreversible degradation by S1P lyase (SPL). S1P is exported from cells by ATP binding cassette (ABC) transporters, where it binds to its five specific receptors (S1PR1-5). Downstream of S1PRs, many cellular signaling pathways are activated, either directly or via G-proteins ($G_i$, $G_q$, $G_{12/13}$). Among these are pathways mediated by phospholipase C (PLC), Rac, p38, extracellular signal-regulated kinases (ERK), phosphatidylinositol-3 kinase (PI3K), Rho, jun N-terminal kinase (JNK), or adenylyl cyclase (AC).

Although considerable amount of data concerning S1P related signaling have been obtained, mechanistic explanation how S1P, after being produced inside cells, surmounts the plasma membrane to bind to its specific receptors in an autocrine or paracrine fashion are limited. Once activated, SphK1 translocates and binds to the plasma membrane, a process bringing S1P in close proximity to putative transporter proteins. Indeed, ATP binding cassette (ABC) family

transporters facilitate the release of S1P from mast cells (105) and platelets (106). Alternatively, a splice variant of SphK1 (SphK1a), is exported from cells, provoking extracellular production of S1P, which contributes to the high vascular S1P concentration observed in mice (107).

### 3.4.1  Sphingosine kinases

S1P is produced by phosphorylation of sphingosine by sphingosine kinases, an enzyme family consisting of two isoenzymes, SphK1 and 2, which, although facilitating the same reaction, may have distinct or even antithetic biological virtues (108). Sphingosine kinases are conserved across most eukaryotic organisms. They contain five conserved domains termed C1 to 5 (Figure 6). The C1-C3 domains comprise the putative catalytic domain of SphKs, with the C2 domain containing the ATP binding site. In the C4 domain, which is unique for SphKs, resides the sphingosine binding site (109). In humans, alternative splice variants for both enzymes have been described recently (107, 110). For SphK1 three proteins (SphK1a to c), consisting of 384, 398 and 470 amino acids are known, whereas the two SphK2 isoenzymes (SphK2S and L) consist of 618 and 654 amino acids (111). SphK2 diverges from SphK1 in its central region and has an elongated amino terminus. Although single knock-out mice have no unusual phenotype, SphK1/SphK2 double knock-out is lethal, due to defects in neurogenesis and angiogenesis as well as increased apoptosis (112). This means that SphKs, also often unlike in their function, may compensate for each other during development.

SphKs exhibit different kinetic properties and also have dissimilar expression profiles during development as well as in tissues (113). They differ in their substrate specificity, where special attention has been paid to the property of SphK2 to phosphorylate the immunomodulatory sphingosine analogue FTY720 (114, 115). Phosphorylated FTY720 is an agonist for S1PRs, where it either mimics S1P responses or induces their down-regulation upon activation (116). S1PR1 down-regulation inhibits lymphocyte migration towards S1P gradients, which may be critical for prevention of immune responses to allograft transplants (115). N,N-Dimethylsphingosine (DMS) inhibits both

SphKs, but is a competitive inhibitor of SphK1 and a noncompetitive one of SphK2 (117). Last, SphKs react in opposite ways to increasing salt concentrations, addition of detergents and serum proteins like BSA (117). Both SphKs are activated by anionic phospholipids, especially PS, although mechanistic explanations are limited.

SphKs vary not only in their responses to their biochemical ambiance, but also in terms of activation and the congruent physiological functions. A good deal of data is available dealing with the activation of SphK1, but substantially less is known for SphK2. Indeed, most of the functions of S1P listed in the previous paragraph were attributed to SphK1 activity (113). In the following, I will focus on regulation of apoptosis, where the opposing roles of the two SphK isoforms are most prominent (Figure 6).

Many studies in various cell types observed that overexpression of SphK1 and thus increased S1P production promotes cell growth (118). SphK1 accounts for the elevated levels of S1P downstream to growth factor signaling, transmitting their pro-proliferative and anti-apoptotic functions. S1P formed such a like may furthermore inhibit ceramide synthesis, shifting the ceramide/S1P balance, i.e. apoptosis or survival, further in the direction of S1P and survival (108). Inversely, efficient apoptosis induction may require SphK1 degradation. TNF-α or DNA damage induce SphK1 cleavage by the p53 driven activation of cystein protease cathepsin B, which leads to a decrease in intracellular levels of S1P (119). In sharp contrast, SphK2 overexpression suppresses cell growth by inhibition of DNA synthesis directly via its nuclear localization (120). Furthermore it induces apoptosis through cytochrome c release and caspase-3 activation, which is surprising, since both SphK isoforms catalyze the same reaction. One possible mechanism for SphK2-dependent apoptosis was revealed, when a BH3 domain was identified in its amino acid sequence (121). SphK2, like other BH3-only proteins, physically interacts with an anti-apoptotic Bcl-2 family protein, in this case Bcl-$x_L$, and thus may induce apoptosis as described in chapter 1.1.2. Nevertheless, disruption of SphK2 interaction with Bcl-$x_L$ only partly reduced its apoptosis-inducing capability (108).
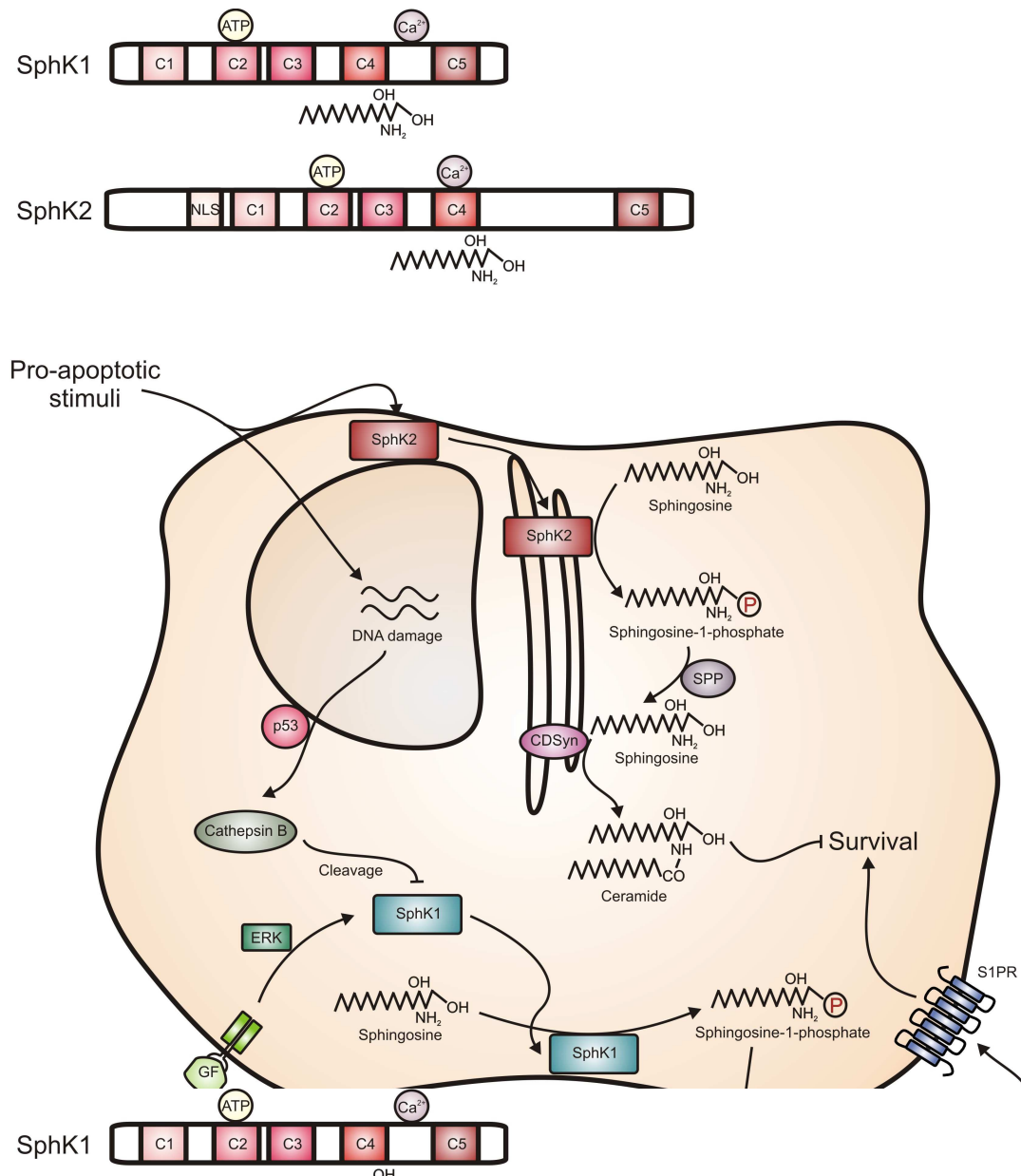
Figure 6: Sphingosine kinases and their different functions in apoptosis. Sphingosine kinases (SphK) contain five conserved domains (C1-5), with an ATP binding site residing in C2, the sphingosine binding site in C4 and a calcium/calmodulin binding site ($Ca^{2+}$). Compared to SphK1, SphK2 is elongated at its N-terminus (containing a nuclear localization signal (NLS)) and between C4 and C5. SphK1 is phosphorylated by extracellular signal-regulated kinases (ERK) upon binding of growth factors (GF) to their receptors, translocates to the plasma membrane where it phosphorylates sphingosine to sphingosine-1-phosphate (S1P). S1P is externalized, binds to its receptors (S1PR) to induce survival. During apoptosis, DNA damage leads to activation of cathepsin B via p53, which cleaves SphK1, thereby terminating its pro-survival properties. SphK2 translocates to the endoplasmatic reticulum (ER), produces S1P, which is reconverted to sphingosine by S1P phosphohydrolase (SPP). Pro-apoptotic ceramide is then synthesized from sphingosine by ceramide synthase (CDSyn) at the ER.

The proposed mechanism was that SphK2 and S1P phosphohydrolase act in concert with ceramide synthase at the ER to convert recently produced S1P back to sphingosine, and subsequently to ceramide. Therefore, the differential virtues of SphKs and S1P production during apoptosis may depend on their subcellular localization.

### 3.4.2   Sphingosine-1-phosphate and cancer

As outlined in chapter 1.1.3, tumor cells are notorious for being opportunistic in utilizing all possible means to escape from physiological cell death. Given the importance of S1P in this regard, it is not surprising that several mutations interfering with its bioregulation were found in tumors. Over-expression of SphK1 as well as reduced expression of S1P-Lyase has been reported recently. In accordance, down-regulation of SphK1 in cancer cells reduced growth and enhanced chemosensitivity (122). This raises the possibility that SphK1 is an oncogene, and represents a suitable target for chemotherapy. Furthermore, both SphK isoforms promote migration of cancer cells towards growth factors, indicating implications in cancer metastasis (123, 124).

The most direct evidence implicating S1P in tumorigenesis emerged from studies investigating its effects on tumor angiogenesis. A monoclonal antibody directed against S1P itself, induced substantial retardation of tumor progression in nude mice xenografted with human breast, ovarian and lung cancer cells (125). Furthermore, the antibody neutralized S1P-stimulated release of pro-angiogenic cytokines like vascular endothelial growth factor (VEGF) and IL-8, as well as VEGF-induced angiogenesis *in vivo*. Although an antibody against S1P might be interesting regarding cancer therapy, its action surely will be broadly unspecific. More specific solutions will be targeting specific S1PRs on the cellular surface. Interestingly, FTY720 reduced primary and metastatic tumor growth in a mouse model by internalization of S1PRs (126). Additionally, or as a prerequisite, it inhibited tumor-associated angiogenesis and increased tumor cell apoptosis. Taken together, highly significant evidence links S1P to tumor growth and angiogenesis. It will be beneficial to understand exactly, how S1P is produced in tumors, and how it transmits signals for promotion of tumor growth. Hopefully, this will result in

identification of drugable targets in the S1P pathway, leading to the development of new anticancer pharmaceuticals.

## 3.5   Aims of this study

Cells entering the route of programmed cell death are recognized and removed by professional phagocytes. The uptake of AC prior to cell membrane disintegration, averts an inflammatory response in the surrounding tissue by preventing contact of neighboring cells with cellular constituents derived from secondary necrosis. During the last decade, it became apparent that suppression of inflammation is an intrinsic feature of apoptotic cell death, achieved furthermore via induction of an anti-inflammatory phenotype in macrophages. Such a macrophage phenotype, also termed M2 polarized, is observed as well in several solid human tumors. Detailed information regarding alternative macrophage activation and its induction by AC is needed to understand how inflammation is regulated. Since this phenomenon may be utilized by human tumors, mechanistic insights will provide targets for tumor therapy.

The first part of my studies dealt with the question whether macrophage survival is influenced by AC. The phenotype alterations in macrophages regarding this topic, as well as the level of interaction between macrophages and AC required to modify macrophage survival, were investigated.

Macrophage survival was induced by liberation of S1P from AC. Thus I performed experiments to elucidate the underlying mechanistic principles. More specifically, I questioned whether classical signals elicited during cell death, such as caspase activation or PS exposure participated in this process. To determine a connection between development of the macrophage phenotype observed in tumors and tumor cell death, I designed a co-culture system of human macrophages with different tumor cell lines. I asked whether macrophages were capable of inducing tumor cell death, and whether this would then induce M2 polarization. Again, a special focus was put on the responsible macrophage/AC interaction.

After exploring the mechanisms that enabled apoptotic tumor cells to induce alternative macrophage polarization, I planned to validate these principal investigations in an *in vivo* tumor xenograft model in nude mice.

Thus, the aims of this study were to identify new characteristics of AC-dependent macrophage polarization. Since macrophage activation by AC is very controversially discussed at present, especially concerning the required signals provided by AC, my studies attempted to provide respective new mechanistic insights. Furthermore, I was interested in investigating whether there was a connection between tumor cell death and pro-tumor macrophage polarization. Again, insights in mechanisms how AC polarize macrophages, will be critical in order to develop therapeutic strategies for the treatment of human diseases depending on inflammation and/or apoptosis.

# 4 Materials and Methods

## 4.1 Materials

### 4.1.1 Chemicals and Reagents

All chemicals were of the highest grade of purity commercially available.

| | |
|---|---|
| 3,3'-Dihexyloxacarbocyanine iodide ($DiOC_6(3)$) | Molecular Probes, Leiden (Netherlands) |
| 4´,6-Diamidino-2-Phenylindol (DAPI) | Sigma-Aldrich Chemie GmbH, Deisenhofen |
| 40% Acrylamide/Bis-acrylamide (37.5% : 1.0% w/v) | Roth GmbH, Karlsruhe |
| 5,5',6,6'-tetrachloro-1,1',3,3'-tetraethyl-benzimidazolylcarbocyanine chloride (JC-1) | Biomol GmbH, Hamburg |
| Accutase | PAA Laboratories GmbH, Cölbe |
| Adenosine triphosphate (ATP) | Roche Diagnostics GmbH, Mannheim |
| Agar-Agar | Roth GmbH, Karlsruhe |
| Agarose | peqLab Biotechnologie GmbH, Erlangen |
| Ammonium chloride ($NH_4Cl$) | Sigma-Aldrich Chemie GmbH, Deisenhofen |
| Ammonium persulfate (APS) | Sigma-Aldrich Chemie GmbH, Deisenhofen |
| Ampicillin | Biomol GmbH, Hamburg |
| Blocking buffer | Rockland Immunochemicals Inc, Gilbertsville (USA) |
| Bovine Serum Albumin (BSA) | Sigma-Aldrich Chemie GmbH, Deisenhofen |
| Brome phenol blue | Fluka GmbH, Buchs |
| Capase-3 substrate (Ac-DEVD-AMC) | Alexis Biochemicals, Grünberg |
| CHAPS | Sigma-Aldrich Chemie GmbH, Deisenhofen |
| Chloroform | Merk Eurolab GmbH, Darmstadt |
| Dimethylsulfoxide (DMSO) | Roth GmbH, Karlsruhe |
| Dithiothreitole (DTT) | Roth GmbH, Karlsruhe |
| Ethanol | Roth GmbH, Karlsruhe |
| Ethylene diamine tetra acetate (EDTA) | Sigma-Aldrich Chemie GmbH, Deisenhofen |
| Ethylene glycol tetra acetate (EGTA) | Sigma-Aldrich Chemie GmbH, Deisenhofen |
| Geneticindisulfate (G418) | Roth GmbH, Karlsruhe |
| Glucose | Roth GmbH, Karlsruhe |

| | |
|---|---|
| Glycerol | Roth GmbH, Karlsruhe |
| Glycine | Serva GmbH, Heidelberg |
| HEPES | Roth GmbH, Karlsruhe |
| Isopropanol | Merck EuroLab GmbH, Darmstadt |
| LB-Broth (Lennox) | Roth GmbH, Karlsruhe |
| L-glutamine | PAA Laboratories GmbH, Cölbe |
| Lymphocyte separation medium (Ficoll) | PAA Laboratories GmbH, Cölbe |
| Magnesium chloride ($MgCl_2$) | Roth GmbH, Karlsruhe |
| Magnesium sulfate ($MgSO_4$) | Roth GmbH, Karlsruhe |
| Methanol (MeOH) | Roth GmbH, Karlsruhe |
| Milk powder | Merck EuroLab GmbH, Darmstadt |
| Neomycin (G 418) | PAA Laboratories GmbH, Cölbe |
| Nonidet P-40 | ICN Biomedicals GmbH, Eschwege |
| Omega(7-nitro-2-1,3-benzoxadiazol-4-yl)-D-*erythro*-Sphingosine (NBD-Sphingosine) | Avanti Polar Lipids, Alabaster (USA) |
| Paraformaldehyde (PFA) | Sigma-Aldrich Chemie GmbH, Deisenhofen |
| Phenylmethylsulphonylfluoride (PMSF) | Sigma-Aldrich Chemie GmbH, Deisenhofen |
| poly(dI-dC) | Pharmacia, Uppsala (Sweden) |
| Potassium chloride (KCl) | Merck EuroLab GmbH, Darmstadt |
| Potassium hydrogen carbonate ($KHCO_3$) | Merck EuroLab GmbH, Darmstadt |
| Potassium hydrogen phosphate ($KH_2PO_4$) | Merck EuroLab GmbH, Darmstadt |
| Protease inhibitor mix | Roche Diagnostics GmbH, Mannheim |
| Roti®-Fect | Roth GmbH, Karlsruhe |
| Semicarbazide | Sigma-Aldrich Chemie GmbH, Deisenhofen |
| Sodium borate | Merck EuroLab GmbH, Darmstadt |
| Sodium chloride (NaCl) | Merck EuroLab GmbH, Darmstadt |
| Sodium fluoride (NaF) | Sigma-Aldrich Chemie GmbH, Deisenhofen |
| Sodium hydrogen phosphate ($Na_2HPO_4$) | Merck EuroLab GmbH, Darmstadt |
| Sucrose | Roth GmbH, Karlsruhe |
| Tetraethylendiamine (TEMED) | Roth GmbH, Karlsruhe |
| Tris-HCl | Roth GmbH, Karlsruhe |
| Triton X-100 | Roth GmbH, Karlsruhe |
| Tryptone | Sigma-Aldrich Chemie GmbH, Deisenhofen |
| Tween 20 | Roth GmbH, Karlsruhe |
| Yeast extract | Life Technologies, Paisley (Scotland) |
| β-glycerophosphate | Sigma-Aldrich Chemie GmbH, Deisenhofen |
| β-mercaptoethanol | Sigma-Aldrich Chemie GmbH, Deisenhofen |

## 4.1.2  Buffers and Solutions

Antibody solution:

| | |
|---|---|
| TBS | 50% (v/v) |
| Blocking Buffer | 50% (v/v) |
| Tween 20 | 0.06% (v/v) |

Blocking solution:

| | |
|---|---|
| Triton X-100 | 0.1% |
| BSA | 3% |
| In PBS | |

10 x blotting buffer:

| | |
|---|---|
| Tris-HCl | 250 mM |
| Glycine | 1.9 M |
| pH | 8.3 |

Buffer D:

| | |
|---|---|
| HEPES/KOH | 20 mM |
| Glycerol | 20% (v/v) |
| KCl | 100 mM |
| EDTA | 0.5 mM |
| Nonidet P-40 | 0.25% (v/v) |
| DTT | 2 mM |
| PMSF | 0.5 mM |
| pH | 7.9 |

Buffer F:

| | |
|---|---|
| Ficoll | 20% (v/v) |
| HEPES/KOH | 100 mM |
| KCl | 300 mM |
| DTT | 10 mM |
| PMSF | 0.5 mM |

pH                                                          7.9


Caspase buffer:

HEPES                                                  100 mM

Sucrose                                                10% (v/v)

CHAPS                                                  0.1% (v/v)

EDTA                                                    1 mM

pH                                                          7.5


EMSA running buffer:

Running buffer (glycerol tolerant)          Amersham      Biosciences      Europe
                                                              GmbH, Freiburg


Fractionation buffer:

Tris-HCl                                                20 mM

EDTA                                                    2 mM

EGTA                                                    5 mM

DTT                                                      1 mM

Protease inhibitor mix                            1 x

pH                                                          7.5


Fixation buffer:

PFA                                                       4% (v/v)

Sucrose                                                10% (v/v)

In PBS


2 x HBS:

HEPES                                                  50 mM

NaCl                                                      280 mM

$Na_2HPO_4$                                         1.5 mM

pH                                                          7.05


Hypotonic cell lysis buffer:

HEPES                                                  10 mM

| MgCl$_2$ | 2 mM |
|---|---|
| EDTA | 100 µM |
| KCl | 10 mM |
| DTT | 1 mM |
| PMSF | 0.5 mM |
| pH | 7.9 |

LB agar:

| Tryptone | 10 g/l |
|---|---|
| Yeast extract | 5 g/l |
| NaCl | 10 g/l |
| Agar-Agar | 15 g/l |

LB medium:

| Tryptone | 10 g/l |
|---|---|
| Yeast extract | 5 g/l |
| NaCl | 10 g/l |

Leucocyte washing buffer:

| EDTA | 2 mM |
|---|---|
| In PBS | |

Lower Tris Buffer:

| Tris/HCl | 1.5 M |
|---|---|
| pH | 8.8 |

Nuclear lysis buffer:

| HEPES | 50 mM |
|---|---|
| KCl | 50 mM |
| NaCl | 300 mM |
| EDTA | 100 µM |
| Glycerol | 10% (v/v) |
| DTT | 1 mM |

| | |
|---|---|
| PMSF | 0.5 mM |
| pH | 7.9 |

p53 lysis buffer:

| | |
|---|---|
| Tris/HCl | 50 mM |
| EDTA | 5 mM |
| NaCl | 150 mM |
| Nonidet P-40 | 150 mM |
| PMSF | 0.5 mM |
| DTT | 1 mM |
| Protease inhibitor mix | 1 x |
| pH | 8.0 |

PBS:

| | |
|---|---|
| NaCl | 137 mM |
| KCl | 2.7 mM |
| $Na_2HPO_4$ | 8.1 mM |
| $KH_2PO_4$ | 1.5 mM |
| pH | 7.4 |

4% PFA for perfusion:

| | |
|---|---|
| PFA | 4% (v/v) |
| Sodium borate | 3.8% (v/v) |
| pH | 9.5 |
| In PBS | |

Potassium phosphate buffer:

| | |
|---|---|
| $KH_2PO_4$ | 1 M |
| pH | 8.5 |

4 x SDS-PAGE sample buffer:

| | |
|---|---|
| Tris/HCl | 125 mM |
| 10% SDS | 2% (v/v) |

| | |
|---|---|
| Glycerol | 20% (v/v) |
| Brome phenole blue | 0.002% (w/v) |
| DTT | 5 mM |
| pH | 6.9 |

SDS separating gel (10%):

| | |
|---|---|
| $H_2O$ distilled | 4.9 ml |
| Lower Tris buffer | 2.5 ml |
| 40% Acrylamide/Bis-acrylamide (37.5% : 1.0% w/v) | 2.5 ml |
| SDS 10% (w/v) | 100 µl |
| Ammonium persulfate 10% (w/v) | 50 µl |
| TEMED | 5 µl |

SDS stacking gel (4%):

| | |
|---|---|
| $H_2O$ distilled | 6.4 ml |
| Upper Tris buffer | 2.5 ml |
| 40% Acrylamide/Bis-acrylamide (37.5% : 1.0% w/v) | 1 ml |
| SDS 10% (w/v) | 100 µl |
| Ammonium persulfate 10% (w/v) | 50 µl |
| TEMED | 5 µl |

10 x SDS running buffer:

| | |
|---|---|
| Tris/HCl | 250 mM |
| Glycine | 1.9 M |
| SDS | 7 mM |
| pH | 7.1 |

SOC medium:

| | |
|---|---|
| Tryptone | 20 g/l |
| Yeast extract | 5 g/l |
| NaCl | 0.5 g/l |
| $MgCl_2$ | 10 mM |

| MgSO$_4$ | 10 mM |
|---|---|
| Glucose | 2 mM |

Sphingosine kinase 2 assay buffer:

| HEPES | 50 mM |
|---|---|
| MgCl$_2$ | 15 mM |
| KCl | 1 M |
| NaF | 10 mM |
| Semicarbazide | 1.5 mM |
| pH | 7.4 |

Sphingosine kinase lysis buffer:

| Tris/HCl | 20 mM |
|---|---|
| Glycerol | 20% (v/v) |
| β-mercaptoethanol | 1 mM |
| EDTA | 1 mM |
| NaF | 15 mM |
| β-glycerophosphate | 40 mM |
| Protease inhibitor mix | 1 x |
| pH | 7.4 |

10 x TBS:

| Tris/HCl | 500 mM |
|---|---|
| NaCl | 1.5 M |
| pH | 7.4 |

5 x Tris borate EDTA buffer (TBE):

| Tris/HCl | 445 mM |
|---|---|
| Sodium borate | 445 mM |
| EDTA | 10 mM |

TE (Trypsin/EDTA):

| Trypsin | 0.5 g/l |
|---|---|
| EDTA | 0.2 g/l |

0.2%/0.1% Triton X-100:

| | |
|---|---|
| Triton X-100 | 0.2%/0.1% |

In PBS


1 x TTBS:

| | |
|---|---|
| TBS | 1 x |
| Tween 20 | 0.06% (v/v) |


Upper Tris Buffer:

| | |
|---|---|
| Tris/HCl | 0.5 M |
| pH | 6.8 |


## 4.1.3  Kits

| | |
|---|---|
| Annexin V-FITC/PI Apoptosis Kit | Coulter-Immunotech GmbH, Hamburg |
| BD Cytometric Bead Array Flex Sets IL-8, IL-10, TNF-α | BD Biosciences, Heidelberg |
| BD Cytometric Bead Array Human Inflammation Kit | BD Biosciences, Heidelberg |
| Cell Line Nucleofector Kit V | Amaxa AG, Cologne |
| HiSpeed Plasmid Maxi Kit | Qiagen GmbH, Hilden |
| QIAprep Spin Miniprep Kit | Qiagen GmbH, Hilden |
| QuickChange XLII Kit | Stratagene GmbH, Amsterdam (Netherlands) |
| Standard DC Protein Assay Kit | Bio-Rad Laboratories GmbH, Munich |
| p*Silencer*™ 4.1-CMV neo Kit | Ambion Inc, Austin (USA) |


## 4.1.4  Antibodies

Primary antibodies:

| | |
|---|---|
| Anti-actin (rabbit, polyclonal) | Sigma-Aldrich Chemie GmbH, Deisenhofen |
| Anti-Bad-Ser136 (rabbit, polyclonal) | Cell Signalling Technology Inc., Beverly (USA) |
| Anti-Bcl-2 (mouse, monoclonal) | BD Transduction Laboratories, Heidelberg |
| Anti-Bcl-$X_L$ (rabbit, polyclonal) | BD Transduction Laboratories, Heidelberg |

| | |
|---|---|
| Anti-Caspase-1 (rabbit, polyclonal) | Cell Signalling Technology Inc., Beverly (USA) |
| Anti-CD31 (rat polyclonal) | BD Transduction Laboratories, Heidelberg |
| Anti-CD44-PE (mouse monoclonal) | Ancell, Bayport (USA) |
| Anti-F4/80 (rat polyclonal) | EBioscience Inc, San Diego (USA) |
| Anti-HA (mouse, monoclonal) | Covance, Richmond (USA) |
| Anti-p50 (rabbit polyclonal) | Santa Cruz Biotechnology, Heidelberg |
| Anti-p65 (rabbit, polyclonal) | Santa Cruz Biotechnology, Heidelberg |
| Anti-S1P1 (rabbit, polyclonal) | Orbigen Inc, San Diego (USA) |
| Anti-SphK1 (rabbit, polyclonal) | Exalpha Biologicals Inc, Maynard (USA) |
| Anti-SphK2 (rabbit, polyclonal) | Exalpha Biologicals Inc, Maynard (USA) |
| Anti-SphK2-C (rabbit, polyclonal) | Abgent Inc, San Diego (USA) |
| Anti-SphK2-N (rabbit, polyclonal) | Abgent Inc, San Diego (USA) |
| Anti-V5 (rabbit, polyclonal) | Abgent Inc, San Diego (USA) |

## Secondary antibodies:

| | |
|---|---|
| IRDye800-labelled anti-mouse | Li-COR Biosciences GmbH, Bad Homburg |
| Alexa Fluor 488-labelled anti-mouse | Invitrogen Corporation, Carlsbad |
| Alexa Fluor 546-labelled anti-rabbit | Invitrogen Corporation, Carlsbad |
| Cy3-labelled anti-rat | Jackson Immunoresearch, West Grove (USA) |
| IRDye680-labelled anti-mouse | Li-COR Biosciences GmbH, Bad Homburg |
| IRDye680-labelled anti-rabbit | Li-COR Biosciences GmbH, Bad Homburg |
| IRDye800-labelled anti-rabbit | Li-COR Biosciences GmbH, Bad Homburg |

## 4.1.5  Media and reagents for cell culture

| | |
|---|---|
| Bovine insulin | Sigma-Aldrich Chemie GmbH, Deisenhofen |
| DMEM high glucose | PAA Laboratories GmbH, Cölbe |
| EMEM | PAA Laboratories GmbH, Cölbe |
| FCS | PAA Laboratories GmbH, Cölbe |
| L-glutamine | PAA Laboratories GmbH, Cölbe |
| Lymphocyte separation medium | PAA Laboratories GmbH, Cölbe |
| Non essential amino acids | PAA Laboratories GmbH, Cölbe |
| PBS (Instamed 9.55 g/ml) | Biochrom AG, Berlin |
| Penicillin/Streptomycin | PAA Laboratories GmbH, Cölbe |
| RPMI 1640 | PAA Laboratories GmbH, Cölbe |
| Sodium pyruvate | PAA Laboratories GmbH, Cölbe |

## 4.1.6  Stimulants and Inhibitors

| | |
|---|---|
| 12-Tetradecanoyl-phorbol-13-acetate (TPA) | Sigma-Aldrich Chemie GmbH, Deisenhofen |
| Ac-YVAD-CMK | Alexis Biochemicals, Grünberg |
| Anti-Fas | Immunotools, Frisoythe |
| Bapta-AM | Molecular Probes, Leiden (Netherlands) |
| Cycloheximide | Sigma-Aldrich Chemie GmbH, Deisenhofen |
| Cytochalasin D | Sigma-Aldrich Chemie GmbH, Deisenhofen |
| Dimethylsphingosine (DMS) | Biomol GmbH, Hamburg |
| Etoposide | Alexis Biochemicals, Grünberg |
| FTY720 | Cayman Chemical, Ann Arbor (USA) |
| Interferon-γ (IFN-γ) | Roche Diagnostics GmbH, Mannheim |
| Lipopolysacharide (LPS) | Sigma-Aldrich Chemie GmbH, Deisenhofen |
| LY294002 | Alexis Biochemicals, Grünberg |
| Lysophosphatidic acid (LPA) | Avanti Polar Lipids, Alabaster (USA) |
| Lysophosphatidylcholine (LPC) | Avanti Polar Lipids, Alabaster (USA) |
| PD98059 | Alexis Biochemicals, Grünberg |
| Platelet activating factor (PAF | Avanti Polar Lipids, Alabaster (USA) |
| Sphingosine-1-phosphate (S1P) | Biomol GmbH, Hamburg |
| Staurosporine (Sts) | Sigma-Aldrich Chemie GmbH, Deisenhofen |
| Tumor necrosis factor-α (TNF-α) | Biomol GmbH, Hamburg |

## 4.1.7  Oligonucleotides

All oligonucleotides were from biomers.net GmbH (Ulm), unless stated otherwise.

**IRD-700 labeled oligonucleotides for EMSA analysis:**
NF-κB  (consensus site in boldface letters) (127) :
5'-GCC AGT TGA **GGG GAC TTT CC**C AGG C-3'
3'-C GGT CAA CT**C CCC TGA AAG G**GT CCG-5'

**Primers for site-directed mutagenesis of SphK2:**
Single base changes in primers compared to wild type SphK2 are indicated with boldface letters.

1) N-terminal caspase-1 cleavage site (D138A):

5'-CGC ACC TTC CGG GCA G**C**T GGG GCC GCC ACC TAC G-3'

5'-C GTA GGT GGC GGC CCC A**G**C TGC CCG GAA GGT GCG-3'


2) C-terminal caspase-1 cleavage site (D552A):

5'-GC CAC CTA GGC GCT G**C**C CTG GTG GCA GCT CCG C-3'

5'-G CGG AGC TGC CAC CAG G**G**C AGC GCC TAG GTG GC-3'


3) Phosphatidylserine binding site (T219A):

5'-C AAC CTC ATC CAG **G**CA GAA CGA CAG AAC CAC G-3'

5'-C GTG GTT CTG TCG TTC TG**C** CTG GAT GAG GTT G-3'


**Sequence specific hairpin siRNA oligonucleotides for SphK2 knock-down:**

5'-GAT CCA CTA AAC AAG CTT GGT ACC TTC AAG AGA GGT ACC AAG CTT GTT TAG TTT A-3'

5'-AGC TTA AAC TAA ACA AGC TTG GTA CCT CTC TTG AAG GTA CCA AGC TTG TTT AGT G-3'


**Sequencing primers for p*Silencer*™ 4.1-CMV neo:**

5'-AGG CGA TTA AGT TGG GTA-3'

5'-CGG TAG GCG TGT ACG GTG-3'


**Specific siRNA:**

Commercially available siRNA against SphK1, SphK2 and caspase-1 was obtained from Qiagen GmbH (Hilden). Sequence information is restricted to the manufacturer. Specificity was assured with siCONTROL non-targeting Duplex #1 from Dharmacon Inc (Lafayette (USA)).

## 4.1.8  Expression plasmids

pRc/CMVbcl2:

Plasmid encodes the Bcl-2 gene, based on the pRc/CMV vector from Invitrogen Corporation (Carlsbad). The vector was established in our lab previously (128).

pmaxGFP:

Expression plasmid for green fluorescent protein (GFP), obtained from Amaxa AG (Cologne).

HA-hSphK2/pCMV5:

The plasmid carries the gene for N-terminally HA-tagged human SphK2 (111), based on the pCMV5 vector. The plasmid was a kind gift from Taro Okada (Kobe University).

V5-mSphK2/pCDNA3.1:

Expression plasmid for murine SphK2 with C-terminal V5-tag (108), based on the pcDNA3 vector from Invitrogen Corporation (Carlsbad). The plasmid was a kind gift from Sarah Spiegel (Virginia Commonwealth University, Richmond).

p*Silencer*™ 4.1-CMV neo:

The plasmid is designed to knock-down specific genes via insertion of hairpin siRNA. It was obtained from Ambion Inc, Austin (USA). Expression is driven by a CMV promoter. The plasmid also carries the gene for resistance against the selection marker neomycin.

## 4.1.9  Cell lines and bacteria

XL1-Blue super competent bacteria from Stratagene GmbH, Amsterdam
Genotype: recA1 endA1 gyrA96 thi-1 hsdR17 supE44 relA1 lac [F´ proAB lacIqZ.M15 Tn10(Tetr)].

Primary human monocytes:

Primary human monocytes were isolated from Buffy Coats, which were obtained from DRK-Blutspendedienst Baden-Württemberg-Hessen, Frankfurt.

Jurkat T cells:

Jurkat T cells are derived from a 14 year old boy with acute lymphatic leukemia (ALL). This T cell line was established in 1977 (129).

HEK293 cells:

HEK 293 cells were generated by transformation of human embryonic kidney cell cultures with sheared adenovirus 5 DNA, and were first described in 1977 (130).

MCF-7 cells:

MCF-7 human breast adenocarcinoma cells were established from the pleural effusion of a 69-year-old Caucasian woman with metastatic mammary carcinoma (after radio- and hormone therapy) in 1970 (131).

THP-1 cells:

THP-1 human monocytes were obtained from the peripheral blood of a 1-year-old boy with acute monocytic leukemia (AML) at relapse in 1978 (132).

RKO cells:

The RKO cell line is a poorly differentiated colon carcinoma cell line, which was developed by Michael Brattain in 1984 (133).

RAW 264.7 cells:

RAW 264.7 mouse monocytes/macrophages were established from ascites of a tumor induced in a male mouse by intraperitoneal injection of Abselon Leukaemia Virus (A-MuLV) in 1977 (134).

Colo 201 cells:

Colo 201 human colon adenocarcinoma cells are derived from ascitic fluid of a 70 year old Caucasian male with carcinoma of the colon (135).

HepG2 cells:

HepG2 hepatocellular carcinoma cells were established from a 15 year old Caucasian male in 1980 (136).

NIH 3T3 cells:

NIH 3T3 mouse fibroblasts were established from a NIH Swiss mouse embryo in 1969 (137).

A549 cells:

A549 lung carcinoma cells are derived from a 58 year old Caucasian male (138).

Caco-2 cells:

Caco-2 colon adenocarcinoma cells were isolated from a primary colonic tumor in a 72-year-old Caucasian male in 1977 (139).

## 4.1.10 Mice

MCF-7 xenograft models were accomplished with seven-week-old NMRI-*nu/nu* female mice obtained from Harlan Winkelmann GmbH, Borchen. These experiments were performed in close cooperation with the Institute of Clinical Pharmacology, especially with Dr. Susanne Schiffmann. The Institute of Clinical Pharmacology bought the mice and cared for approval by the local Ethics Committee for Animal Research.

## 4.1.11 Instruments

| | |
|---|---|
| Autoclave HV 85 | BPW GmbH, Süssen |
| B250 Sonifier | Branson Ultrasonics, Danbury (USA) |
| Bacteria clean bench UVUB 1200 | Uniequip GmbH, Martinsried |
| Bacteria incubator B5042 | Heraeus GmbH, Hanau |
| CASY® | Schärfe System, Reutlingen |
| Centrifuge 5415 R | Eppendorf GmbH, Hamburg |

| | |
|---|---|
| Centrifuge CR 3.22 | Jouan GmbH, Unterhaching |
| Centrifuge MR 23i | Jouan GmbH, Unterhaching |
| Centrifuge ZK380 | Hermle GmbH, Wehingen |
| Cryotome Jung CM 3000 | Leica Microsystems, Bensheim |
| FACSCanto flow cytometer | BD Biosciences GmbH, Heidelberg |
| Fluorescence microscope Axiovert 200M | Carl Zeiss MicroImaging Inc, Göttingen |
| Holten LaminAir clean bench | Jouan GmbH, Unterhaching |
| IG 150 (cell culture incubator) | Jouan GmbH, Unterhaching |
| LabLine Orbit Shaker | Uniequip GmbH, Martinsried |
| Magnetic stirrer Combimag RCH | IKA Labortechnik GmbH & Co. KG, Staufen |
| Mastercycler Thermocycler | Eppendorf GmbH, Hamburg |
| Mini-PROTEAN 3 System (SDS-PAGE) | Bio-Rad Laboratories GmbH, München |
| Mithras LB940 multimode reader | Berthold Technologies, Bad Wildbad |
| NanoDrop ND-1000 | Peqlab Biotechnologie GmbH, Erlangen |
| Nucleofector | Amaxa AG, Cologne |
| Odyssey infrared imaging system | Li-COR Biosciences GmbH, Bad Homburg |
| Pipettes (10 µl, 100 µl, 1.000 µl) | Eppendorf GmbH, Hamburg |
| Plastic material (cell culture) | Greiner Bio-One GmbH, Frickenhausen |
| Pure water system Purelab Plus | ELGA LabWater GmbH, Siershahn |
| Sub-Cell® GT electrophoresis system | Bio-Rad Laboratories GmbH, München |
| Thermomixer 5436 | Eppendorf GmbH, Hamburg |
| Trans-Blot SD blotting machine | Bio-Rad Laboratories GmbH, München |
| Ultra-Sonifier | MSE, Loughborough (England) |
| UV-Transilluminator gel documentation system | Raytest GmbH, Straubenhardt |

## 4.1.12 Software

| | |
|---|---|
| Aida Image Analyzer v 3.11 | Raytest GmbH, Straubenhardt |
| AxioVision Software | Carl Zeiss MicroImaging Inc, Göttingen |
| BD FACSDiva[TM] Software | BD Biosciences GmbH, Heidelberg |
| FCAP Array v 1.0.1 | Soft Flow, Burnsville (USA) |
| MikroWin 2000 | Berthold Technologies Bad Wildbad |
| Peptide Cutter | Freeware on the www |
| WoLF PSORT | Freeware on the www |

## 4.2  Methods

### 4.2.1  Cell culture

RAW 264.7 mouse monocytes/macrophages, THP-1 human monocytes, Jurkat T cells, MCF-7 breast carcinoma cells, Colo 201 human colon adenocarcinoma cells and Hep-G2 hepatocellular carcinoma cells were maintained in Roswell Park Memorial Institute (RPMI) 1640. HEK293 embryonal kidney, RKO colon carcinoma cells and NIH 3T3 mouse fibroblasts were cultured in Dulbecco's modified eagle medium (DMEM) with 4.5 g/l D-glucose, A549 lung carcinoma cells in DMEM/Ham's F12 and Caco-2 colon adenocarcinoma in Earle's minimal essential medium (EMEM). All media were supplemented with 5 mM glutamine, 100 U/ml penicillin, 100 µg/ml streptomycin and 10% heat-inactivated FCS. HEK293 medium also contained 1 mM sodium pyruvate, Caco-2 medium contained 1 x non essential amino acids and MCF-7 medium was supplemented with 1mM sodium pyruvate, 1 x non essential amino acids and 10 µg/ml bovine insulin. Cells were kept in a humidified atmosphere of 5% $CO_2$ in air at 37°C and were transferred twice a week.

### 4.2.2  Human monocyte isolation and culture

Human monocytes were isolated essentially as described (140). In brief, monocytes were isolated from buffy coats (DRK-Blutspendedienst Baden-Württemberg-Hessen, Institut für Transfusionsmedizin und Immunhämatologie Frankfurt am Main, Frankfurt, Germany) using Ficoll-Hypaque gradients. 50 ml Falcon tubes were layered with 15 ml lymphocyte separation medium, blood cells were added, followed by density gradient centrifugation (1000 x g, 10 min, RT). Peripheral blood mononuclear cells (PBMCs) were collected, washed twice with PBS and were allowed to adhere to culture dishes (Primaria 3072, BD Becton Dickinson GmbH, Heidelberg) for 1 h at 37°C. Non-adherent cells were removed. Monocytes we re then differentiated into macrophages with RPMI 1640 containing 10% AB-positive human serum for 7 days.

### 4.2.3   Induction of apoptosis and necrosis

For the generation of apoptotic cells (AC), cells were cultured in appropriate medium (4.2.1) without FCS. Apoptosis in macrophages was generally induced in full medium (141). Inhibitors were added 2 h prior to cell death induction. Stimulus concentrations are listed in Table 1. Subsequently, AC were washed twice prior to the addition to macrophages. Necrosis was induced by heating Jurkat cells for 30 min at 56°C (77). Cell death was quantified by flow cytometry after staining with annexin-V and propidium iodide (4.2.6). Agonist concentrations and incubation times were chosen to provoke roughly 80% apoptotic cell death.

Table 1: Induction of apoptosis

| **Cell line** | **Stimulus** | **Concentration** |
|---|---|---|
| Human primary macrophages | TNF-α/CHX | 10 ng/ml/10 µg/ml |
| THP-1 monocyte-derived macrophages | Etopopside | 250µM |
| RAW 264.7 | Etoposide | 250 µM |
| Jurkat | Staurosporine | 0.5 µg/ml |
|  | Anti-Fas | 0.05 ng/ml |
|  | Etoposide | 100 µM |
| RKO | Staurosporine | 0.5 µg/ml |
| MCF-7 | Staurosporine | 0.5 µg/ml |
| HEK293 | Staurosporine | 0.5 µg/ml |
|  | TNF-α/CHX | 50 ng/ml/10 µg/ml |
| NIH 3T3 | Staurosporine | 0.5 µg/ml |

### 4.2.4   Production and characterization of conditioned media

To produce apoptotic cell conditioned medium (ACM), cells were washed twice with PBS subsequent to apoptosis-induction, followed by an incubation

for another 4 h in appropriate medium (4.2.1) with 10% FCS. ACM was harvested by centrifugation (13.000 x g, 5 min) and filtration through 0.2 µm pore filters, to remove apoptotic bodies (35, 142). Conditioned media from necrotic (NCM) or viable (VCM) cells were prepared respectively. Two different protocols were used for protein degradation in conditioned media. First, for heat inactivation, media were heated at 100°C for 1 h. Second, enzyme digestion was carried out with 50 µg/ml proteinase K or 0.1% trypsin at 37°C for 1 h. Afterwards, enzymes were inactivated by heat treatment and/or the use of excess soybean trypsin inhibitor. Extraction of lipids was performed with 1 volume of chloroform and was repeated at least twice (35). Specific extraction of S1P was performed essentially as described (143). In brief, a two step partitioning protocol with chloroform/methanol/HCL (100:200:1) was used, first in alkaline conditions followed by re-extraction under acidic conditions. The acidic organic phase was evaporated to dryness and the lipid extract was resolved in PBS containing 0.4% fatty acid free BSA for cell culture, or ethanol for quantitative analysis, for 30 min at 37°C, followed by sonication for 10 sec. Macrophages were generally exposed to conditioned media for 16 h. Inhibitors were added 2 h prior to conditioned medium.

## 4.2.5  Co-culture experiments

Different co-culture set-ups with THP-1 monocyte-derived macrophages or primary human macrophages were performed. THP-1 cells were differentiated to macrophages at a density of $2x10^5$ cells/ml, with 50 nM TPA for 24 h. TPA was removed by washing and the cells were cultured for another 24 h without TPA. Apoptotic, necrotic or viable cells were added at a ratio of 1:5. Co-cultures were maintained for 16 h at 37°C. Afterwards residual AC were washed off. Conditioned media from co-cultures were produced as described in 4.2.4. In one set of experiments, transwell inserts (Greiner Bio-One GmbH, Frickenhausen) were used to ensure spatial separation between macrophages and AC (144). Primary human monocyte-derived macrophages were cultured at a density of $2x10^5$ cells/ml. Following differentiation, tumor cells were added at the same density. Co-cultures were maintained for 5

days. Subsequently, residual tumor cells were removed from the plates by incubations with accutase (145) for 5 min, which left adherence of macrophages unaltered. Remaining macrophages were treated with 1 µg/ml LPS and 100 U/ml IFN-γ or exposed for a second time to equal amounts of tumor cells. In some experiments, higher ratios of tumor cells compared to macrophages were used, as indicated.

### 4.2.6  Quantification of cell death

To distinguish apoptosis from necrosis, the annexin V-FITC/propidium iodide (PI) apoptosis kit was used. Annexin V-FITC (extinction: 492 nm; emission: 520 nm) binds to PS on the surface of apoptotic and necrotic cells, but the DNA intercalating dye PI (extinction: 550 nm; emission: 617 nm) only enters a cell when its cell membrane integrity is lost during necrosis. Cells were harvested by centrifugation (500 x g, 5 min, 4℃) a nd resolved in 500 µl 1 x binding buffer. Annexin V-FITC (5 µl) and PI (2 µl) where added and the cell solution was incubated on ice for 10 min, protected from direct light exposure. The measurement of annexin V-FITC and/or PI positive cells was performed with the FACSCanto flow cytometer and the BD Cell Quest Pro Software. To quantify cell death at the level of the mitochondria, the mitochondrial dye JC-1 was used. JC-1 stains mitochondria in living cells in a membrane potential ($\Delta\Psi$)-dependent fashion. JC-1 monomer is in equilibrium with so called J-aggregates, which are favored at higher mitochondrial membrane potential. The monomer JC-1 has green fluorescence (emission: 527 nm), while the J-aggregates have red fluorescence (emission: 590 nm). In AC, the dye stays in the cytoplasm and fluoresces green, while in healthy cells, the dye aggregates in the mitochondria and fluoresces red (146). Cells were harvested, resolved in PBS, 1 µM JC-1 was added, and cells were kept on ice for 20 min prior to analysis via flow cytometry. Alternatively, $DIOC_6(3)$, a positively charged dye (emission: 501 nm), which accumulates selectively in the mitochondria, was used to monitor the mitochondrial membrane potential ($\Delta\Psi$). Cell suspensions were incubated with 40 nM $DIOC_6(3)$ for 30 min on ice, followed by analysis using the FACSCanto flow cytometer.

### 4.2.7 Cell death quantification in co-cultures

Co-cultures of human macrophages and tumor cells were harvested after 12, 24 or 48 h by incubation with accutase for 30 min, which removed both macrophages and tumor cells. Cell death was quantified by flow cytometry after incubations with a monoclonal human CD44 antibody coupled to phycoerythrin (PE), to discriminate between macrophages and tumor cells, followed by the annexin V-FITC method (4.2.6) to detect cell death. In detail, quantification of macrophage vs. tumor cell contents in co-cultures was performed using α-CD44-PE (extinction 530 nm; emission: 565 nm). The macrophage population was identified by staining control macrophages, thereby gating on this population, which was used to identify macrophages in co-cultures. All remaining cell counts were attributed to tumor cells.

### 4.2.8 Caspase activity assays

Caspase-3 or -1 activity was quantified following the cleavage of specific substrates as described (147). Briefly, cells were lysed in 200 µl caspase buffer, sonicated for 10 sec, followed by centrifugation (15000 x g, 10 min, 4°C). After that, the protein concentration in the supernatant was determined with the Lowry method (4.2.9). 30 µg protein were filled up to 140 µl with caspase buffer and mixed with 10 µl caspase substrate (200 µM Ac-DEVD-AMC for caspase-3 or 1 mM Ac-YVAD-AMC for caspase-1) in 96 well plates. The cleavage of the caspase substrate was followed for 1 h at 30°C with measurements being performed every 2 min on the Mithras LB 940 multimode reader (extinction: 360 nm; emission: 465 nm). Caspase activities were calculated as substrate cleavage per minute relative to controls using the MikroWin 2000 software.

### 4.2.9 Protein determination (Lowry method)

The protein content of cell lysates was determined using the DC Protein Assay kit, based on the Lowry method (148). Briefly, a standard dilution series of BSA in $H_2O$ was prepared (0.625 to 10 mg/ml). Samples as well as standards (2 µl) were pipetted in duplicates into a 96-well plate, 20 µl solution

A were added, and then the colorimetric reaction was started by addition of 160 µl solution B. After incubation for 15 min (RT with shaking), extinction was measured at 750 nm using the Mithras LB 940 multimode reader.

### 4.2.10 SDS-PAGE and Western blot analysis

For Western blot analysis, cells were incubated as indicated in the individual experiments, scraped off, lysed in 200 µl p-53 lysis buffer and sonicated for 3 sec. Lysates were incubated on ice for 30 min and vortexed each 10 min for 10 sec, followed by centrifugation (15000 x g, 30 min, 4°C). Subsequently, protein concentrations were determined with the Lowry method (4.2.9). 80 µg protein and 10 µl 4 x SDS-PAGE sample buffer (4.1.2) were mixed, filled up to 40 µl with $H_2O$, denatured at 100°C for 10 min and put on ice immediately for 2 min. Proteins were resolved on 10% SDS polyacrylamide gels (4.1.2) with 1 x SDS running buffer (4.1.2). After that, proteins were blotted onto a nitrocellulose membrane using a semi-dry transfer cell. Unspecific binding was blocked with 5% milk in TBS (4.1.2) for 1h, followed by washing with TTBS for 10 min. Primary antibody was added in antibody solution (4.1.2) and incubated overnight at 4°C. Membranes were washed three for 10 min each with TTBS. For protein detection, blots were incubated with an appropriate (anti-rabbit or anti-mouse) secondary near infrared dye (IRDye) conjugated antibody (4.1.4) in antibody solution for 1 h. Thereafter, membranes were washed 3 times for 10 min with TTBS, followed by detection of specific proteins using the Odyssey infrared imaging system. Specific protein expression was quantified compared to actin expression using the Odyssey infrared imaging system or AIDA software.

### 4.2.11 Cellular fractionation

Cellular fractions were obtained by lysis of cell pellets in fractionation buffer (4.1.2) followed by incubation on ice for 1 h, with regular vortexing. Lysates were passed 40 times through 25-gauge needles. Nuclei were pelleted by centrifugation (300 x g, 10 min, 4°C), supernatants were removed and the

membrane fraction was obtained by centrifugation at 16.000 x g (30 min, 4°C). Supernatant was used as the cytosolic fractio n.

## 4.2.12 Electrophoretic mobility shift assays (EMSA)

An established EMSA method, with slight modifications, was used (149). 5 x $10^6$ cells were suspended in 200 µl ice cold hypotonic cell lysis buffer (4.1.2) and incubated on ice for 10 min. Nuclei were collected (500 x g, 30 min, 4°C), resolved in 50 µl nuclear lysis buffer, incubated on ice for 20 min and pelleted (12000 x g, 20 min, 4°C). Protein content in the su pernatant was determined using the Lowry method (4.2.9.). Nuclear protein (20 µg) was incubated for 30 min at room temperature with 2 µg poly(dl-dC), 2 µl buffer D (4.1.2), 4 µl buffer F (4.1.2), and 250 fmol 5'-IRD700-labelled oligonucleotide in a final volume of 20 µl. Specific p65 and p50 supershift antibodies (2 µg) were added as indicated. DNA–protein complexes were resolved at 200 V for 2 h using native 4% polyacrylamide gels, and visualized with the Odyssey infrared imaging system. Supershift analysis was performed with α-p65 and α-p50 from Santa Cruz Biotechnology (Heidelberg, Germany). The latter antibody is known to attenuate the protein-DNA interaction rather than causing a classical supershift (150).

## 4.2.13 Quantification of cytokine release from co-cultures

For the measurement of cytokine contents in the supernatants of human primary macrophages from co-cultures with tumor cells, BD CBA Flex Sets or the CBA Human Inflammation Kit were used. In brief, 50 µl supernatant were incubated with beads, coated with antibodies against TNF-α, IL-10, IL-8 or IL-12-p70 and a PE-labeled detection reagent for 3 h. The samples were acquired with the FACSCanto flow cytometer and analyzed with the FCAP Array software. The performance matched the specifications of the manufacturer. Minimal detection limits were 1.9 pg/ml for TNF-α, 3.8 pg/ml for IL-10, 4.9 pg/ml for IL-8 and 4.8 pg/ml for IL-12-p70. Routinely, medium from co-culture set-ups were changed every 24 h. Thus, cytokine production reflects a sampling period corresponding to the last 24 h of the co-culture,

only. If not stated otherwise, co-cultures lasted for 5 days with changing the medium every 24 h.

## 4.2.14 Down-regulation of S1PR1

Internalization of S1PR1 was induced as described (116). Briefly, primary human macrophages were incubated with 100 nM FTY720, an agonist inducing internalization upon binding, for 1 h. After that, cells were washed twice with PBS, cultured for another 48 h and used for further experiments. S1PR1 down-regulation was controlled by Western blotting compared to un-stimulated controls.

## 4.2.15 S1P quantification in cell culture supernatants

S1P quantification using liquid chromatography-tandem mass spectrometry (LC-MS/MS) analysis, was performed in the Institute of Clinical Pharmacology by Helmut Schmidt (151). Therefore, cells were cultured in medium devoid of FCS, prior to stimulation. Alternatively, the medium in co-cultures of human macrophages and MCF-7 cells was replaced by medium free of FCS after 24 h. Co-cultures were maintained for another 24 h and supernatants were harvested. Afterwards, lipids were extracted from supernatants of cell cultures with chloroform/HCl (50:1) after addition of the internal standard C17-sphingosine-1-phosphate (C17-S1P). Extraction was repeated three times to achieve maximum recovery. The combined organic phases were evaporated to dryness and resolved in ethanol for quantification. After liquid-liquid extraction, concentrations of S1P and the internal standard were determined by liquid chromatography coupled to tandem mass spectrometry. HPLC analysis was done under gradient conditions using a Luna C18 column (150 cm x 2 mm ID, 5 μm particle size and 100 Å pore size, Phenomenex, Aschaffenburg). MS/MS analyses were performed on a 4000 Q TRAP triple quadrupole mass spectrometer with a TurboIonSpray source (Applied Biosystems, Darmstadt). Precursor-to-product ion transitions of m/z 380→82 for S1P and 366→250 for C17-S1P were used for the Multiple Reaction Monitoring (MRM). Concentrations of the calibration standards, quality

controls and unknowns were evaluated by Analyst software 1.4 (Applied Biosystems, Darmstadt). Linearity of the calibration curve was proven from 1 to 250 ng/ml. The coefficient of correlation for all measured sequences was at least 0.99. The lower limit of quantification (LLOQ) was 0.5 ng/ml. Variations in accuracy and intra-day and inter-day precision (n = 6 for each concentration, respectively) were <15% over the range of calibration.

## 4.2.16  Sphingosine kinase activity assay

Activity of sphingosine kinase 2 was followed as phosphorylation of NBD-sphingosine to NBD-S1P. An established protocol with slight modifications was used (152). For preparation of whole cell lysates, cells were harvested, washed with ice cold PBS and solved in 100 µl ice cold sphingosine kinase lysis buffer. Subsequently, lysates were sonicated for 5 sec, followed by centrifugation (1600 x g, 30 min, 4℃). 10 µl of th e supernatant or 15 µl cell culture supernatants were then added to 100 µl sphingosine kinase assay buffer, together with 10 µM NBD-Sphingosine and 1 mM ATP, for 1 h at 30℃. The proximate addition of 1 volume alkaline potassium phosphate buffer, followed by chloroform/methanol (500 µl, 2:1) extraction ensured separation of the substrate (NBD-Sphingosine) to the lipid phase and of the product (NBD-S1P) to the aqueous phase. 100 µl of the aqueous phase were then analyzed for NBD-S1P-dependent fluorescence (extinction: 485 nm, emission: 538 nm) in the Mithras LB 940 multimode reader.

## 4.2.17  Transformation of bacteria by the heat shock protocol

XL1-Blue supercompetent bacteria were transformed using the heat shock protocol. For this purpose, bacteria were thawed on ice, and 100 ng of plasmid DNA or specific reaction templates were added. After gentle mixing by pipetting up and down, cells were incubated on ice for 30 min. After a heat shock (45 sec, 42℃), they were kept on ice for 2 m in. Then, 400 µl of SOC medium were added to the cells, followed by incubation for 60 min at 37℃ with continuous shaking. To select transformed bacteria, 200 µl of the cultures were inoculated on ampicillin-containing (100 µg/ml) LB agar plates. Single

clones were picked, cultured overnight at 37℃, and subsequently used for plasmid preparation.

## 4.2.18 Bacterial culture and plasmid preparation

For preparation of plasmids, 2 ml LB medium with bacteria containing the required plasmid, were transferred to 400 ml LB medium (100 µg/ml ampicillin) and grown at 37℃ overnight. The isolation of the plasmid from bacteria was performed using the HiSpeed Plasmid Maxi Kit. In detail, after pelting the bacteria by centrifugation (6000 x g, 15 min, 4℃), the pellets were resuspended in 10 ml buffer P1. Then, buffer P2 (10 ml) was added and the suspension was mixed gently but thoroughly, by inverting 5 times, followed by 5 min incubation at RT. Thereafter, 10 ml chilled buffer P3 were added, immediately mixed and the lysate was transferred to a QIAfilter cartridge, where it was incubated for 10 min at RT. Subsequently, the lysate was filtered into a previously equilibrated (with 10 ml buffer QBT) HiSpeed Maxi Tip and the filters were washed using 60 ml buffer QC. Then, the DNA was eluted using 15 ml buffer QF and precipitated by addition of 10.5 ml isopropanol (5 min, RT). The precipitation reaction was filtered through the QIAprecipitator Maxi Module applying constant pressure. The bound DNA was washed with 70% ethanol, followed by drying and elution with 1 ml $H_2O$. The resulting DNA content was quantified using the NanoDrop ND-1000.

## 4.2.19 Site-directed mutagenesis

Site-directed mutagenesis for generation of point mutations in SphK2, was performed using the QuickChange XLII kit. The HA-hSphK2/pCMV5 construct was used as a template (4.1.8). Oligonucleotides were designed according to the manufacturer's specifications. 10 ng of the vector was mixed with the specific oligonucleotides (4.1.7) in reaction buffer, followed by addition of *PfuTurbo* DNA polymerase. An initial denaturation step was performed at 95℃ for 1 min, followed by 18 cycles at 95℃ for 5 0 s, annealing at 60℃ for 50 s, and extension at 68℃ for 7 min. A final exte nsion phase was performed at 68℃ for 7 min. Next, the nonmutated parental DN A template was digested

with 10 U DpnI (37℃, 1 h) and the mutated plasmids were transfected into XL1-Blue supercompetent bacteria using the heat shock method (4.2.17). Positive clones were selected and plasmid DNA was extracted using the QIAprep Spin Miniprep Kit. Correct sequence of the generated vectors was verified by sequencing, performed by AGOWA GmbH (Berlin), with pCMV5 specific primers.

## 4.2.20  Transfection of eukaryotic cells

MCF-7 cells and Jurkat cells were transfected with the respective plasmids or siRNA using Cell Line Nucleofector Kit V on the Nucleofector. The required amount of cells was harvested by centrifugation. Then the cells were resolved in Nucleofector solution and mixed with 2 µg plasmid or siRNA. The mixtures were transferred to an appropriate cuvette, which where transferred to the Nucleofector. After nucleofection, cells were seeded in 6 well plates in 1 ml full medium and incubated for 48 h, prior to use in individual experiments. HEK 293 cells were transiently transfected by $CaPO_4$-precipitation. In detail, $H_2O$, $CaCl_2$ and the 2 µg of plasmid were mixed. 2 x HBS (4.1.2) was added, followed by vigorous vortexing. The resulting mix was incubated for 20 min at room temperature, to allow precipitation. Subsequently, an appropriate amount of mix was added to cells, which then were incubated at 37℃ for 24 h. Medium was changed prior to the experiments. For transfection of NIH 3T3 cells, 2 µg plasmid were mixed with 100 µl medium devoid of antibiotics, and 10 µl Roti®-Fect, in 100 µl medium without antibiotics and serum, were added. The solution was mixed by pipetting up and down, followed by incubation for 30 min at RT. The mixture was added to cells in medium devoid of antibiotics for 6 h at 37℃. Then, medium was re placed by full medium and cells were used for experiments after further incubation at 37℃ for 20 h. Transfection efficiencies were measured by default via control transfection with pmaxGFP (4.1.8) and subsequent analysis of GFP expression using fluorescence microscopy. Overexpression or knock-down of proteins was controlled by Western blot analysis (4.2.10). Specificity of siRNA knock-down was ensured by control transfection with siCONTROL non-targeting siRNA (4.1.7).

## 4.2.21 Stable SphK2 knock-down

For SphK2 knock-down, sequence specific siRNA oligonucleotides, designed following the guidelines of Ambion's siRNA design tool on their website (4.1.7), were ligated into the p*Silencer*<sup>TM</sup> 4.1-CMV neo vector (4.1.8). Oligonucleotides were annealed in DNA Annealing solution provided with the vector construction kit to obtain annealed hairpin siRNA at a concentration of 8 ng/µl. 1 µl annealed siRNA insert was mixed with 1 µl DNA Annealing Solution, 6 µl Nuclease-free water, 1 µl 10X T4 DNA Ligase Buffer, 1 µl p*Silencer* 4.1-CMV neo vector and 1 µl T4 DNA ligase (5 U/µl). Ligation was performed for 1 h at 22°C. pSilencer-siSphK2 was then transformed into bacteria using the heat shock protocol (4.2.17). Plasmids were amplified, extracted from bacteria (4.2.18) and were sequenced using specific primers (4.1.7) to verify efficient ligation. pSilencer-siSphK2 was transfected into MCF-7 cells using Nucleofector technology (4.2.20). Stability of transfection was ensured by keeping MCF-7-siSphK2 cells under selective pressure using 500 µg/ml of Neomycin (G418) during cell culture. Efficient knock-down was verified by Western blot analysis (4.2.10).

## 4.2.22 Immunofluorescence staining

HEK293 cells were seeded directly onto a slide, and transiently transfected by CaPO$_4$-precipitation (4.2.20) with HA-SphK2 or the mutated constructs. After transfection, cells were used for experiments and treated as indicated. Cells were incubated for 1 h at RT in fixation buffer, followed by permeabilization for 20 min in 0.2% Triton X-100. After that, cells were incubated for 2 h with a mouse anti-HA antibody and rabbit anti-caspase-1 antibody followed by washing thrice with PBS. Secondary antibodies (2 h) were goat α-rabbit labeled with Alexa Fluor 546 and goat α-mouse labeled with Alexa Fluor 488. Cells were counterstained with DAPI (1 µg/ml in PBS for 15 min). After a final 5-min washing step in PBS, cells were covered with Vectashield mounting medium and a cover slip. Localization of wild type and mutated HA-SphK2 as well as caspase-1 was analyzed using the AxioScope fluorescence microscope with the ApoTome upgrade (lens 63./0.6 NA; ocular 10) at room temperature, documented by a charge-coupled device camera and the

AxioVision Software. Alternatively, tumor cryosections were analyzed. Slides were washed with PBS for 5 min at RT, incubated in 0.1% Triton X-100 for another 5 min, followed by incubation for 1 h in blocking solution at RT. After that, slides were incubated overnight with rat anti-CD31 or rat anti-F4/80 antibody in blocking solution, washed thrice with PBS, followed by incubation with a Cy3-labelled anti-rat antibody in blocking solution for 2 h. Nuclei were counterstained with DAPI for 15 min, washed for 5-min in PBS and slides were covered with Vectashield mounting medium and a cover slip prior to fluorescence imaging.

### 4.2.23 Tumor growth in nude mice

Seven-week-old NMRI-*nu/nu* female mice were used (4.1.10). MCF-7 (n = 8) or MCF-7-siSphK2 cells (n = 6) (suspended in cell culture medium devoid of antibiotics) were injected subcutaneously at the right and left dorsal flank ($1{\times}10^7$ cells per mouse). The mice received 10 mg/kg estradiolvalerate i.m. one week before tumor cell injection, followed by further weekly estradiolvalverate-injection. The tumor volume was assessed three times a week with the calliper rule, as soon as control tumors started growing. Tumor volume was calculated according to the following formula: $V = (a \times b)^2/2$ (V = tumor volume, a = length, b = breadth). After three weeks, mice were killed, followed by perfusion. In detail, mice were anesthetized and the thoracic cavity was opened to expose the heart. An 18-gauge needle, connected to a pump, was inserted into the left ventricle, followed by opening of the right atrium. Mice were perfused with approximately 50 ml PBS (RT), followed by perfusion with 50 ml ice cold 4% PFA. Afterwards, tumors were removed, fixed in 4% PFA overnight at 4°C, followed by a further overnight incubation in 30% sucrose (4%) for cryoprotection. Fixed tumors were stored at -80°C and 8 µm cryosections were prepared using the Jung CM 3000 cryotome. Macrophage infiltration (F4/80), as well as blood vessel formation (CD31), was then monitored in tumor cryosections by immunofluorescence staining (4.2.22). In all experiments the ethics guidelines for investigations in conscious animals were obeyed and the experiments were approved by the local Ethics Committee for Animal Research.

### 4.2.24 Statistical analysis

For Western analysis one representative experiment is displayed. *p*-values were calculated using one-factor ANOVA or a two-tailed Student's t-test modified by Bonferroni's multiple comparison test. Differences were regarded as significant for $p < 0.05$, unless indicated otherwise.

# 5 Results

## 5.1 Macrophages cheat death after interaction with apoptotic cells

Macrophages exert key functions in termination of inflammation, at least in part due to their interaction with AC. Therefore it should be warranted, that their immunosuppressive and curative properties carry on during the whole process of tissue regeneration, e.g. in wound healing. One vital means to provide this security is resistance against cell death, as potentially harmful substances are aboard especially during inflammation. The first question I addressed was whether AC influence macrophage resistance against inducers of cell death or not.
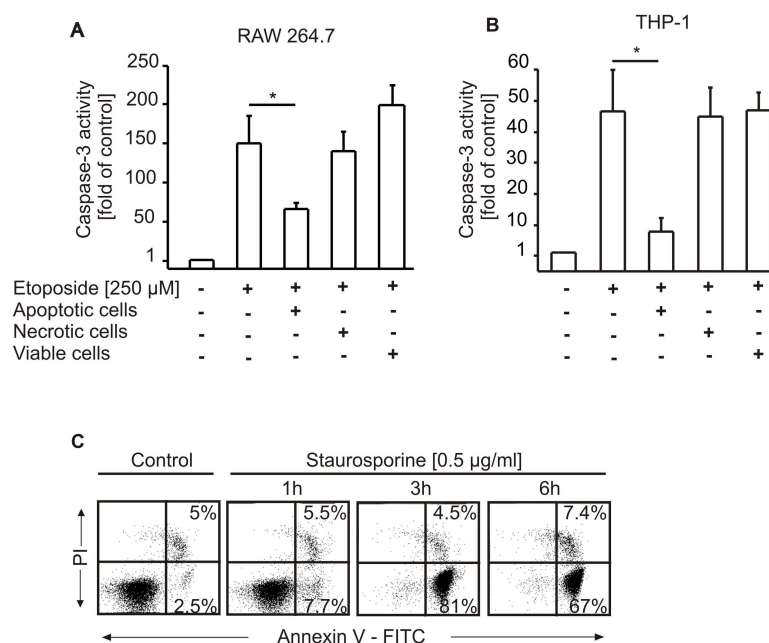


Figure 7: AC attenuate caspase-3 activation in murine and human macrophages. Caspase-3 activity in (A) murine RAW 264.7 macrophages and (B) human monocyte-derived THP-1 macrophages normalized to untreated control cells. Macrophages were pre-treated with AC, NC, VC or remained as controls for 16 h. Cell death was induced for 8 h with 250 µM etoposide. Data are presented as the mean ± SD from three independent experiments. Differences between untreated and AC-treated cells are statistically significant ($p < 0.05$). (C) Apoptosis in Jurkat cells induced with 0.5 µg/ml staurosporine followed by annexin-V/PI staining after 1, 3 and 6 h. Parameters were assessed by flow cytometry.

### 5.1.1 Macrophage protection against apoptosis by apoptotic cells

The first approach to determine the impact of AC in protection of macrophages from apoptosis was incubation of RAW 264.7 mouse macrophages (Figure 7A) and THP-1 human monocyte-derived macrophages (Figure 7B) with apoptotic Jurkat cells, and subsequent induction of apoptosis with etoposide, an inhibitor of topoisomerase II (153). The amount of apoptosis in Jurkat cells was around 80% after 3 h-treatments with 0.5 µg/ml staurosporine (Sts), the time point when AC were applied to macrophages, while necrosis only started to increase from 6 h onwards (Figure 7C). In contrast to necrotic (NC) or viable (VC) Jurkat cells, co-cultures with AC attenuated caspase-3 activation in RAW 264.7 as well as THP-1 cells, compared to controls. Similar results were obtained with alternative apoptosis-inducing stimuli such as nitric oxide (NO) or TNF-α in combination with cycloheximide (CHX) (data not shown).
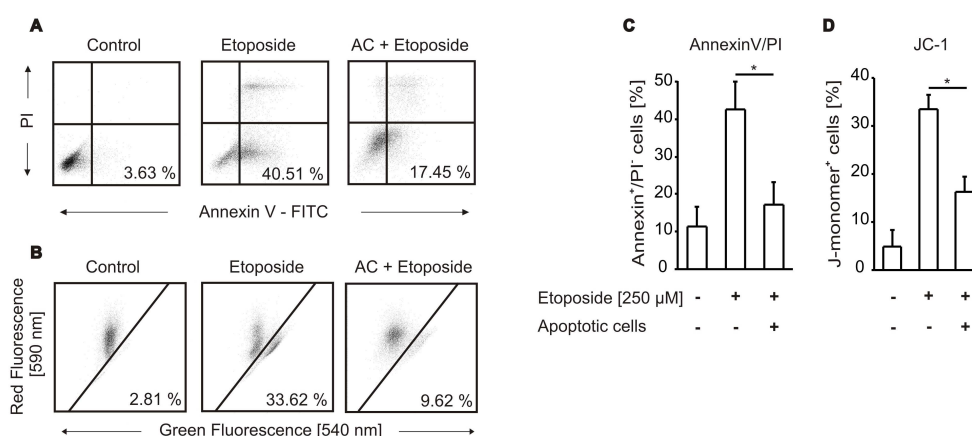


Figure 8: AC attenuate macrophage apoptosis. (A to D) THP-1 cells were untreated or pre-treated with AC for 16 h. Apoptosis was induced for 8 h with 250 µM etoposide. Viability was assessed by (A and C) annexin-V/PI staining, (B and D) JC-1 staining and subsequent analysis by flow cytometry. (C and D) Data are presented as the mean ± SD from four independent experiments. Differences between untreated and AC-treated cells are statistically significant ($p < 0.05$) for both parameters shown.

Measurement of alternative apoptotic markers, which were phosphatidylserine exposure and mitochondrial membrane integrity, confirmed that AC indeed attenuated etoposide-induced apoptosis (Figure 8A to D). THP-1 cells pre-

incubated with AC showed significantly less annexin-V binding following treatment with etoposide as compared to controls (Figure 8A and C). Macrophage staining with the fluorescent dye JC-1, which differentiates between metabolically active (red fluorescence) and defective (green fluorescence) mitochondria, further verified prevention of cell death (Figure 8B and D). The presence of AC preserved mitochondrial integrity in macrophages, which otherwise was lost upon etoposide treatment.
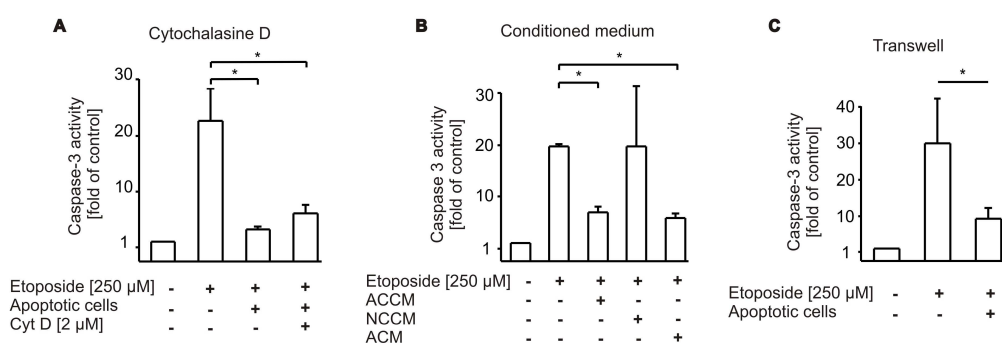


Figure 9: Macrophage protection is caused by an apoptotic cell-derived soluble factor. (A-C) Caspase-3 activity in etoposide-treated (8 h, 250 µM) THP-1 macrophages normalized to untreated controls. Cells and media were pre-incubated for 16 h. Data are presented as the mean ± SD from three independent experiments. Statistical differences between samples are marked with asterisk ($p < 0.05$). (A) Cells remained untreated, were treated with AC alone or in combination with 2 µM cytochalasin D. (B) Cells remained untreated or were treated with conditioned media from macrophages co-cultured with AC (ACCM), necrotic cells (NCCM) or conditioned medium from AC (ACM). (C) Cells remained untreated or were pre-exposed to AC in transwell inserts for 16 h prior to stimulation with etoposide.

## 5.1.2 Survival is transmitted by a soluble factor

I questioned the type of interaction between AC and macrophages that was required to attenuate etoposide-evoked cell death. Therefore cytochalasin D, an inhibitor of phagocytosis via disruption of cytoskeletal rearrangement (154), was added to THP-1 macrophages prior to incubation with AC (Figure 9A). Upon stimulation with etoposide, there was no difference in the ability of AC to protect from cell death, irrespective of the presence or absence of

cytochalasin D. This excluded a contribution of phagocytosis in conveying protection.

Next, conditioned medium from macrophage/AC co-cultures (ACCM) was collected to check whether or not a macrophage-derived soluble factor might be involved. For control reasons, conditioned medium of macrophage/NC co-cultures (NCCM) and conditioned medium from AC (ACM) only was used (Figure 9B). Interestingly, not only ACCM but also ACM protected THP-1 cells from etoposide-induced apoptosis, while NCCM did not (Fig 9B). This finding strongly suggested the release of a protective factor from AC. For further validation, transwell experiments were performed, separating macrophages and AC by a permeable membrane to exclude direct cell/cell contacts. Spatial separation of macrophages and AC still conveyed protection (Figure 9C). These results argued for a soluble, apoptotic cell-derived factor, mediating macrophage protection towards etoposide-induced cell death.

### 5.1.3  Survival is irrespective of AC cell line and pro-apoptotic stimulus

To analyze whether the production of an anti-apoptotic factor by AC was an inherent feature of apoptotic cell death, apoptosis was induced in different cell lines by activating intrinsic (Sts) as well as extrinsic pathways (TNF-α, anti-Fas) of apoptosis. ACM from Jurkat, RKO, HEK293 or MCF-7 cells elicited protection against etoposide-induced THP-1 macrophage apoptosis (Table 2). These results imply that macrophage protection by AC resembles a general principle because it was reproduced by using distinct cell lines treated either with extrinsic or intrinsic pro-apoptotic stimuli. Moreover, by using caspase-3 negative MCF-7 cells (35), an involvement of caspase-3 activation in the production of the protective factor was excluded.

Table 2: Macrophage protection by ACM from different cell lines and stimuli

_____

| Cell line and stimulus | Protection (%)[*] | SD (n ≥ 3) |
| --- | --- | --- |
| **Jurkat** | | |
| Staurosporine [0.5 µg/ml, 3 h] | 100 | ± 0 |
| Anti-Fas [0.05 ng/ml, 5 h] | 91.1 | ± 18.6 |
| **RKO** | | |
| Staurosporine [0.5 µg/ml, 5 h] | 103.3 | ± 23.6 |
| **MCF-7** | | |
| Staurosporine [0.5 µg/ml, 4 h] | 91.3 | ± 12.9 |
| **HEK293** | | |
| Staurosporine [0.5 µg/ml, 8 h] | 80.5 | ± 19.7 |
| TNF-α/CHX [50 ng/ml/10 µg/ml, 24 h] | 106.7 | ± 27.5 |

_____

[*]100% protection is set as the difference in caspase-3 activity (fold of control) between untreated THP-1 macrophages and those treated with ACM (16 h) from Jurkat cells killed with staurosporine, followed by induction of apoptosis in macrophages with 250 µM etoposide for 8 h. Caspase-3 activity in whole cell lysates was quantified as described in Materials and Methods. Differences in caspase-3 activity between untreated and ACM-treated macrophages were significant ($p < 0.05$) for each cell line and stimulus indicated.

## 5.1.4  Characterization of the protective factor

With the intention to characterize the nature of the protective factor present in ACM, I noticed that neither heating conditioned medium at 100°C, nor digestion with proteinase K or trypsin abrogated the protective principle (Table 3), thus ruling out a protein factor. However, extracting lipids from ACM with chloroform completely eliminated protection (Table 3). These experiments argued for a lipid factor as the messenger in question.

Table 3: Macrophage protection by ACM

_____

| ACM-Treatment | Protection (%) [*] | SD | $p$-value (n ≥ 3)[†] |
|---|---|---|---|
| none | 100 | ± 0 | - |
| heat inactivation [100°C] | 87.4 | ± 2.4 | 0.4 |
| proteinase K digestion [50 μM] | 98.5 | ± 8.2 | 0.39 |
| trypsin digestion [0.1%] | 99.2 | ± 12 | 0.46 |
| chloroform extraction | -5.2 | ± 17.5 | 0.007 |

_____

[*]100% protection is set as the difference in caspase-3 activity (fold of control) between untreated and ACM-treated (16 h) THP-1 macrophages after induction of apoptosis with 250 μM etoposide for 8 h. Caspase-3 activity in whole cell lysates was quantified as described in Materials and Methods. [†]Statistical analysis was performed using the paired Student's $t$-test.

### 5.1.5  Characterization of the protective principle

To establish the time-dependency for protection, THP-1 cells were incubated with ACM for 1 to 6 h prior to stimulation with etoposide. Significant protection was first detected after 6 h, with the further notion that protection once established lasted for 48 h (data not shown). Additional examinations confirmed protection by ACM in primary human monocyte-derived macrophages, as determined by annexin-V/PI staining and caspase-3 activity measurements (Figure 10A). To characterize protective signaling pathways, I used pharmacological inhibitors known to interfere with anti-apoptotic pathways. LY294002, an inhibitor of PI3K-signaling, PD98059, an inhibitor of ERK1/2, and Bapta-AM, a calcium chelator, restored caspase-3 activation in human primary macrophages upon pre-incubation with ACM. Inhibitor studies implied that preferentially a PI3K-sensitive pathway transmits protection in response to ACM, while $Ca^{2+}$ as well as ERK1/2 signaling contributes to protection to a lower extent (Figure 10B).
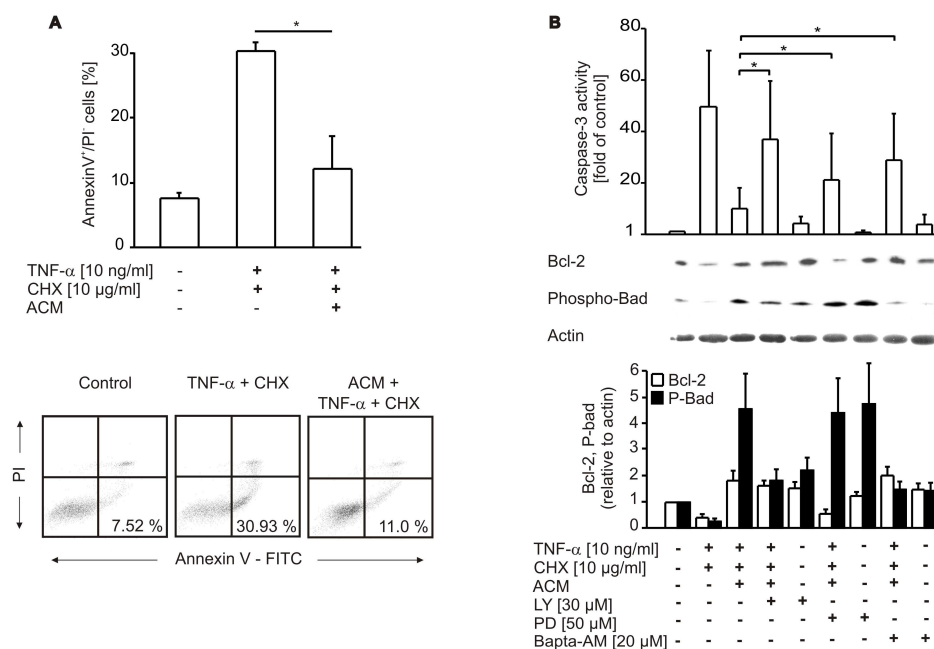
Figure 10: Protection of primary human macrophages by ACM is PI3K-, Ca2+- and ERK1/2-dependent. (A) Human primary monocyte-derived macrophages remained untreated or were exposed to ACM for 16 h. Following a medium change, apoptosis was induced for 8 h with 10 ng/ml TNF-α and 10 µg/ml CHX. Viability was assessed by annexin-V/PI staining and FACS-analysis. Data in histograms are presented as the mean ± SD from three independent experiments. Statistical differences are marked (p < 0.05). The lower part shows typical FACS traces. (B) Human primary macrophages were not treated, exposed to ACM for 16 h in the presence or absence of LY92004, PD98059 or Bapta-AM at the indicated concentrations. Apoptosis was induced for 8 h with 10 ng/ml TNF-α and 10 µg/ml CHX. The upper histogram shows caspase-3 activity. Data are presented as the mean ± SD from six independent experiments. Significant differences between samples are marked by asterisks (*p* < 0.05). Western analysis shows expression of Bcl-2 and phospho-Ser136-Bad. One representative experiment out of three is displayed. Lower histograms show quantification of Western data normalized to actin by using AIDA software. Data are presented as the mean ± SEM from four independent experiments.

Supportive argumentation comes from Bcl-2 expression and Ser136-Bad phosphorylation. Treatment of human primary macrophages with TNF-α and CHX decreased Bcl-2 levels and Bad-phosphorylation, compared to controls, with the notion that these changes were restored by ACM. In analogy to caspase activity, PD98059 reduced Bcl-2 stabilization while Bad-phosphorylation was decreased to control levels by LY294002 and Bapta-AM

(Figure 10B). In order to investigate the contribution of other Bcl-2 family members towards protection, expression of Mcl-1 and Bcl-$X_L$, which is known to be relevant for macrophage survival (155, 156), was analyzed in response to ACM. Although Mcl-1 was not significantly induced by ACM in macrophages, up-regulation of Bcl-$X_L$ was obvious (Figure 11B). I concluded that the ACM-protective principle is reflected at the level of pro- and/or anti-apoptotic Bcl-2-family members. This is further supported by JC-1 experiments (Figure 8B and C), which imply the involvement of mitochondria.

### 5.1.6   Contribution of sphingosine-1-phosphate towards protection

Results so far pointed to a lipid mediator in protection of macrophages against apoptotic cell death. Therefore, I tested candidates such as platelet-activating factor (PAF), lysophosphatidic acid (LPA), lysophosphatidylcholine (LPC) or sphingosine-1-phosphate (S1P), known to manipulate apoptosis in other test systems. Increasing concentrations of each compound, compared to ACM, were added to primary macrophages in combination with the apoptosis-inductors TNF-α/CHX (Table 4). Only S1P induced significant protection at a rather low concentration of 1 µM (Table 4). LPC attenuated cell death at higher concentrations, only, and PAF as well as LPA increased rather than decreased death.

Considering a potential impact of S1P, the effect of ACM-extracted lipids, the ACM aqueous phase as well as conditioned medium derived from necrotic cells (NCM), was analyzed regarding the modulation of death in primary human macrophages (Figure 11A). TNF-α/CHX-evoked caspase-3 activation was attenuated by the lipid but neither by the aqueous phase of ACM nor by NCM. Protection conveyed by ACM as well as S1P was reflected at the level of Bcl-2, Bcl-$X_L$, and phosphorylated Bad (Figure 11B). ACM and S1P increased Bcl-2 as well as Bcl-$X_L$ expression and provoked Bad phosphorylation in analogy to results shown in Figure 10B. To strengthen a protective role of S1P, dimethylsphingosine (DMS), an inhibitor of sphingosine kinases, was applied to Jurkat cells 3 h prior to initiation of cell death. ACM derived from DMS-treated Jurkat cells did not protect macrophages from TNF-α/CHX-induced apoptosis (Figure 11A).

Table 4: Bioactive lipids and human macrophage survival

_____

| Treatment | | Caspase-3 activity[*] | SD | $p$-value (n ≥ 3) [†] |
|---|---|---|---|---|
_____
| none | | 30.6 | ± 4 | - |
| ACM | | 5.3 | ± 3.6 | 0.02 |
| LPA | [1 µM] | 30.1 | ± 12.8 | 0.35 |
| | [10 µM] | 33.8 | ± 19.7 | 0.49 |
| | [100 µM] | 39.5 | ± 20.8 | 0.35 |
| S1P | [1 µM] | 13.2 | ± 9.2 | 0.05 |
| | [10 µM] | 10 | ± 6.3 | 0.02 |
| | [100 µM] | 6.1 | ± 4 | 0.006 |
| PAF | [1 µM] | 40.5 | ± 5.1 | 0.4 |
| | [10 µM] | 61.1 | ± 41.3 | 0.15 |
| | [100 µM] | 97.2 | ± 59.6 | 0.09 |
| LPC | [1 µM] | 54.2 | ± 27.8 | 0.25 |
| | [10 µM] | 32.1 | ± 18.4 | 0.44 |
| | [100 µM] | 20 | ± 5.2 | 0.2 |
_____

[*]Human primary macrophages were exposed to ACM, LPA, S1P, PAF or LPC at the indicated concentrations for 16 h. Apoptosis was induced with 10 ng/ml TNF-α and 10 µg/ml CHX for 8 h. Caspase-3 activity in whole cell lysates was quantified as described in Materials and Methods. [†]Statistical analysis was performed using the paired Student's $t$-test.

To further substantiate a role of S1P in protection, I used a lipid extraction procedure, designed to be specific for S1P (143). The lipid extract from ACM gained with this method reproduced protection (Figure 11A), which underscores the assumption that indeed S1P is released from AC to protect macrophages from entering pathways of cell demise.
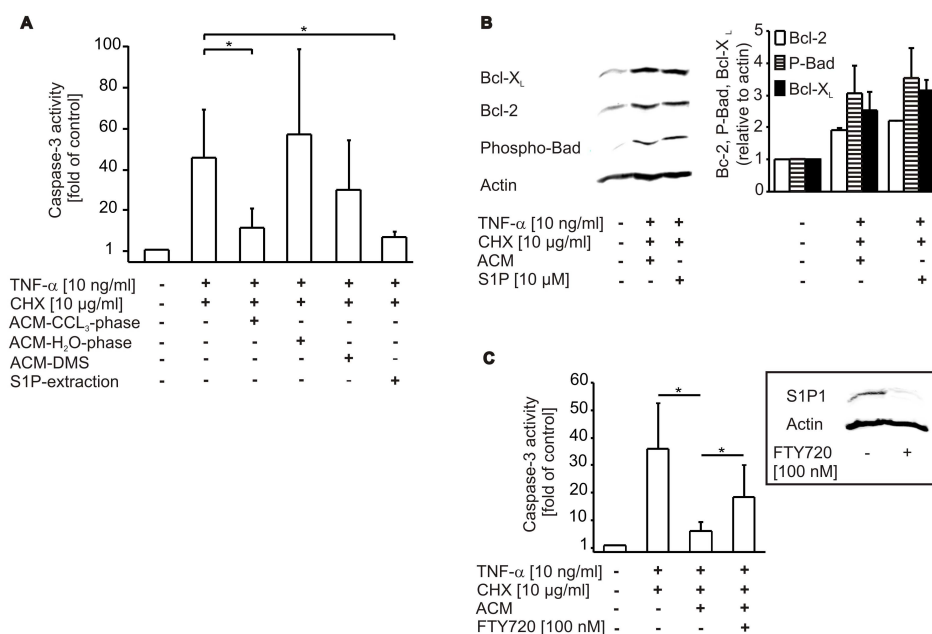
Figure 11: Sphingosine-1-phosphate conveys protection. (A to C) Apoptosis in human primary macrophages was induced for 8 h with 10 ng/ml TNF-α and 10 µg/ml CHX. (A) Cells remained untreated or were treated with ACM, the ACM-lipid fraction, the ACM-aqueous fraction, with ACM derived from Jurkat cells exposed to DMS prior to initiation of apoptosis (ACM-DMS) or treated with the ACM-lipid fraction specific for S1P extraction (S1P-extraction), 16 h prior to induction of cell death. Caspase-3 activity was quantified as described in Materials and Methods. Data are presented as the mean ± SD from four independent experiments. Significant differences between samples are marked by asterisk ($p < 0.01$). (B) Cells were not treated, exposed to the ACM or stimulated with 10 µM S1P for 16 h. Western analysis shows expression of Bcl-2, Bcl-$X_L$ and phosphorylated Ser136-Bad. One representative experiment out of three is displayed. Histograms show quantification of Western data normalized to actin by using AIDA software. Data are presented as the mean ± SEM from three independent experiments. (C) Cells remained untreated, were exposed for 16 h to ACM alone or to ACM after pre-treatment with 100 nM FTY720 for 1 h followed by further incubations of 48 h. Afterwards TNF-α/CHX-treatments lasted for 8 h. Data are presented as the mean ± SD from four independent experiments. Significant differences between samples are marked by asterisks ($p < 0.05$).

Next, the identity of the subtype of S1P receptor being expressed on human macrophages and participating in protection was questioned. Primary human macrophages were pre-stimulated with 100 nM of the S1P-receptor agonist FTY720, which induces internalization of S1PR1 after 48 h when applied for 1 h (116). Western blot analysis revealed a strong down-regulation of S1PR1 following pre-stimulation with FTY720, compared to controls (Figure 11C).

When ACM was added to macrophages with S1PR1 being down-regulated, protection was significantly but not completely diminished in comparison to macrophages incubated only with ACM (Figure 11C). Since pre-stimulation of macrophages with 100 nM FTY720 was shown to specifically induce internalization of S1P-receptor subtypes 1 and 5 (116), I concluded that S1PR1 was at least partially responsible for macrophage protection by S1P because macrophages do not express S1PR5 (157, 158).
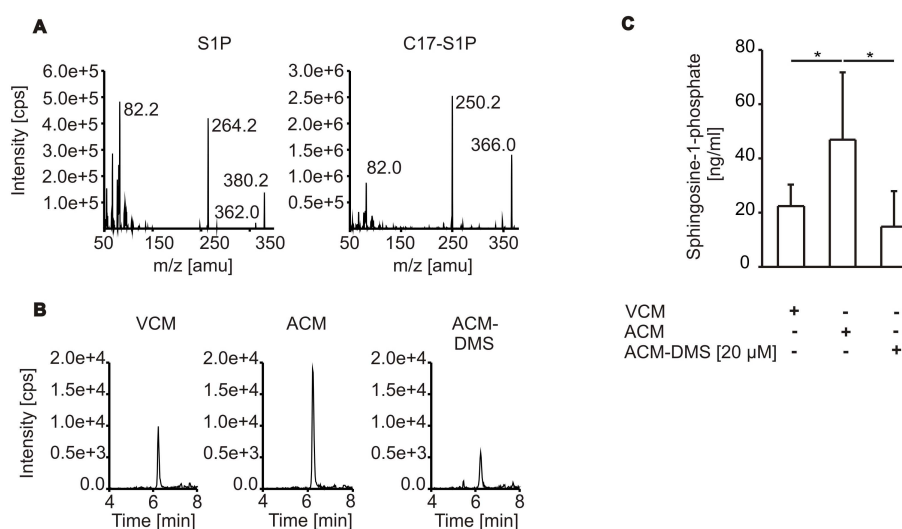


Figure 12: Measurement of S1P-secretion by AC. (A) Fragment spectra of S1P and the internal standard C17-S1P by using product ion scans in the positive ionization mode. Product ion scans were obtained by infusion of 100-1000 ng/ml of the respective analyte in methanol with a flow of 10 µl/min. (B to C) Jurkat cells were cultured in FCS free medium, remained as controls (VCM) or were treated with 0.5 µg/ml staurosporine with (ACM-DMS) or without (ACM) the previous addition of DMS for 3 h. After changing medium, incubation continued for another 2 h and conditioned media were analyzed for the S1P content with liquid chromatography-tandem mass spectrometry. (B) Exemplary chromatograms of S1P representing 22.0, 42.1 and 12.2 ng/ml, respectively. (C) Quantification of S1P release in the supernatant of Jurkat cells. Data are presented as the mean ± SD from six independent experiments. Significant differences between samples are marked by asterisks ($p < 0.05$).

Many hints pointed to a mechanism involving S1P release from AC. The finally prove this assumption, conditioned medium from viable Jurkat cells, ACM and ACM from DMS-treated Jurkat cells was analyzed for S1P amounts in cooperation with the Institute of Clinical Pharmacology, using liquid

chromatography-tandem mass spectrometry analysis (Figure 12). Induction of Jurkat cell apoptosis with Sts increased the release of S1P into the cell supernatant as compared to non-stimulated cells (Figure 12B and C). Moreover, S1P release from AC was blocked by the sphingosine kinase inhibitor DMS (Figure 12B and C). These data corroborated the release of the anti-apoptotic molecule S1P from AC.

### 5.1.7 S1P production during apoptosis is performed by SphK2

Since two isoforms of SphK are known up to date, and DMS attenuates the activity of both enzymes, siRNA technology was used to determine which SphK isoform catalyzes S1P production during apoptotic cell death.
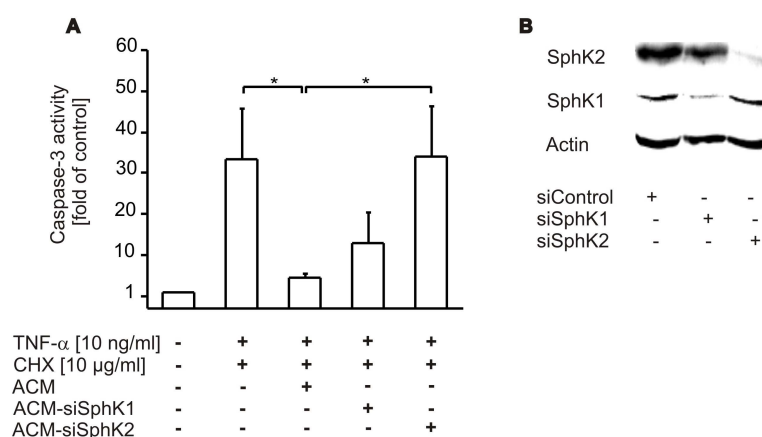


Figure 13: SphK2 expression in AC contributes to the release of S1P. (A) Apoptosis in human primary macrophages was induced for 8 h with 10 ng/ml TNF-α and 10 µg/ml CHX. Cells remained untreated or were treated with ACM or ACM from Jurkat cells nucleofected with siRNA to target SphK1 or SphK2, 16 h prior to induction of cell death. Caspase-3 activity was quantified as described in Materials and Methods. Data are presented as the mean ± SD from four independent experiments. Significant differences between samples are marked by asterisks ($p < 0.05$). (B) Jurkat cells were nucleofected with control siRNA or siRNA against SphK1 or SphK2. Western analysis shows SphK1 and SphK2 expression. One representative experiment out of three is displayed.

Therefore, Jurkat cells were nucleofected with siRNA for both SphK-isoforms, prior to being used for the preparation of ACM. Importantly, induction of apoptosis with Sts in Jurkat cells was not affected by knock-down of either SphK1 or SphK2 (data not shown). Western blot analysis revealed strong down-regulation of SphK1 and SphK2 in Jurkat cells after nucleofection with corresponding siRNA, compared to control siRNA (Figure 13B). Incubation of human primary macrophages with ACM-siSphK2 significantly reduced protection compared to the efficacy of ACM, whereas ACM-siSphK1 was marginally effective, only (Fig 13A). These data strongly suggested a role of SphK2 in the production of S1P in AC. Concluding, I can say that AC release S1P, which transmits a shift in the Bcl-2 family member profile towards anti-apoptotic via S1PR1 in macrophages, thus protecting them from cell death.

## 5.2   The mechanism of S1P production by apoptotic cells

S1P was produced and released during apoptotic cell death (5.1), a phenomenon that likely enhances its biological importance, since apoptosis plays a fundamental role in the pathogenesis of many human diseases (26). Therefore I desired to understand the underlying mechanistic principle, since this could lead to the identification of targets for the treatment of disease.

### 5.2.1   A truncated sphingosine kinase 2 is released during apoptosis

Little is known how S1P is transferred from inside a cell to its surrounding. To approach the mechanism of its production in AC, I investigated subcellular expression and activity of SphK2 in Jurkat cells, prior and subsequent to apoptosis-induction using Sts (Figure 14). Corroborating a previous report (108), reduced expression of SphK2, both of the L- and S-isoform (111), in the nuclear, membrane and cytosolic fractions was noticed during apoptosis (Figure 14A). New data emerged when I observed a protein of lower molecular weight in the supernatant of Sts-treated cells (Figure 14A), that was only visible with an antibody recognizing the C-terminus of SphK2, but not with an antibody binding to the N-terminus. Using a fluorescence-based activity assay (152), a decrease in intracellular SphK2 activity in apoptotic

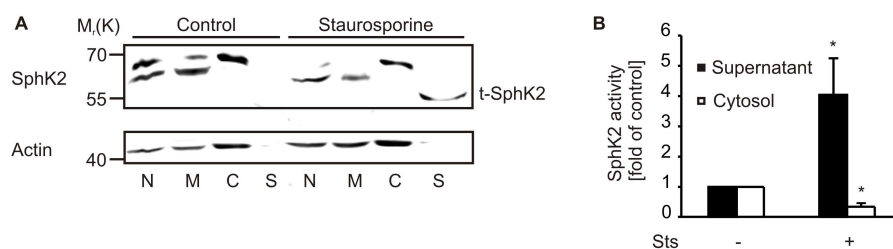Jurkat cells was revealed, whereas extracellular SphK2 activity was significantly elevated (Figure 14B).



Figure 14: A truncated active SphK2 (t-SphK2) is released into the supernatant of apoptotic Jurkat cells. (A and B) Jurkat cells remained as controls or were treated with staurosporine as described in Materials and Methods. (A) Western analysis of SphK2 expression in subcellular fractions (nuclear (N), membrane (M), cytosolic (C)) or the cell supernatant (S). (B) SphK2 activity in cell lysates (white bars) and cell supernatants (black bars). Data are means ± SEM from four independent experiments. Asterisks indicate significant differences (* = $p < 0.05$).

## 5.2.2 Caspase-1 cleavage sites in SphK2

Since cleavage of SphK2 was not previously reported, I used PeptideCutter, a free tool on the ExPASy Proteomics Server, to identify potential protease cleavage sites. With a focus on proteases activated during apoptosis, two putative caspase-1 cleavage sites were identified in human SphK2, at D138 and D552, both of them being well conserved in mammals (Figure 15). Furthermore, the N-terminal cleavage site showed homology to a caspase-1 cleavage site in pro-IL-β (12) (Figure 15). To ask for potential consequences of SphK2 cleavage by caspase-1 regarding protein distribution, I used WoLF PSORT (159), to predict localization of full length as well as cleaved SphK2. The prediction for full length SphK2 to be localized mainly nuclear and cytosolic, concurs with experimental data (120). Putative localization of the C-terminal caspase-1 cleavage product was identical with the full length protein. Interestingly, the product generated by N-terminal cleavage was predicted, among other compartments, to localize extracellular (data not shown).

**A**

N-terminal cleavage site

```
Rat_SphK2      95    RATRTFRADGAATYVE
Rhesus_SphK2   94    RTTRTFRTDGATTYEE
Dog_SphK2     131    RAPRTFRADGAATYEE
Human_SphK2   130    RATRTFRADGAATYEE
Mouse_SphK2    95    RATRTFRADGATTYEE
```

C-terminal cleavage site

```
Rat_SphK2     507    ILPSHLCADLMAAPHA
Rhesus_SphK2  508    ISPSHLGADLVAAPHA
Dog_SphK2     553    ISPSHLGADLVAAPHA
Human_SphK2   544    ISPSHLGADLVAAPHA
Mouse_SphK2   508    ILPSHLCADLMAAPHA
```

**B**

| Peptide | Cleavage site | Resulting fragments [aa] |
|---|---|---|
| Pro-IL-1β: | 24 FEAD/G | 27, 242 |
| SphK2: | 135 FRAD/G | 138, 516 |
|  | 549 LGAD/L | 552, 102 |

Figure 15: Caspase-1 cleavage sites in SphK2 are conserved in mammals. (A) Alignment of putative caspase-1 cleavage sites (bold letters) in SphK2 from different mammalian species is displayed. (B) Comparison of caspase-1 cleavage sites in human SphK2 with the N-terminal caspase-1 cleavage site in pro-interleukin 1β. Fragment sizes (aa) resulting from cleavage are displayed.

### 5.2.3 Caspase-1 inhibition abrogates SphK2 release

Taking this theoretical information into account, caspase-1 was inhibited with Ac-YVAD-CMK, which indeed prevented SphK2 cleavage and the concomitant release of the C-terminal fragment into the supernatant of apoptotic, i.e. Sts-treated cells (Figure 16A). My previous studies showed that ACM containing S1P attenuated etoposide-induced caspase-3 activation in THP-1 macrophages and upregulated Bcl-2 (5.1). These alterations were reversed, when ACM was generated from Jurkat cells treated with Sts in the presence of the caspase-1 inhibitor Ac-YVAD-CMK or the sphingosine kinase inhibitor DMS (Figure 16B).

To obtain more direct evidence for the involvement of caspase-1 in provoking SphK2 release, caspase-1 expression in Jurkat cells was targeted with siRNA. Expression of pro-caspase-1 and the active p20 subunit was reduced below the control level with caspase-1 being knocked down. Sts initiated the release of the truncated SphK2 to the supernatant, which was attenuated in caspase-1 knock-down cells (Figure 16C). Intracellular expression of SphK2 in apoptotic caspase-1 knock-down Jurkat cells was comparable to that seen in controls. Sts also increased caspase-1 as well as caspase-3 activity, but only caspase-1 activity was reduced in caspase-1 knock-down cells, shown via fluorescence-based caspase activity assays (Figure 16C). Along that line,

ACM from caspase-1 knock-down Jurkat cells failed to protect THP-1 macrophages against etoposide, compared to ACM from Jurkat cells transfected with non-targeting siRNA, as demonstrated by caspase-3 measurements (Figure 16D). I concluded that caspase-1 provokes SphK2 cleavage and release of the truncated SphK2 during apoptosis.
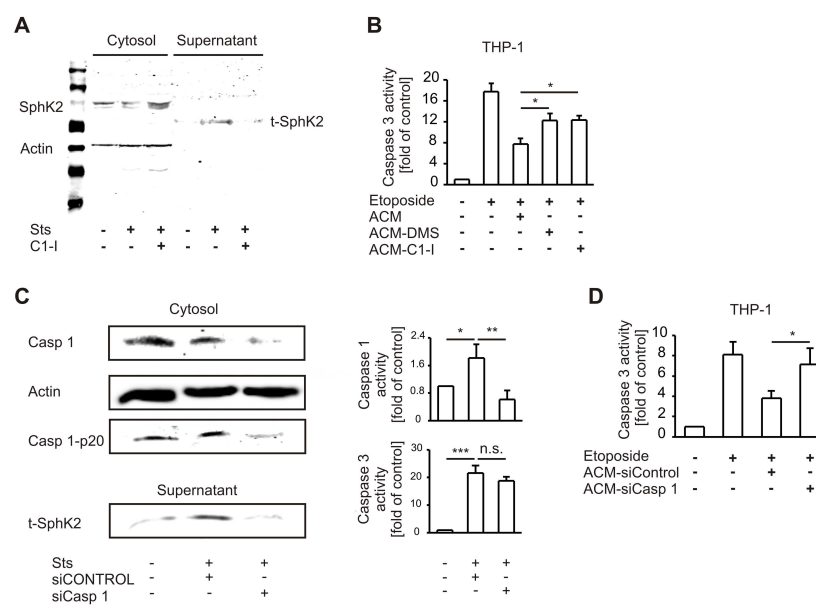


Figure 16: Release of SphK2 demands active caspase-1. (A) Western analysis of SphK2 expression in the cytosol and supernatants of Jurkat cells left as controls, treated with staurosporine (Sts) or Sts in combination with the caspase-1 inhibitor Ac-YVAD-CMK (C1-I). (B) THP-1 macrophages were pretreated with supernatants of apoptotic Jurkat cells (ACM), or supernatants of AC generated with either DMS (ACM-DMS) or Ac-YVAD-CMK (ACM-C1-I) being present. Apoptosis was induced for 8 h with 250 µM etoposide. Caspase-3 activity in THP-1 macrophages normalized to untreated cells is shown. Data are means ± SEM from four independent experiments. (C) Jurkat cells were controls or transfected with either siCONTROL or siRNA directed against caspase-1 prior to induction of apoptosis with staurosporine. Western analysis shows expression of pro-caspase-1 and the caspase p20 subunit in the cytosol and t-SphK2 in the cell supernatant. Histograms display caspase-3 or caspase-1 activity normalized to controls. Data are means ± SEM from four independent experiments. (D) THP-1 macrophages were pretreated with supernatants of apoptotic Jurkat cells transfected with siCONTROL (ACM-siControl) or siRNA targeting caspase-1 (ACM-siCasp 1). Apoptosis was induced for 8 h with 250 µM etoposide. Caspase-3 activity in THP-1 macrophages was normalized to untreated cells. Data are means ± SEM from five independent experiments. (B to D) Asterisks indicate significant differences (* = $p<0.05$; ** = $p<0.01$; *** = $p<0.001$; n.s. = not significant).

### 5.2.4  Mutational analysis of caspase-1 cleavage sites in SphK2

The following experiments were planed to establish a system allowing overexpression of SphK2, which at the same time could be utilized for mutational analysis of caspase-1 cleavage sites. HEK293 cells are easy to transfect and exhibit low basal SphK2 expression. Some extracellular SphK2 activity was elicited in supernatants of apoptotic HEK293 cells induced by Sts or tumor necrosis factor (TNF)-α, but again, this attenuated by the caspase-1 inhibitor or by adding DMS, which was used as an internal control to block all SphK2 activity in the *in vitro* assay (Figure 17A). HEK293 cells were then transfected with a plasmid encoding human N-terminal HA-tagged full length SphK2 (111). Induction of apoptosis in transfectants induced high extracellular SphK2 activity compared to controls. Intracellular expression of HA-tagged SphK2 was decreased and truncated SphK2 appeared in the supernatant. Again, this phenotype was ablated when caspase-1 was blocked with Ac-YVAD-CMK (Figure 17). Eliminating cleavage and release of SphK2 with the caspase-1 inhibitor was as potent as direct inhibition of SphK2 activity with DMS in the supernatant (Figure 17B). Interestingly, SphK2 cleavage and release during apoptosis also occurred in the murine system. This was shown by using a plasmid encoding murine C-terminal V5-tagged SphK2 transfected into NIH3T3 cells (Figure 17C). Unlike in the human system, several intracellular V5-tagged fragments appeared during the time course of V5-SphK2 cleavage which may indicate further digestion by proteases, at least in the murine system (Figure 17C).
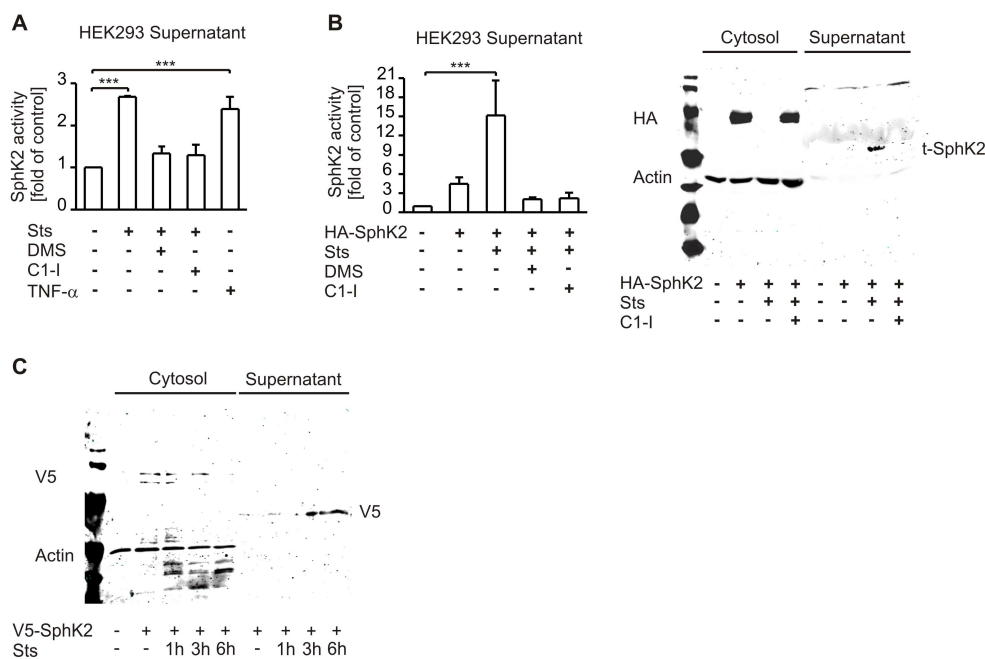
Figure 17: Overexpression of SphK2 in HEK293 and NIH 3T3 cells. (A) Apoptosis in HEK293 cells was induced with staurosporine in the presence/absence of Ac-YVAD-CMK (C1-I), or using TNF-α. SphK2 activity in the supernatant, normalized to controls, is displayed. DMS was used as an internal control, added during the kinase assay. Data are means ± SEM from four independent experiments. (B) HEK293 cells were transfected with HA-hSPHK2/pCMV5. Cells were left as controls or treated with staurosporine alone or in combination with Ac-YVAD-CMK. Histograms show SphK2 activity in the supernatant normalized to controls. DMS was used as an internal control. Data are means ± SEM from five independent experiments. Western analysis shows cytosolic expression of HA-SphK2 and t-SphK2 in the cell supernatant. (C) NIH 3T3 cells were transfected with V5-mSphK2/pCDNA3.1. Cells were left as controls or treated with staurosporine for times as indicated. Western analysis displays intra- and extracellular expression of V5-SphK2. (A and B) Asterisks indicate significant differences (*** = p<0.001).

To substantiate N-terminal cleavage of SphK2 by caspase-1, I used site-directed mutagenesis to introduce point mutations in the plasmid encoding HA-SphK2, changing aspartate to alanine in both putative caspase-1 cleavage sites. Mutated and wild type SphK2 were expressed in HEK293 cells to check basal SphK2 activity. Overexpression of the naïve plasmid vs. expression of the mutants produced comparable intracellular SphK2 activity (Figure 18A). Then, apoptosis was induced with Sts and extracellular SphK2 activity was measured. Expression of wild type HA-SphK2 resulted in increased SphK2

activity in the supernatant of apoptotic HEK293 cells. The same behavior was seen when expressing HA-SphK2-D552A. However, in cells expressing HA-SphK2-D138A, extracellular SphK2 activity was drastically decreased (Figure 18B). Checking for intracellular and extracellular protein expression revealed comparable information. Wild type and mutated proteins were expressed to a similar extent. Degradation of intracellular HA-tagged constructs was seen when expressing HA-SphK2 or HA-SphK2-D552A, but was absent with the HA-SphK2-D138A mutant (Figure 18C). In line, the release of truncated SphK2 was detectable in supernatants from apoptotic HEK293 cells expressing HA-SphK2 or HA-SphK2-D552A, but not in cells transfected with HA-SphK2-D138A (Figure 18D).

### 5.2.5  Caspase-1 and SphK2 co-localize at the plasma membrane

In the following experiments I determined localization of SphK2 before and after apoptosis induction with Sts. Therefore, paraformaldehyde fixed HEK293 cells, expressing HA-SphK2 or HA-SphK2-D138A, were stained for the HA-tag and caspase-1. Caspase-1 was stained as a marker for the cytosol and to possibly monitor co-localization with SphK2, while nuclei were counterstained using DAPI in control cells or following treatment with Sts for 2 h or 12 h. HA-SphK2 was visible throughout the cytosol in HEK293 cells as described previously (120) (Figure 18E, panel 1). The same holds for caspase-1. When Sts was added, HA-SphK2 translocated to the plasma membrane, where it co-localized with caspase-1 (Figure 18E, panel 2). After 12 h of Sts, cell death was visible based on chromatin condensation (white arrows) and HA-SphK2 was scarcely detectable any more (Figure 18E, panel 3). The same observation was made for caspase-1, which is known to be shed from dying cells and/or degraded subsequent to its activation. HA-SphK-D138A localized near or at the plasma membrane in untreated HEK293 cells (Figure 18F, panel 1) and remained at the plasma membrane when Sts was added for 2 h (Figure 18F, panel 2). In contrast to HA-SphK2, HA-SphK2-D138A was not degraded, remained visible after 12 h Sts treatment and stayed membrane associated or was cytosolic (Figure 18F, panel 3).
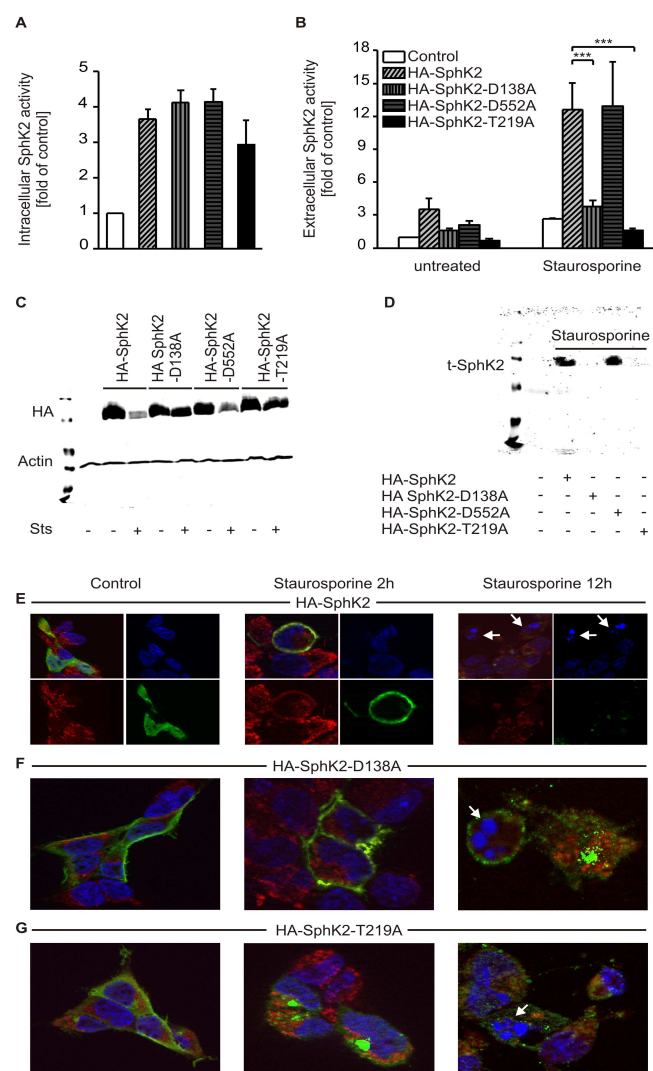
Figure 18: Mutation of the N-terminal caspase-1 cleavage site or the phosphatidylserine binding site in SphK2 inhibits cleavage and release of SphK2 during apoptosis. (A to D) HEK293 cells were transfected with HA-SphK2 or mutated constructs. (A) Intracellular SphK2 activity normalized to controls. Data are means ± SEM from four independent experiments. (B and C) Transfectants were left as controls or treated with staurosporine. (B) Extracellular SphK2 activity normalized to naïve controls is shown. Data are means ± SEM from five independent experiments. Asterisks indicate significant differences (*** = $p$<0.001). (C) Western analysis showing intracellular expression of wild type and mutated HA-SphK2. (D) Western analysis showing extracellular t-SphK2 expression in transfectants stimulated with staurosporine. (E to G) HEK293 cells, seeded on cover slips were transfected with (E) HA-SphK2, (F) HA-SphK2-D138A or (G) HA-SphK2-T219A. Cells remained as controls or were treated with staurosporine for 2 or 12 h. Cells were fixed and stained for HA (green) and caspase-1 (red). Nuclear staining was performed with DAPI (blue). White arrows indicate nuclear fragmentation. Each experiment was performed four times and representative images are shown.

Data so far indicated co-localization of SphK2 with caspase-1 after 2 h at the plasma membrane following induction of apoptosis with Sts and suggested that HA-SphK2-D138A, although located at the membrane, was not cleaved by caspase-1. These observations supported the assumption that caspase-1 cleaves SphK2 at its N-terminus during apoptosis, with concomitant release to the extracellular space.

### 5.2.6  Mutation of the PS binding site in SphK2 prevents its cleavage

As noticed in Figure 16C I observed a residual activity of caspase-1 in Jurkat cells, which was also evident in most other cell lines that were used. Therefore, additional regulatory mechanisms, besides caspase-1 activation, must be critical in regulating SphK2 release during apoptosis. Interestingly, SphK2 as well as SphK1 contain phosphatidylserine (PS) binding sites, which are well conserved between both isoenzymes (Figure 19). Indeed, PS was shown to stimulate the activity of both isoforms (117). PS exposure on the outer leaflet of AC is considered to be a hallmark of apoptosis and crucial for provoking anti-inflammatory macrophage polarization after their interaction with AC (160). I therefore questioned whether PS exposure would affect the release or activity of SphK2 during apoptosis. The critical amino acid residues for PS binding to SphK1 have been identified and were shown to have a profound impact on SphK1 membrane targeting (161). I used this knowledge and mutated the analogous threonine 219 to alanine in SphK2.

Mutation of the PS binding site did not significantly affect intracellular SphK2 activity compared to the naïve plasmid, although a slight reduction was noticed (Figure 18A). However, upon induction of apoptosis in cells expressing HA-SphK2-T219A, extracellular SphK2 activity was absent compared to cells transfected with the *wt* plasmid (Figure 18B). In concordance, expression of HA-SphK2-T219A was only slightly reduced when comparing viable and apoptotic HEK293 cells (Fig 18C) and the release of truncated SphK2 was absent (Figure 18D). Taking comparable effects on mutation of the N-terminal caspase-1 cleavage site and the PS binding site into account (Fig 18A to D), intracellular localization of the mutant was determined. HEK293 cells transfected with HA-SphK2-T219A were fixed with

paraformaldehyde and stained for the HA-tag and caspase-1. In contrast to cells expressing HA-SphK2 (Figure 18E) or HA-SphK2-D138A (Figure 18F), the HA-SphK2-T219A mutant remained cytosolic upon induction of apoptosis with Sts and was not degraded (Figure 18G). Apparently, binding of SphK2 to PS at the plasma membrane is critical for its cleavage and release.

**Phosphatidylserine binding sites in human sphingosine kinase isoforms**

```
hSphK2   175 LLPRPPRLLLLVNPFGGRGLAWQWCKNHVLPMISEAGLSFNLIQTERQNHARELVQGLSL
hSphK1    10 VLPRPCRVLVLLNPRGGKGKALQLFRSHVQPLLAEAEISFTLMLTERRNHARELVRSEEL
             **** * * * ** ** * * *    ** *   ** ** *  *** *******   *

hSphK2   235 SEWDGIVTVSGDGLLHEVLNGLLDRPDWEEAVKMPVGILPCGSGNALAGAVNQHGGFEPA
hSphK1    70 GRWDALVVMSGDGLMHEVVNGLMERPDWETAIQKPLCSLPAGSGNALAASLNHYAGYEQV
             ** * ***** *** ***  ***** *   *  ** *******   *    * *
```

Figure 19: PS binding site is highly conserved between human SphK1 and SphK2. Sequence alignment of the PS binding sites in hSphK1 and hSphK2. The threonine residue, mutated in this study, is in bold.

### 5.2.7 Lowering PS exposure attenuates SphK2 release

To obtain more information on the role of PS, I applied two strategies to modulate PS exposure during apoptosis. Besides initiating apoptosis in Jurkat cells with Sts, etoposide was used, which is known to induce apoptosis with only minor PS exposure (162). Furthermore, PS exposure was attenuated during Sts- or etoposide-induced apoptosis with 100 µM nifedipine, which is an inhibitor of L-type calcium channels (163). Apoptosis in Jurkat cells elicited by Sts induced PS exposure, mitochondrial membrane depolarization (ΔΨ) and cell shrinkage (Figure 20A and B). Nifedipine applied in combination with Sts significantly reduced PS exposure, whereas mitochondrial membrane depolarization (ΔΨ) and cell shrinkage remained unchanged (Figure 20A and B). Jurkat cells killed with etoposide showed a loss of ΔΨ comparable to Sts, but less PS exposure, the latter one being further reduced in the presence of nifedipine (Figure 20B). These conditions allowed initiating Jurkat cell apoptosis associated with a variable degree of PS exposure.

SphK2 activity in supernatants of Sts- or etoposide-treated cells with/without the addition of nifedipine was reduced in parallel to PS exposure (Figure 20C vs. Figure 20B). This behavior was reflected at the level of SphK2 expression

in whole cell lysate or supernatants. SphK2 was released into the supernatant of apoptotic Jurkat cells. Attenuating PS exposure decreased the release of truncated SphK2, while a cleaved SphK2 fragment accumulated inside the cells (Figure 20D). Again, the inverse correlation between released SphK2 and accumulation of the cleaved fragment inside cells correlated with PS exposure.
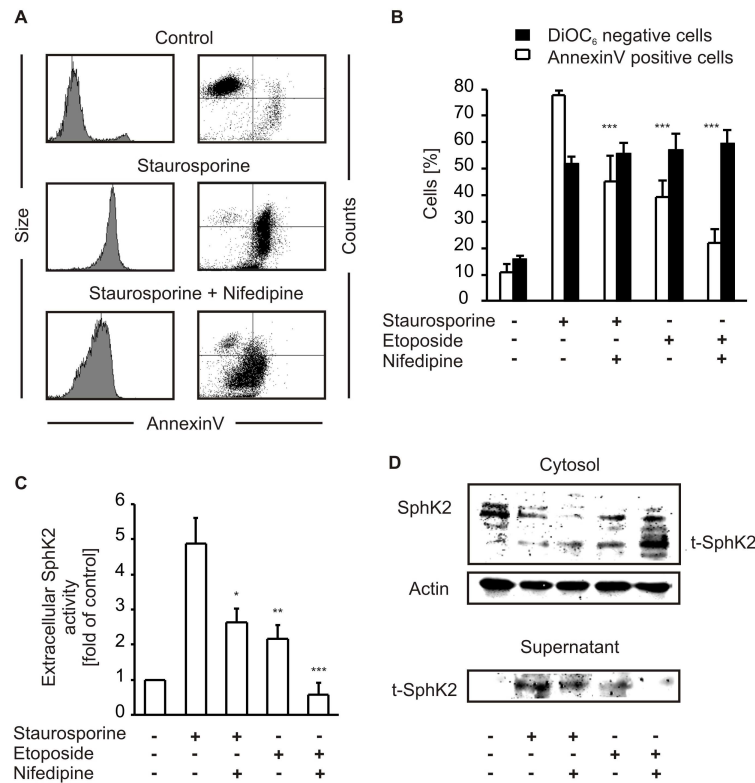


Figure 20: SphK2 release during apoptosis is coupled to phosphatidylserine exposure. (A to D) Jurkat cells were killed with staurosporine or etoposide in the absence/presence of 100 µM nifedipine. (A) Left FACS histograms show phosphatidylserine exposure visualized with Annexin V-FITC. Right FACS dot blots display phosphatidylserine exposure visualized with Annexin V-FITC compared to cell size, with cell shrinkage indicating cell death. Representative data out of four experiments are shown. (B) Cells were stained with Annexin V-FITC (white bars) or $DiOC_6$ (black bars) and analyzed by flow cytometry. Data are means ± SEM from four independent experiments. (C) Extracellular SphK2 activity normalized to controls is shown. Data are means ± SEM from four independent experiments. (D) Western analysis of intra- and extracellular SphK2 expression. (B and C) Asterisks indicate significant differences compared to cells treated with staurosporine alone (* = $p<0.05$;** = $p<0.01$; *** = $p<0.001$).

Taken together, I showed that a truncated, enzymatically active SphK2 is shed from AC upon cleavage by caspase-1 at its N-terminus. This pictures a new mechanism how S1P is released from cells. The outcome of this mechanism is the release of a protein factor, which could be a suitable target for therapeutics, like neutralizing antibodies or putative specific SphK2 inhibitors.

## 5.3   Tumor cell apoptosis polarizes macrophages via S1P

As mentioned in the introduction (3.3.3), TAM are comparable to AC-stimulated macrophages regarding their activation profile. Tumors may utilize the properties of macrophages in tissue repair and angiogenesis by providing signals comparable to AC. Since S1P is highly associated with tumor angiogenesis (3.4.2), the connection between AC-derived S1P and TAM development seemed striking. My next aim was to investigate this putative connection.

### 5.3.1   Co-cultured MCF-7 cells alter the cytokine profile of macrophages

In a first experimental approach, I asked whether or not a co-culture of breast carcinoma cells (MCF-7) with primary human monocyte-derived macrophages affected the cytokine profile in the latter ones. Therefore, macrophages were incubated with an equal amount of MCF-7 cells for 5 days and the contents of TNF-α, IL-10 and IL-8 in the co-culture supernatants were quantified at different time points (Figure 21). The co-culture provoked induction of TNF-α and IL-10 at 24 h, followed by a decrease from 48 to 120 h, which was markedly stronger in case of TNF-α (Figure 21A) as compared to IL-10 (Figure 21B). In contrast, IL-8 production did not peak after 24h, but increased steadily up to 120 h (Fig 21C). Cytokine production in either control macrophages or MCF-7 cells, cultured for 24 h, was low. Interestingly, adding fresh MCF-7 cells for 24 h to the culture systems that already lasted for 120 h (2nd co-culture), failed to induce TNF-α (Figure 21A), but elicited an increase in IL-10 (Figure 21B), whereas IL-8 production remained high (Fig 21C). This suggested that MCF-7 cells, co-cultured with macrophages elicited a transient

pro-inflammatory response, followed by an early production of TNF-α, a more persistent formation of the anti-inflammatory cytokine IL-10 and a strong induction of IL-8.
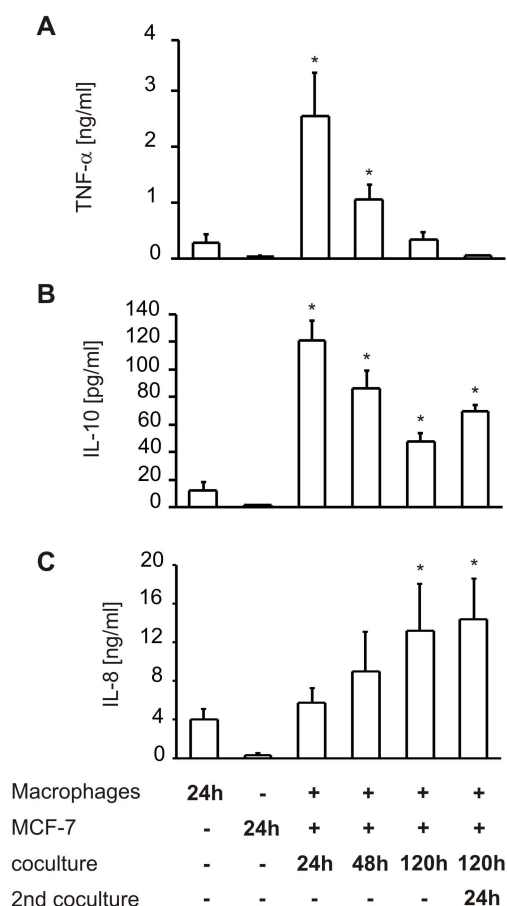


Figure 21: Co-culture of human macrophages with MCF-7 cells induced a cytokine shift. Supernatants of human monocyte-derived macrophages, MCF-7 cells or from co-cultures of macrophages with MCF-7 cells were assayed at times indicated for TNF-α (A), IL-10 (B) or IL-8 (C). Quantification was by FACS with BD Cytometric Bead Array Flex Sets as described under Materials and Methods. Data are presented as the mean ± SEM from four independent experiments. Differences between supernatants from control macrophages and co-cultures marked with an asterisk are statistically significant ($p < 0.05$).

To prove that a prolonged co-culture set-up provoked an alternative activation profile in macrophages, macrophages were stimulated with LPS/IFN-γ at the end of the 5 days co-culture with MCF-7 cells and compared to control macrophages (Figure 22A). Residual MCF-7 cells were removed by

incubations with accutase for 5 min, which left adherence of macrophages unaltered, thus proving, that this set-up exclusively determined cytokine production from macrophages (Figure 22B). Activation of naïve macrophages with LPS/IFN-γ stimulated the production of TNF-α and IL-10 but not of IL-8 as compared to resting cells. Addition of LPS/IFN-γ to macrophages from the co-culture set-up produced significantly less TNF-α, revealed markedly increased levels of IL-8, while IL-10 remained unchanged.

In the past, decreased production of pro-inflammatory IL-12-p70 has been connected to alternative macrophage activation and was attributed to increased IL-10 (164). Since IL-10 levels in macrophages from co-cultures were enhanced as compared to naïve macrophages even without LPS/IFN-γ stimulation (Figure 21B), I measured the amount of IL-12-p70 in the co-culture system. Administration of LPS/IFN-γ strongly induced IL-12-p70 in control macrophages, but remained significantly less effective when stimulating macrophages from the co-culture set-up (Figure 22A).

These results suggested that MCF-7 cells provoked a macrophage phenotype shift towards an alternative activation profile. Activation of macrophages from co-cultures with LPS/IFN-γ substantiated this phenotype switch, when following the production of classical pro- versus anti-inflammatory mediators. Although principal observations pointing to alternative macrophage activation during co-culture with MCF-7 cells were obvious (Figure 21), stimulation of naïve vs. co-culture primed macrophages with LPS/IFN-γ made the phenotype shift more definite. Therefore, LPS/IFN-γ stimulation was used in further experiments to demonstrate macrophage phenotype alterations.

Infiltrating macrophages may comprise up to 50% of the tumor cell mass (88). Nevertheless, it was interesting whether or not higher cell numbers of tumor cells would change the phenotypic alterations that were observed. When ratios of 5:1 or 10:1 were used in co-cultures, the decrease of TNF-α became more pronounced with more tumor cells added to macrophages, whereas the increase in IL-8 was unaffected (Figure 22C).
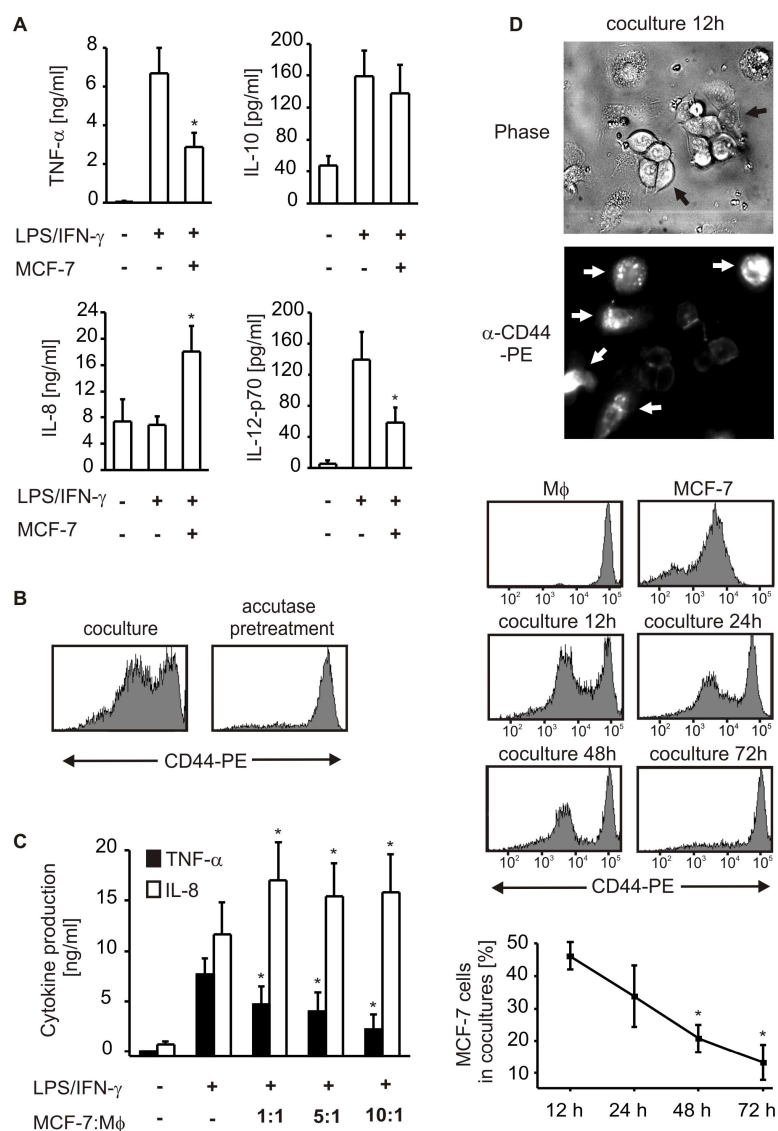
Figure 22: Co-culture with MCF-7 cells induced an alternative activation profile in human macrophages. (A and C) Human primary macrophages were controls or were incubated with MCF-7 cells for 5 days. Subsequently residual MCF-7 cells were removed from co-cultures and 1 µg/ml LPS and 100 U IFN-γ were added to macrophages from co-cultures or control macrophages for 6 h. TNF-α (A and C), IL-10 (A), IL-8 (A and C) and IL-12-p70 (A) contents in supernatants were quantified by FACS with BD Cytometric Bead Array Flex Sets. Data are presented as the mean ± SEM from at least six independent experiments. Differences between supernatants from LPS/IFN-γ treated macrophages and macrophages from co-cultures marked with an asterisk are statistically significant ($p < 0.05$). (B) Macrophages and MCF-7 cells were co-cultured for 12 h. Co-cultures were harvested after incubation with accutase for 30 min, with or without accutase pre-treatment for 5 min followed by washing, subsequent staining with α-CD44-PE, and analysis by FACS. (D) Co-cultures of human primary macrophages with MCF-7 cells were maintained for the times indicated. Co-cultures, control macrophages or MCF-7 cells were incubated for 30 min with accutase, harvested,

stained with α-CD44-PE as a discrimination marker between macrophages and MCF-7 cells, and analyzed by FACS or fluorescence microscopy. Images display phase contrast and α-CD44-PE staining of macrophage/MCF-7 co-cultures after 12 h. White arrows mark α-CD44 positive macrophages, black arrows mark MCF-7 cell colonies. FACS traces are representative for three independent experiments. The lower graph shows quantification of FACS data. Statistically significant ($p < 0.05$) reduced cell numbers of MCF-7 cells in co-cultures are marked with asterisks.

### 5.3.2  Viability changes of cancer cells in co-cultures with macrophages

To follow the ratio of macrophages to MCF-7 cells, co-cultures were stained with anti-CD44. CD44 proved to be a valid discrimination marker between highly CD44-positive macrophages and weakly CD44-expressing tumor cells (165) in the co-culture system (Figure 22D). I noticed a continuous reduction of MCF-7 cells starting at 24 h after initiating the co-culture, which resulted in a complete loss of tumor cells at 72 h (Figure 22D). To ensure that MCF-7 did not simply up-regulate CD44, the morphology of cells in co-cultures was additionally monitored. On the basis of morphological criteria, MCF-7 cells were completely absent after 72h (data not shown). These data indicated macrophage-induced apoptotic cell death of cancer cells.

To prove this assumption, cells from co-cultures were harvested after 12, 24 and 48 h and stained with anti-CD44 to distinguish between macrophages and MCF-7 cells. In addition, annexin V staining was used to monitor phosphatidylserine exposure as an early marker of cell death. Annexin V positive MCF-7 cells were noticed 24 h after co-culture with macrophages. The amount of apoptotic MCF-7 cells increased to about 50% after 48 h, whereas no significant changes in annexin V binding were observed in macrophages from co-cultures or control macrophages, i.e. cultured in the absence of MCF-7 cells (Figure 23A).
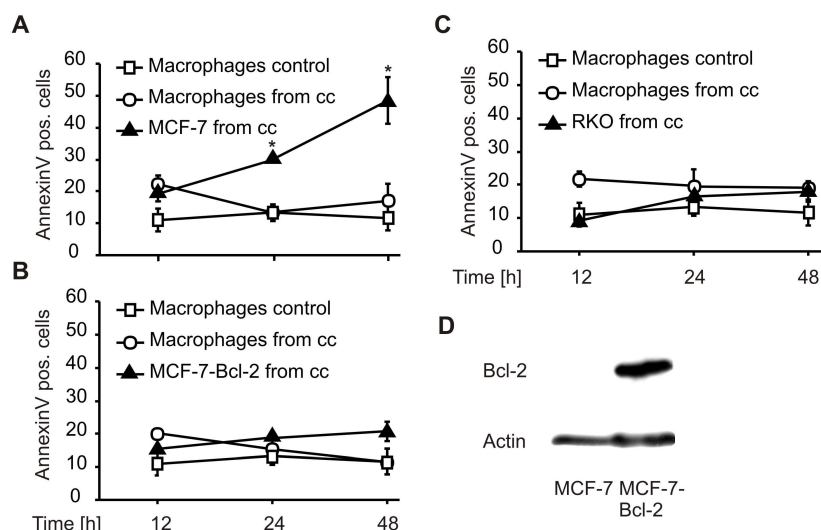
Figure 23: Impact of human primary macrophages on the viability of different human cancer cell lines. Human primary macrophages remained as controls or were incubated with MCF-7 cells (A), Bcl-2-overexpressing MCF-7 cells (B) or RKO cells (C) for the times indicated. Co-cultures and control macrophages were incubated for 30 min with accutase, harvested, stained with α-CD44-PE as a discrimination marker between macrophages and tumor cells, followed by annexin V-FITC staining as a marker for cell death, and analyzed by FACS. Data are presented as the mean ± SEM from three independent experiments. Differences between annexin V binding of macrophages and MCF-7 cells from co-culture (cc) marked with an asterisk are statistically significant ($p < 0.05$). (D) Western analysis shows Bcl-2 expression of control MCF-7 cells and MCF-7 cells transfected with a plasmid encoding human Bcl-2 (MCF-7-Bcl-2). One representative experiment out of two is displayed.

The working hypothesis predicted that only apoptotic tumor cells would evoke phenotype changes in macrophages. Therefore, two cells lines that were resistant to cell death induced by co-cultured macrophages were used in further experiments. First, I used MCF-7 cells that over-express Bcl-2 (Figure 23B and D) and second, I employed RKO cells, which turned out to be naturally resistant (Figure 23C). The reason for RKO cell survival in co-cultures remained unknown. However, they expressed higher amounts of Bcl-2 than naïve MCF-7 cells, which may account for apoptosis resistance (data not shown). A 48-h lasting co-culture of MCF-7-Bcl-2 or RKO cells with human macrophages showed no signs of cell death, neither in tumor cells nor in macrophages. Under these conditions, tumor cells and macrophages

coexisted, without initiation of cell death parameters. This was in contrast to the co-culture of apoptosis sensitive MCF-7 cells exposed to macrophages.

### 5.3.3 Alternative macrophage activation demands tumor cell apoptosis

The notion that Bcl-2-overexpressing MCF-7 cells (MCF-7-Bcl-2) and RKO do not enter the route of programmed cell death upon co-culture with macrophages qualified these cells, compared to sensitive MCF-7 cells, to study LPS/IFN-γ-evoked cytokine responses after 5 days of co-culture (Figure 24).
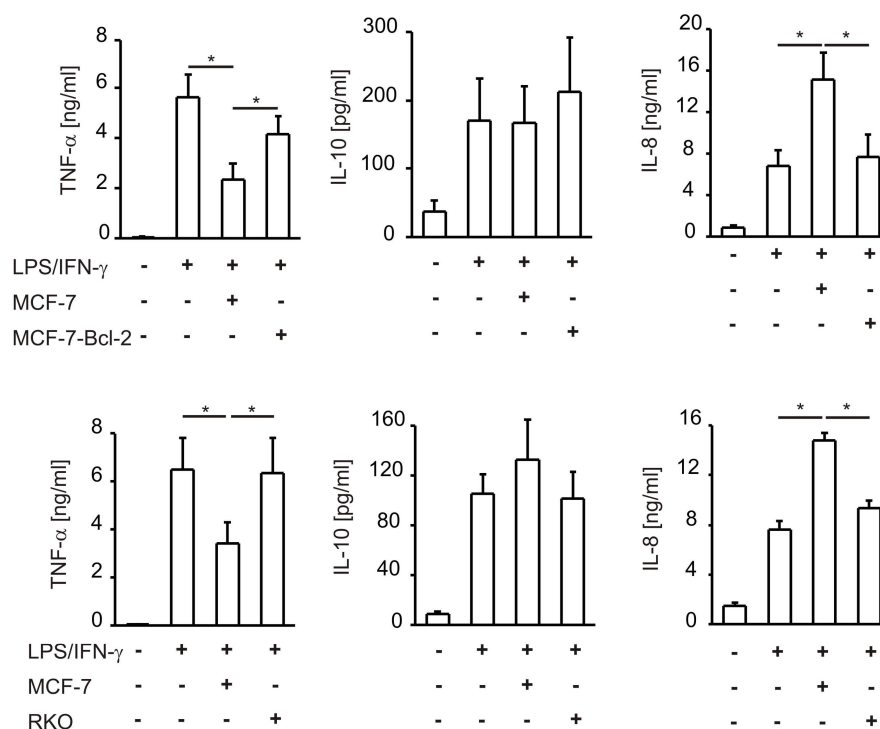


Figure 24: Activation profile of human macrophages after co-culture with different human tumor cell lines. Human primary macrophages remained as controls or were incubated with MCF-7 cells, Bcl-2-overexpressing MCF-7 cells (MCF-7-Bcl-2) or RKO cells for 5 days. Residual tumor cells were removed from co-cultures with 5 min accutase-treatment. Afterwards, 1 µg/ml LPS and 100 U IFN-γ were added to macrophages from co-cultures and control macrophages for 6 h. TNF-α, IL-10 and IL-8 contents in supernatants were quantified by FACS with BD Cytometric Bead Array Flex Sets. Data are presented as the mean ± SEM from five independent experiments. Statistically significant differences ($p < 0.05$) are marked with an asterisk.

Production of TNF-α, IL-10 and IL-8 in naïve macrophages following LPS/IFN-γ-addition was significantly increased compared to un-stimulated controls. Activation of macrophages coming from co-cultures with MCF-7-Bcl-2 or RKO cells revealed a cytokine profile resembling that of naïve macrophages following classic stimulation with LPS/IFN-γ. In contrast, cytokine formation of macrophages derived from co-cultures with apoptosis sensitive MCF-7 cells was different. TNF-α was lower, IL-8 was higher while IL-10 remained unaltered. Apparently, MCF-7-Bcl-2 as well as RKO cells did not change the ability of macrophages to respond to LPS/INF-γ with the production of these cytokines compared to naïve cells. Only the co-culture with MCF-7 cells, which underwent apoptotic cell death upon co-culture with macrophages, altered cytokine production following LPS/IFN-γ stimulation.

To corroborate that tumor cell death indeed was essential for alternative macrophage polarization, apoptosis was induced in RKO and MCF-7 cells with Sts and conditioned medium from these apoptotic tumor cells was collected, which then was added to macrophages for 24 h. After changing the medium, macrophages were stimulated with LPS/IFN-γ. Supernatants from apoptotic tumor cells alone induced significant changes in the macrophage cytokine profile, independent of direct tumor cell/macrophage contacts. Secretion of IL-10 and IL-8 was enhanced, whereas IL-12-p70 production was decreased compared to naïve macrophages (Figure 25A). Supernatants of apoptotic RKO or MCF-7 cells *per se* did not contain detectable amounts of cytokines (data not shown), except for IL-8 (around 200 pg/ml), which was nevertheless extremely low compared to the amounts that were produced by macrophages. Stimulation of macrophages exposed to tumor cell conditioned medium with LPS/IFN-γ elicited those phenotypic alterations that were observed in direct co-cultures, where tumor cell death occurred. TNF-α and IL-12-p70 were decreased, IL-8 was enhanced, whereas IL-10 was high, but not significantly different from control macrophages (Figure 25A). I concluded that the macrophage phenotype shift was dependent on tumor cell apoptosis, rather than representing intrinsic features of different tumor cell lines. Moreover, since supernatants of apoptotic tumor cells evoked macrophage phenotype alterations, macrophage polarization demanded soluble, apoptotic cell-derived factors.
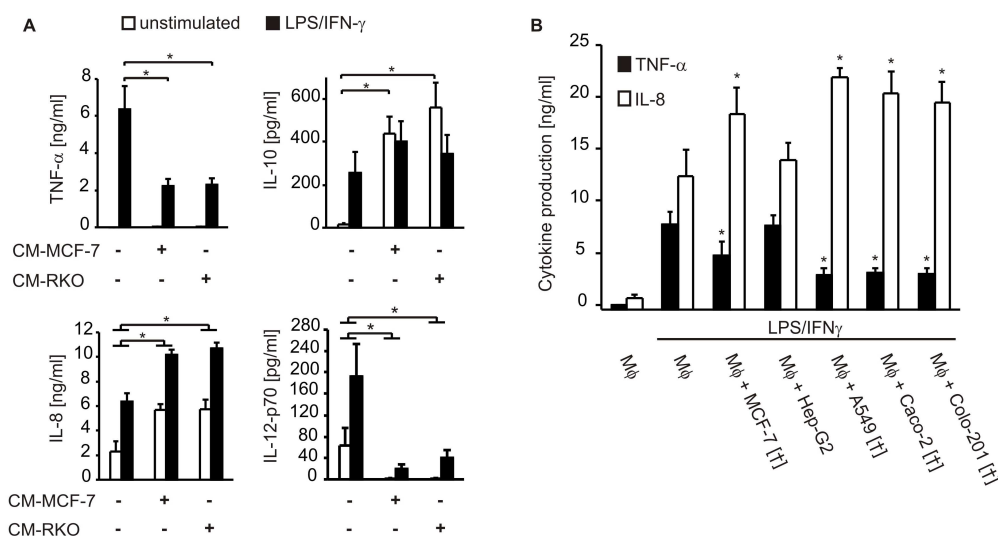
Figure 25: Activation profile of human macrophages induced by conditioned medium of apoptotic tumor cells and different tumor cell lines. (A) Human primary macrophages remained as controls or were incubated with conditioned medium from apoptotic MCF-7 (CM-MCF-7) or RKO (CM-RKO) cells for 24 h. Thereafter, supernatants were removed, cells were washed with PBS, fresh medium was added and macrophages were stimulated with 1 µg/ml LPS and 100 U IFN-γ for 6 h. Production of TNF-α, IL-10, IL-8 and IL-12-p70 was quantified by FACS with BD Cytometric Bead Array Flex Sets. Data are presented as the mean ± SEM from five independent experiments. Statistically significant differences ($p < 0.05$) are marked with an asterisk. (B) Human macrophages were controls or incubated with different tumor cell lines, as indicated. Tumor cell death in co-cultures is marked with [†]. Residual tumor cells were removed from co-cultures with 5 min accutase-treatment. Afterwards, 1 µg/ml LPS and 100 U IFN-γ were added to macrophages from co-cultures and control macrophages for 6 h. TNF-α and IL-8 contents in supernatants were quantified by FACS with BD Cytometric Bead Array Flex Sets. Data are presented as the mean ± SEM from six independent experiments. Statistically significant differences compared to LPS/IFNγ-stimulated control macrophages ($p < 0.05$) are marked with an asterisk.

For validation concerning independence from specific tumor cell lines, I used four additional well characterized tumor cell lines, such as the colon carcinoma cell lines Caco-2 and Colo201, the lung cancer cell line A549 and the hepatocellular carcinoma cell line Hep-G2 in the co-culture system. After 5 days of co-culture, Caco-2, Colo201 and A549 cells were absent from co-cultures, whereas Hep-G2 cells were growing normally (data not shown). After removal of residual tumor cells and stimulation with LPS/IFN-γ, macrophages that had killed tumor cells displayed a cytokine profile comparable, but even

more pronounced, to those derived from MCF-7 co-cultures (Figure 25B). TNF-α was significantly lower in comparison to control macrophages stimulated with LPS/IFN-γ, whereas IL-8 was significantly increased. Macrophages from co-cultures with Hep-G2 cells displayed an activation profile similar to control macrophages, stimulated with LPS/IFN-γ (Figure 25B).

### 5.3.4  MCF-7 cell-derived S1P accounts for macrophage polarization

Since I had evidence that AC release S1P into the culture medium and further considering existing evidence that associates S1P production with tumor vascularization and growth (125, 126), I wanted to know whether S1P production in apoptotic MCF-7 cells contributed to macrophage polarization. This question was approached by using siRNA technology to knock-down SphK1 vs. SphK2 in MCF-7 cells. Knock-down of either SphK isoforms in MCF-7 cells was successful (Figure 26D). SiRNA supplied was isoform specific and a control siRNA further proved specificity. As an additional control, an interference of SphK1 or SphK2 knock-down on induction of MCF-7 cell death upon co-culture with macrophages was ruled out (Fig 26E).

Naïve macrophages, macrophages derived from a co-culture with MCF-7 cells or cells from a co-culture of MCF-7 cells with either SphK1 or SphK2 being knocked down were then used in the co-culture system (Figure 26). After 5 days of co-culture, tumor cells were removed and macrophages were stimulated with LPS/IFN-γ to follow cytokine production of TNF-α (Figure 26A), IL-10 (Figure 26B), or IL-8 (Figure 26C). As seen in previous experiments, macrophages from co-cultures with MCF-7 cells displayed reduced TNF-α, increased IL-8 but unaltered IL-10 production compared to naïve macrophages exposed to LPS/IFN-γ. Knock-down of SphK1 did not alter macrophage cytokine production as compared to changes provoked by apoptotic MCF-7 cells. However, knock-down of SphK2 affected the ability of MCF-7 cells to alter cytokine production in macrophages upon LPS/IFN-γ stimulation. With SphK2 being suppressed in MCF-7 cells during the co-culture, the macrophage response upon LPS/IFN-γ addition was similar to naïve cells in producing high TNF-α, low IL-8, with no changes in IL-10.
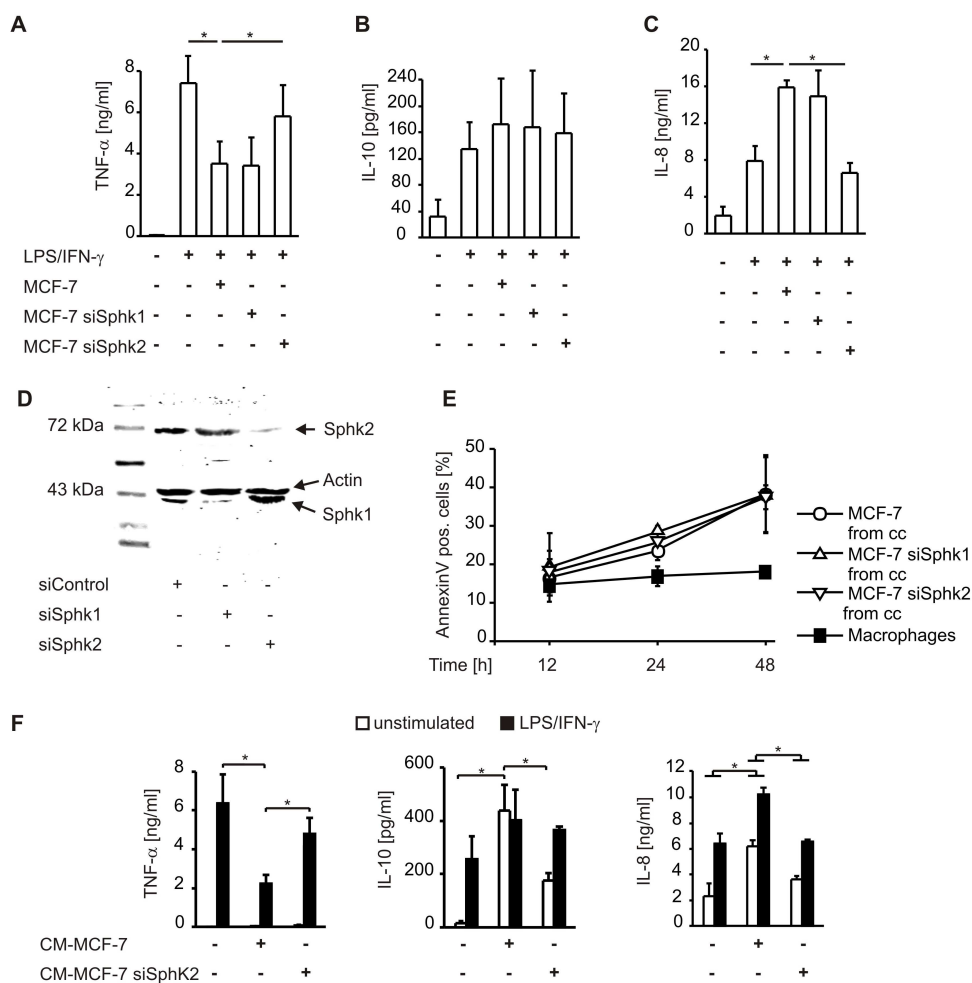
Figure 26: Knock-down of SphK2, but not SphK1 in MCF-7 cells restored a classical activation profile in human macrophages upon co-culture. Human primary macrophages remained as controls or were incubated for 5 days with MCF-7 cells or MCF-7 cells with SphK1 or SphK2 being knocked down with specific siRNA. Residual tumor cells were removed from co-cultures with 5 min accutase-treatment and 1 µg/ml LPS and 100 U IFN-γ were added to macrophages from co-cultures and control macrophages for 6 h. TNF-α (A), IL-10 (B) and IL-8 (C) contents in supernatants were quantified by FACS with BD Cytometric Bead Array Flex Sets. Data are presented as the mean ± SEM from five independent experiments. Statistically significant differences ($p < 0.05$) are marked with an asterisk. (D) Western analysis shows SphK1 and SphK2 expression in MCF-7 cells transfected either with control siRNA (siControl), siRNA against SphK1 (siSphK1) or SphK2 (siSphK2). One representative experiment out of three is displayed. Western analysis was performed 48 h after nucleofection. (E) Human primary macrophages remained as controls or were incubated with naïve MCF-7 cells or MCF-7 cells with SphK1 or SphK2 being knocked down with specific siRNA for the times indicated. Co-cultures and control macrophages were incubated for 30 min with accutase, harvested, stained with α-CD44-PE as a discrimination marker between macrophages and tumor cells and annexin V-FITC as a marker for cell death, and

analyzed by FACS. Data are presented as the mean ± SEM from three independent experiments. (F) Human macrophages remained as controls or were incubated with conditioned medium from apoptotic MCF-7 (CM-MCF-7) or MCF-7 cells transfected with siRNA against SphK2 (CM-MCF-7 siSphK2) cells for 24 h. Thereafter, supernatants were removed, cells were washed with PBS, fresh medium was added and macrophages were stimulated with 1 µg/ml LPS and 100 U IFN-γ for 6 h. Production of TNF-α, IL-10 and IL-8 was quantified by FACS with BD Cytometric Bead Array Flex Sets. Data are presented as the mean ± SEM from five independent experiments. Statistically significant differences ($p < 0.05$) are marked with an asterisk.

The same was true when supernatants from apoptotic MCF-7 cells, that were previously transfected with siRNA directed against SphK2, were added to macrophages. Compared to supernatants from unmodified apoptotic MCF-7 cells, the release of IL-8 and IL-10 from macrophages was largely suppressed (Figure 26F). Along that line, repression of TNF-α as well as induction of IL-8, elicited with LPS/IFN-γ in macrophages stimulated with supernatants from apoptotic MCF-7 cells, was significantly reduced when SphK2 was knocked down (Figure 26F).

As a final prove that tumor cell apoptosis and SphK2 knock-down affected S1P release, LC-MS/MS to quantify S1P release into supernatants of co-cultures and MCF-7 cell cultures was performed again in cooperation with the Institute of Clinical Pharmacology (Table 5). Supernatants of co-cultures of macrophages with MCF-7 cells, MCF-7 cells overexpressing Bcl-2 and MCF-7 cells with SphK2 being knocked down, were collected at a time when apoptosis was high in MCF-7 cells (24-48 h of co-culturing). Whereas S1P amounts in supernatants of control macrophages, co-cultures of macrophages with Bcl-2-overexpressing- or SphK2-knock-down-MCF-7 cells were below the reliable limit of quantification (0.5 ng/ml), S1P levels in co-cultures of macrophages with naïve MCF-7 cells were significantly elevated (Table 5; $p \leq$ 0.01). The same results where obtained, when S1P was quantified in supernatants of viable or apoptotic MCF-7 cells with or without SphK2 knock-down. Supernatants of viable MCF-7 were devoid of S1P, whereas S1P was released from apoptotic MCF-7 cells. Knock-down of SphK2 abrogated this release significantly (Table 5; $p \leq$ 0.01). These results implied that S1P

generated by SphK2 and derived from dying MCF-7 cells, altered macrophage polarization.

Table 5: S1P release from MCF-7 cells induced by co-culturing or staurosporine

_____

| Sample | S1P [ng/ml]* | SD (n ≥ 5) |
|---|---|---|
| MCF-7 cells: | | |
| Control | n.d. | - |
| | | |
| Staurosporine [0,5 ng/ml] | 4.02 | ± 1.51 |
| siSphK2 + Staurosporine [0,5 ng/ml] | 0.65 | ± 0.12 |
| | | |
| Co-cultures: | | |
| Macrophages | n.d. | - |
| Macrophages + MCF-7 | 5.65 | ± 2.79 |
| Macrophages + MCF-7 siSphK2 | n.d. | - |
| Macrophages + MCF-7-Bcl-2 | n.d. | - |

_____

*S1P contents in supernatants were measured with LC-MS/MS as described in the Materials and Methods section. The lower limit of quantification was 0.5 ng/ml. S1P concentrations in supernatants below this limit are marked with n.d.

### 5.3.5 MCF-7 cells or authentic S1P impair NF-κB activation in macrophages

M2 polarization of TAM has previously been attributed to diminished p65 nuclear translocation and thus to defective NF-κB signaling (98). To validate the co-culture model with respect to this TAM marker, NF-κB activation in macrophages exposed to apoptosis sensitive vs. resistant MCF-7 cells was investigated. EMSA analysis showed NF-κB activation in response to LPS/IFN-γ stimulation in macrophages from co-cultures with MCF-7-Bcl-2 or RKO cells (Figure 27A, lane 4-9). Supershift analysis was evident with an α-p65 antibody while α-p50 reduced NF-κB-DNA binding without shifting the complex to higher molecular mass. When macrophages had been co-cultured with MCF-7 cells prior to stimulation with LPS/IFN-γ, activation of NF-κB was

impaired (Figure 27A, lane 1-3). Negligible activation of NF-κB was also seen when macrophages were pre-exposed for 2 days to authentic S1P (Figure 27B). Statistic quantification of relevant changes is shown in part C of figure 27.
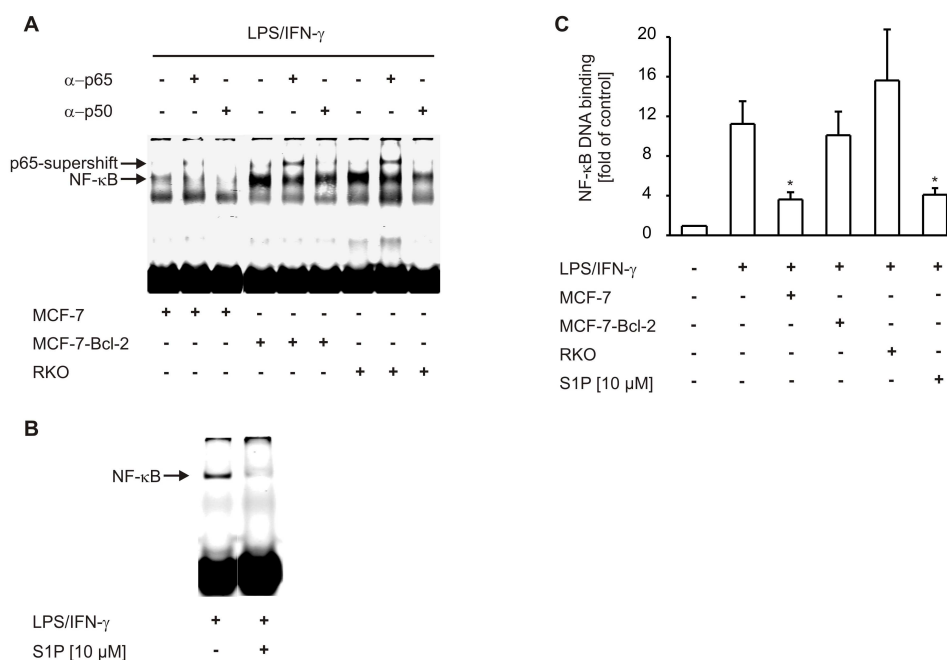


Figure 27: Macrophages display reduced NF-κB activation after co-culture with MCF-7 cells or addition of S1P. Human primary macrophage remained as controls, were incubated with MCF-7 cells, Bcl-2-overexpressing MCF-7 cells (MCF-7-Bcl-2), RKO cells for 5 days or 10 µM S1P for 2 days. Residual tumor cells were removed and 1 µg/ml LPS and 100 U IFN-γ were added to macrophages from co-cultures and control macrophages for 4 h. Activation of NF-κB was analyzed by EMSA using a specific 5'-IRD700-labelled oligonucleotide as described in Materials and Methods. Supershift analysis was performed with p65 and p50 antibodies (Santa Cruz Biotechnology) as indicated. (A) EMSA for NF-κB DNA binding activity in macrophages from co-cultures. One representative experiment out of three is displayed. (B) EMSA for NF-κB DNA binding activity in control and S1P-exposed macrophages following LPS/IFN-γ stimulation. One representative experiment out of three is displayed. Cells were pre-exposed for 48 h with 10 µM S1P prior to stimulation with 1 µg/ml LPS and 100 U IFN-γ. (C) The histogram shows quantification of EMSA data. Data are presented as the mean ± SEM from five independent experiments. Differences between LPS/IFN-γ-stimulated macrophages and macrophages from co-cultures or S1P-treated macrophages marked by asterisks are statistically significant ($p < 0.05$).

Collectively, these data implied that S1P as well as apoptotic tumor cells suppressed activation of NF-κB in macrophages while apoptosis-resistant tumor cells did not share this behavior. Macrophage polarization by apoptotic tumor cell-derived S1P was evident at the level of cytokine production as well as NF-κB activation.

## 5.4 SphK2 is important for tumor growth *in vivo*

Having evidence that SphK2-dependent S1P production in tumor cells was connected to TAM development, and thus possibly to tumor development, I wanted to establish an *in vivo* tumor model. MCF-7 breast cancer cells were efficient inducers of TAM-like macrophage polarization. Furthermore, TAM-dependent tumor promotion is well established for breast cancer (93). Therefore I planned to knock-down SphK2 in MCF-7 breast cancer cells, implant these cells and naïve MCF-7 cells into nude mice, and look for tumor growth and vascularization. Since these experiments are very time-consuming, I was not able to finish them until now. Nevertheless, the first results are promising.

### 5.4.1 Knock-down of SphK2 in MCF-7 cells

For high stability of SphK2 knock-down in MCF-7, specific hairpin siRNA was ligated into p*Silencer*$^{TM}$ 4.1-CMV neo vector, since this expression vector encodes the gene for resistance against the selection marker neomycin (G418). This vector, then named pSilencer-siSphK2, was nucleofected into MCF-7 cells, followed by selection of positive clones (MCF-7-siSphK2) with 500 µg/ml of G418. After three weeks, expression of SphK2 was verified by Western blot analysis in MCF-7-siSphK2 versus naïve MCF-7 cells (Figure 28). MCF-7-siSphK2 cells displayed reduced SphK2 expression down to 25% compared to control MCF-7 cells. For comparison, expression of SphK1 was also investigated. SphK1 levels were not reduced by transfection with pSilencer-siSphK2. On the contrary, it rather seemed up-regulated. This may be a cellular mechanism, ensuring stable intracellular levels of S1P, a compensatory process which was also observed previously in either SphK1 or

SphK2 knockout mice. However, knock-down of SphK2, which was controlled every two weeks, was stable during culture. Therefore, MCF-7-siSphK2 cells were suitable for the mouse model.
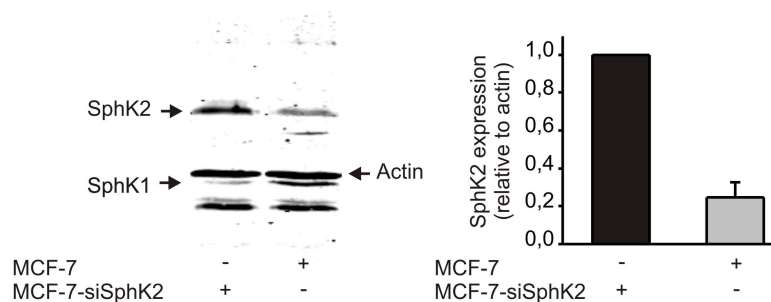


Figure 28: Knock-down of SphK2 in MCF-7 cells. MCF-7 cells were controls or transfected with pSilencer-siSphK2 (MCF-7-siSphK2). Western analysis shows expression of SphK2 and SphK1. One representative experiment out of five is displayed. Histogram shows quantification of Western data normalized to actin. Data are presented as the mean ± SEM from five independent experiments.

## 5.4.2  Growth of MCF-7-siSphK2 tumors is impaired in nude mice

Together with Dr. Susanne Schiffmann from the Institute of Clinical Pharmacology, I started the first *in vivo* experiment. MCF-7 cells and MCF-7-siSphK2 cells were injected subcutaneously at the left and right dorsal flank of female nude mice (166). Three weeks after the MCF-7 control tumors started growing, the mice were sacrificed, perfused and the tumors were extracted. The growth of MCF-7-siSphK2 xenografts was largely impaired in comparison to MCF-7 xenografts (Figure 29). In fact, MCF-7-siSphK2 tumors started growing approximately two weeks after the control tumors. Furthermore, tumor growth appeared to be less structured, since MCF-7-siSphK2 xenografts grew rather flat compared to globular growing control tumors and displayed a spongy texture when touched.

The extracted tumors were used for the preparation of cryosections. Sections from both xenografts were stained for infiltration of mouse macrophages with an antibody against the macrophage marker F4/80 (167), and for presence of blood vessels using an antibody against the endothelial cell marker CD31 (168).
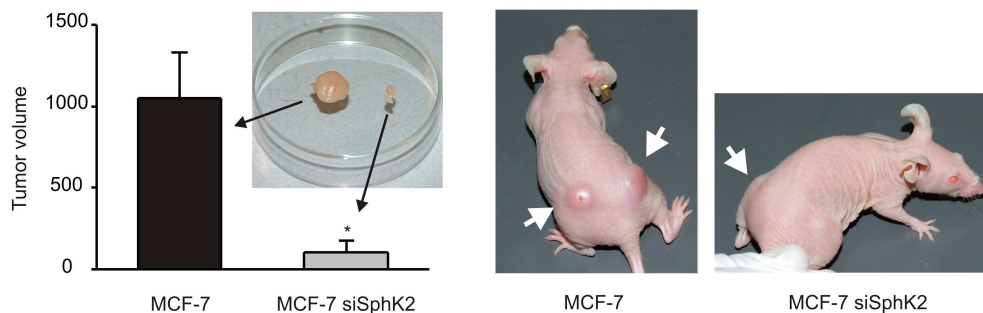
Figure 29: Growth of MCF-7 and MCF-7-siSphK2 xenografts in nude mice. 1 x $10^7$ MCF-7 cells (n = 8) or MCF-7-siSphK2 cells (n = 6) were injected subcutaneously at the both dorsal flanks. The tumor volume is displayed three weeks after MCF-7 xenografts started to grow. Data are the mean ± SEM of the tumor volumes. Growth of MCF-7-siSphK2 tumors was significantly reduced, compared to MCF-7 tumors (* = $p < 0.05$). Photographs display representative mice. Xenografts are indicated with white arrows.
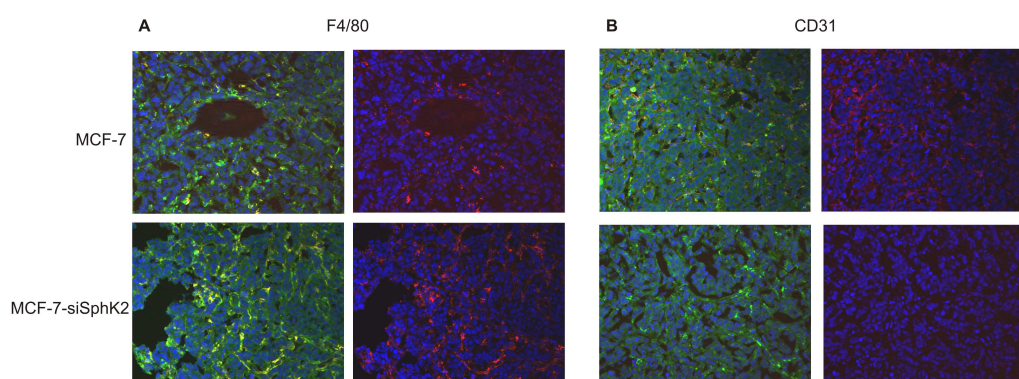


Figure 30: Macrophage infiltration and blood vessel growth in tumor xenografts. Cryosections of MCF-7 or MCF-7-siSphK2 xenografts (A and B) were either stained for the macrophage marker F4/80 (A) or the endothelial cell marker CD31 (B), both counterstained with Cy3-labelled secondary antibody (red). Nuclear staining was performed with DAPI (blue), cytosol is the background of green fluorescence (green). Cryosections of three different tumor xenografts each were stained and representative images are shown.

Strikingly, MCF-7-siSphK2 tumors were almost completely devoid of blood vessels in comparison to MCF-7 tumors (Figure 30B), although both xenografts were infiltrated with macrophages (Figure 30A). Therefore, if reduce tumor growth is due to SphK2 deficiency, it is a result of macrophage polarization rather than macrophage numbers.

# 6      Discussion

Macrophages display opposing activities in human physiology and pathology by adopting different phenotypes. Thereby they shape inflammation (59) as well as diseases that are closely linked to inflammatory dysfunction, including cancer (169) and atherosclerosis (34). Activation patterns of macrophages are reflected at the level of their mediator profile. Macrophages may act as 'killers' (the M1 phenotype), when they produce pro-inflammatory cytokines or present antigens on their surface, thus activating other immune cell populations, or when they release bactericidal/cytotoxic agents like NO, ROS or TNF family proteins (61). 'Killer' macrophages drive the host response against pathogens and destroy tumor cells, but they are also key players in chronic inflammatory disorders. On the other hand, macrophages can also act as 'healers' (the M2 phenotype) by modulation or suppression of immune responses, which is associated with tissue remodeling and promotion of angiogenesis (87). 'Healer' macrophages facilitate the termination of inflammation and promote $T_H2$ immunity, but they also promote tumor development by induction of angiogenesis and tumor cell survival.

Distinct M2 phenotypes have been described (3.3.1), which are believed to be extremes of a continuum rather than fixed patterns (87). Macrophage phenotypes are therefore often considered as extremely versatile, depending on the exact composition of the respective microenvironment. Contradictory, it has been suggested that macrophage activation profiles, once established, are highly stable and nearly inconvertible. This is especially true for M2 macrophages (170). Stable functional responses may be a reason why macrophages are key players in a variety of human pathologies. After activation, reprogramming turns out to be highly intricate. Defects may then lead to prolonged activation, which may be either chronic inflammation, or likewise 'chronic anti-inflammation'. Most interestingly, AC may be one of the rare means to shape macrophage polarization even after activation. Extreme pro-inflammatory macrophage phenotypes associated with the capacity to induce apoptosis of tumor or glumerular cells are suppressed by the uptake of apoptotic debris (171). Taking this into consideration, it is obvious that a

detailed understanding of the mechanisms of macrophage programming may lead to the identification of therapeutic strategies, which are targeted at cutting the Gordian knot in inflammatory disorders (172).

My studies where therefore aimed at a mechanistic understanding of how alternative macrophage polarization is achieved and preserved:

1)      I started with investigations on macrophage survival after interaction with AC and tried to understand its induction, its source and the molecular pathways involved in that process.

2)      Knowing that S1P was released by AC, my aim was to define the underlying mechanistic principle.

3)      Being aware that activation patterns of TAM and AC-primed macrophages are comparable, I investigated a putative connection in an *in vitro* co-culture system.

4)      After I had identified SphK2-dependent S1P production as a prerequisite for macrophage polarization in the co-culture system, I started with an *in vivo* tumor xenograft model to clarify the relevance of SphK2 and S1P in tumor development.

## 6.1   Macrophage survival induced by apoptotic cells

The first part of my studies supports the notion that AC not only modulate pro- vs. anti-inflammatory mediator release from macrophages, but also affect their susceptibility towards apoptosis. Cell protection was initiated by liberating S1P from AC (Figure 31).

So far, two studies have indicated macrophage resistance against apoptosis after interaction with AC. Reddy *et. al.* observed protection of murine macrophages from apoptosis induced by cytokine withdrawal, which demanded phagocytosis of AC and activation of PI3K-signaling as suggested by the use of colchicines and LY294002, respectively (173). Unfortunately,

colchicine is rather unspecific, and besides blocking phagocytosis it depletes calcium from internal stores (174). Therefore, this study cannot determine whether uptake of apoptotic material and/or PI3K activation are distinct or uniform cell responses. However, protection from apoptosis induced by AC was corroborated for macrophages in another study and in addition shown for non-professional phagocytic epithelial cells (175). Specifically, the authors achieved survival effects with supernatants from phagocytes co-cultured with AC. This implied paracrine signaling, which was in contrast to the above-mentioned phagocytosis. Promotion of survival correlated with VEGF secretion from epithelial cells and up-regulation of Bcl-2. Although VEGF is known to act para- and autocrine in regulating epithelial cell survival, in part by PI3K/Akt-induced Bcl-2 expression (176, 177), a direct connection between VEGF secretion and Bcl-2 has not been investigated (175).

Connections to the results I obtained are striking. Macrophage protection in my system against apoptosis was mediated via S1P from AC. The participation of S1P cannot be excluded from the results obtained in the other studies, since no control experiments with ACM were performed. However, the results obtained for activation of the PI3K-pathway and Bcl-2 up-regulation, are supported by my data.

S1P is known to provoke survival in different cell types by binding to its high affinity G-protein coupled receptors (102, 178, 179). Five different receptors for S1P are known to date, of which subtypes 1 to 4 are shown to be predominantly expressed on human macrophages (157, 158). Down-regulation of S1PR1 on primary macrophages partially diminished protection by supernatants from AC. This may indicate that protection of S1P in macrophages is transmitted by more than one S1PR subtype expressed on their surface. Further experiments using knock-down approaches should be performed to clarify the relative contribution of S1PRs towards macrophages protection by S1P.

S1P-receptors activate PI3K and/or ERK1/2 (179). Inhibitor studies pointed to these pathways in conveying protection by ACM, which resulted in phosphorylation of Bad at Ser136. It is an established function of the PI3K/Akt pathway to attenuate the apoptotic machinery (180), among other cells in

macrophages (181). These data are in close concordance with the studies mentioned above.
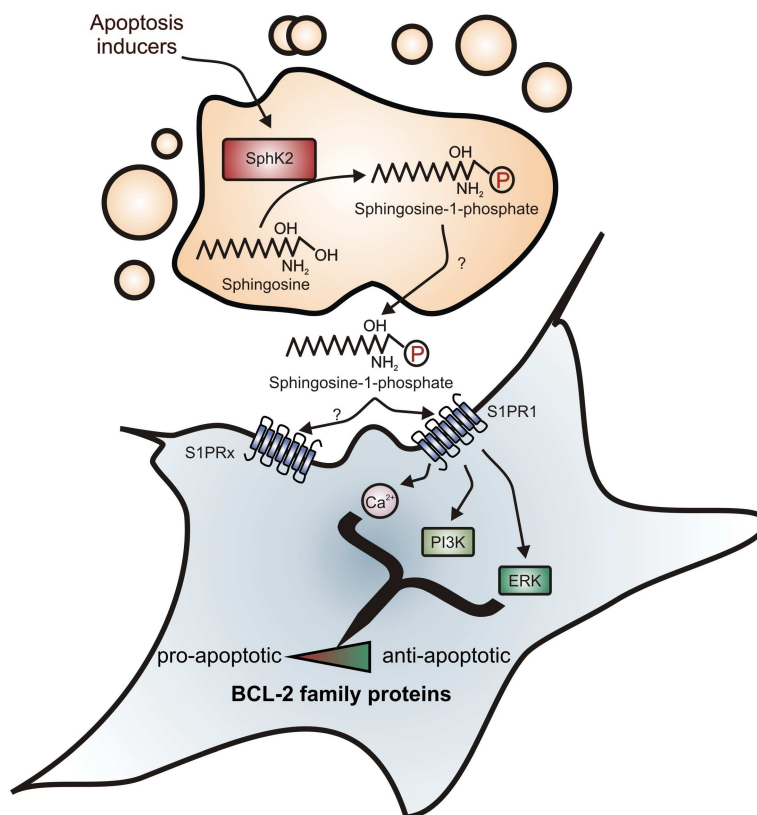


Figure 31: Macrophage protection by AC-derived S1P. AC produce sphingosine-1-phosphate (S1P) depending on sphingosine kinase (SphK) 2. S1P then binds to its specific receptors (S1PRx), especially S1P-receptor 1 (S1PR) on the macrophage surface. S1P activates $Ca^{2+}$-, phosphatidylinosotol-3 kinase (PI3K)- and extracellular signal-regulated kinase (ERK)-dependent signaling, which induces a shift in the macrophage's Bcl-2 family protein activity pattern towards anti-apoptotic.

ERK1/2 activation in macrophages usually is a signal downstream to growth factors or cytokines such as M-CSF, IL-3 or TGF-β (182, 183). TGF-β seems of interest, because it is secreted by AC (83). Yet the possibility that ERK1/2 is activated by TGF-β to contribute to Bcl-2 up-regulation must be excluded under the used experimental conditions, bearing in mind the lipophilic nature of the factor under investigation. It was shown previously that extracellular S1P inhibits bone marrow-derived macrophage cell death induced by M-CSF withdrawal (156). This was related to PKB activation, increased Bcl-$X_L$

expression, and decreased acid sphingomyelinase activity, thus reducing ceramide production. Although I noticed increased expression of Bcl-$X_L$, its induction was not affected by blocking PKB. These data provide evidence that besides PKB, another pathway seems to be involved in Bcl-$X_L$ induction. However, expression of Bcl-2 and Bcl-$X_L$ as well as Bad phosphorylation was noticed with ACM and authentic S1P.

S1P receptor activation triggers intracellular $Ca^{2+}$-signals (102, 178, 179). $Ca^{2+}$-signals are involved in ACM-mediated macrophage survival, as shown by the use of the intracellular $Ca^{2+}$ scavenger Bapta-AM. Although $Ca^{2+}$ signals usually promote apoptosis by mitochondrial $Ca^{2+}$ overload and subsequent release of pro-apoptotic factors (184), there are indications that a modest $Ca^{2+}$ increase elicits anti-apoptotic responses via $Ca^{2+}$/calmodulin-dependent kinase-induced PKB activation, which results in Bad phosphorylation (185). This agrees quite well with my findings showing that Bad phosphorylation not only depends on PI3K- but also on $Ca^{2+}$-signaling. Furthermore, this may explain the results obtained with colchicine by Reddy *et. al.*, since colchicine may block $Ca^{2+}$-mediated responses. It remains to be clarified, whether PI3K- and $Ca^{2+}$-pathways work synergistically or independently. Since either reducing the expression of Bcl-2 or diminishing Ser136-Bad phosphorylation were sufficient to recover caspase-3 activity, I assume that the Bcl-2-family rheostat is more important than expression modulation or phosphorylation of individual proteins such as Bcl-2 or Bad.

Release of S1P from apoptotic Jurkat cells was necessary for macrophage protection, as was demonstrated by transwell experiments, by the use of ACM in combination with the sphingosine kinase inhibitor DMS, and via liquid chromatography-tandem mass spectrometry. Knock-down studies using siRNA revealed a vital role of SphK2 in apoptosis-dependent S1P production. SphK2 activity during apoptosis has been previously reported but was linked to promotion of apoptosis (121, 186). However, knock-down of SphK2 did not diminish the induction of apoptosis in Jurkat cells. So far, my data expanded the role of SphK2 in regulating apoptosis: it is not only involved in apoptosis induction inside cells but also acts as an inhibitor once it releases its product.

Other potential mediators released from AC can formally be excluded to contribute to ACM protection. TGF-ß does not fulfill criteria of a lipid

messenger. LPC (187) only attenuated macrophage apoptosis when supplied at high concentrations of roughly 100 µM, a concentration that is unlikely to be of physiological relevance. Arachidonic acid and/or derived metabolites, released during apoptosis (188) could also be excluded, because they are not extractable with chloroform (35). The new role of S1P as an anti-apoptotic mediator released from AC adds to existing concepts on the anti-inflammatory role of S1P. This might be relevant to fully understand the phenotype switch in macrophages that is induced by AC. As the production and release of S1P during apoptosis have not been reported so far, future studies were needed to define the role of SphK2 in this process, as well as release pathways for S1P.

## 6.2   The mechanism of S1P release from apoptotic cells

Exploring the mechanism of S1P release from AC, I found that a truncated, enzymatically active SphK2 was shed from AC upon cleavage by caspase-1 at its N-terminus (Figure 32). It is important to stress that sphingosine kinases may produce S1P outside the cell because all enzymes necessary for degradation of sphingomyelin to sphingosine are present at the outer leaflet of the plasma membrane or are constitutively secreted (189). This was already corroborated *in vivo* since the presence of catalytically active SphK1 was observed in mouse plasma (107).

SphK2 co-localized with caspase-1 at the plasma membrane during apoptosis. Preventing translocation of SphK2 to the plasma membrane inhibited its cleavage by caspase-1 (Figure 12). In HEK293 cells, SphK2 was distributed mainly throughout the cytosol. Other cell types with predominant nuclear localization have been described, based on the NLS in the N-terminus of SphK2 (120), which raises the question how SphK2 can be cleaved and released under these conditions. However, during apoptosis caspase-1 may also enter the nucleus (190), which may allow nuclear cleavage. Furthermore, a putative nuclear export signal (NES) in SphK2 was identified recently (191). Together with the removal of the NLS by caspase-1, this might prepare SphK2 for nuclear export and release from the cell.

Alternatively to caspase-1 dependent cleavage, other mechanisms preserved in the apoptotic machinery may contribute to SphK2 release from AC. Recently, the sources for apoptotic body membranes were defined (192). Budding of apoptotic bodies from cells is strictly associated with an extension of the cell membrane surface. Franz *et. al.* could verify the ER as a source for apoptotic body membranes in late apoptosis. In one study dealing with the implications of SphKs in apoptosis, SphK2 translocated to the ER during cell death to promote increases in ceramide levels (108). Combining these results, the following pattern might be conceivable: SphK2, being coupled to ER membranes, is recruited to apoptotic bodies, where it produces S1P, which is then transported into the extracellular space by specific ABC family transporters. Although there was no indication for a cleavage-independent release of SphK2 in the time frame of my investigation, this might contribute to S1P production during late apoptosis.

Attenuating PS exposure during apoptosis blocked the release of truncated SphK2 (Figure 20). These findings raise the exciting possibility that PS exposure is directly involved in SphK2 release or even is the primary mechanism. The release of proteins that is linked to PS exposure may require a flipping mechanism, which was previously suggested for annexins (193, 194) and which might work for SphK2 as well. In such a model, SphK2 translocates to the inner leaflet of the plasma membrane early during apoptosis, binds to PS, is cleaved by caspase-1 and subsequently transported to the cell surface together with PS. PS externalization requires the action of scramblase (195). Therefore, knock-down of scramblase would be another approach to prove that SphK2 is directly connected to PS exposure. Obviously, the necessity for caspase-1 dependent cleavage is questionable in this model. One might speculate that regulatory proteins are possibly bound to the N-terminus of SphK2, thus preventing externalization, and are then removed by specific N-terminal cleavage. However, my observations provide a new mechanistic explanation how PS exposure on AC may influence the phenotype of phagocytes by promoting the release of SphK2 with proximate S1P formation. In fact, SphK2 could be another PS 'receptor', in this case provided by AC, transmitting the most prominent cellular alteration during apoptosis to functional responses in macrophages.
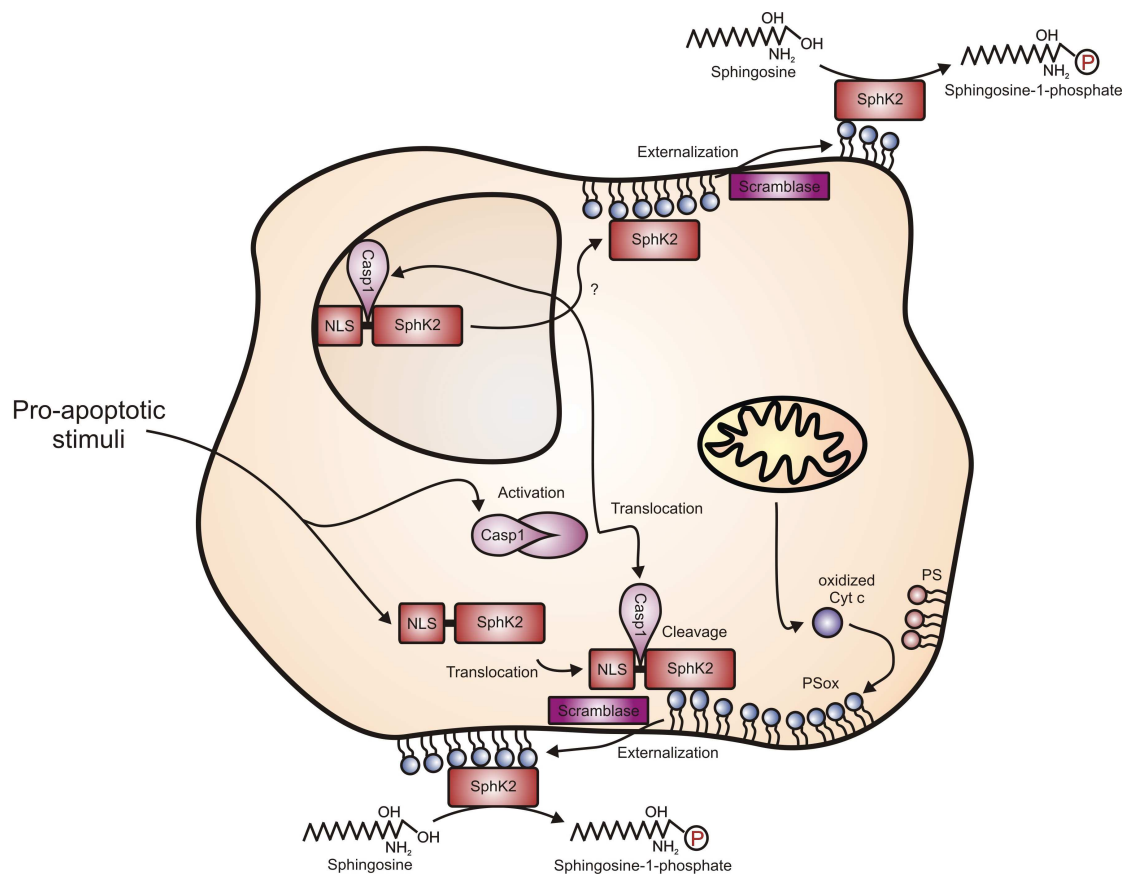
Figure 32: The mechanism of S1P production by AC. Sphingosine kinase (SphK) 2 translocates to the plasma membrane during apoptosis by binding to phosphatidylserine (PS) at the inner leaflet of the plasma membrane. Moreover, caspase-1 (Casp1) is activated and cleaves SphK2 at its N-terminus. Mitochondria-derived oxidized cytochrome c (Cyt c) oxidizes PS, which is transported to the extracellular side of the plasma membrane by scramblase. Cleaved SphK2 is externalized due to its PS-binding. Subsequently, it phosphorylates sphingosine to sphingosine-1-phosphate in the extracellular space. SphK2 may also be localized in the nucleus, where it can be cleaved by Casp1, thereby losing its nuclear localization signal (NLS). SphK2 may then leave the nucleus, bind to PS and be externalized.

Taken together, my results show a hitherto neglected role of caspase-1 in modulating immune responses. Besides promoting the maturation of pro-inflammatory cytokines (14), its activation during apoptosis in combination with PS exposure delivers a signal to cleave and release SphK2, which allows to produce S1P outside of cells. S1P formation is capable of inducing $T_H2$ responses by polarizing immune cell populations such as dendritic cells (196) or T cells (197). This implies the rather surprising conclusion that caspase-1,

in the context of PS exposure, may actually have anti-inflammatory properties regarding immune cell polarization. On the other hand, S1P plays a major role in lymphocyte recruitment (103). Therefore, caspase-1 activation again might secure proper inflammatory responses against invading pathogens by attracting lymphocytes and dendritic cells to inflamed areas via assembling S1P gradients. However, given the importance of S1P in several human pathologies including cancer (125), extracellular SphK2 may represent an interesting drugable target, at least if cell death is involved.

## 6.3 Macrophage polarization by S1P

Increasing evidence suggests TAM as important players in tumor progression. In some human cancers they even emerge as prognostic markers (89, 90). Their pro-tumor activities are associated with polarization towards an M2 phenotype. This alternative activation program is driven by the tumor microenvironment, which includes tumor-derived immunosuppressants as well as tumor hypoxia (92). My studies pointed to tumor cell apoptosis as an additional process in affecting the tumor microenvironment and thus macrophage polarization (198). Previous research has shown that pretreatment of macrophages with apoptotic, but not necrotic, tumor cells reduces their cytotoxicity, i.e. their capability of producing NO and ROS (96). Considering the production of TNF-α as a potentially harmful agent (there is a reason why it is called tumor necrosis factor), my data support the notion that TNF-α is produced in a co-culture of macrophages with MCF-7 cells, with the latter ones being killed. However, once AC had been generated in the co-culture set-up, the production of TNF-α declined and co-cultures produced substantially smaller amounts of the cytotoxic agent upon LPS/IFN-γ stimulation in comparison to activation of naïve macrophages. Moreover, a second administration of fresh tumor cells to macrophages, previously primed by apoptotic tumor cells, did not elicit a new peak of TNF-α formation and did not result in tumor cell killing. Along that line, MCF-7 cells overexpressing Bcl-2 were not killed by macrophages, because Bcl-2-overexpressing cells, especially Bcl-2-expressing MCF-7 cells, are resistant to TNF-α-induced

apoptosis (199). Thus, the presence of AC attenuates TNF-α formation in macrophages, and affects their cytotoxic potential towards tumor cells. Presumably, the interaction with apoptotic tumor cells affects other mechanisms of macrophage cytotoxicity, that were investigated previously (96). Nevertheless, tumor cell killing by macrophages that had been primed with dying tumor cells beforehand was disabled.

Besides reducing macrophage cytotoxicity, AC may further affect the tumor microenvironment because they release immune modulators such as TGF-β and IL-10 (83, 84). In my system, dying tumor cells did not release IL-10 (quantified with the CBA as a control), although this may depend on the tumor cell type. Nevertheless, conditioned medium from apoptotic tumor cells induced phenotype alterations in macrophages.

As in co-cultures with MCF-7 cells, IL-10 production in macrophages was enhanced with conditioned medium from dying tumor cells. Although mechanistically unexplained, an increase in IL-10 was correlated to defective NF-κB binding in TAM (164) and the inability to activate NF-κB was also observed upon recognition of AC by macrophages (79). In the latter system, a short-term binding of AC to macrophages did not affect NF-κB DNA binding, but depleted p300, thus impairing transcriptional activation of NF-κB (79). Importantly, attenuated NF-κB activity is a critical marker of the TAM phenotype (98). My experiments favored S1P, a soluble factor, in blocking NF-κB following long-term exposure of AC to macrophages. This was unexpected, since NF-κB activation rather than inhibition was shown for S1P in other cell systems (200). Despite S1P itself might induce low NF-κB activation also in macrophages, it completely abrogated TNF-α-mediated stimulation of NF-κB in THP-1 human monocytes (201). Further supporting evidence emerged from a study investigating the effect of the S1PR agonist FTY720 in an *in vivo* model of liver injury. FTY720 induced expression of A20 (202), a deubiquitinase capable of terminating Toll-like receptor (TLR)- or TNF receptor-induced NF-κB signaling (203). Up-regulation of A20 started after 6 h and hence was dependent on S1PR activation rather than internalization. Although the impact of S1P on NF-κB signaling is unclear at present, it may help to understand macrophage polarization by apoptotic tumor cells.

Activation vs. inhibition may depend on the S1PR expression profile in different cell types and/or on the duration of S1P exposure, as well as the presence or absence of co-stimuli such as LPS/IFN-γ.

S1P from apoptotic MCF-7 cells changed the LPS/IFN-γ activation profile in macrophages. It suppressed TNF-α formation but increased IL-8 production in macrophages upon LPS/IFN-γ activation and most likely provoked IL-10 liberation during interaction with dying cells. Reduced TNF-α production may result from a diminished NF-κB activity, whereas alterations in interleukin production may be associated with activation of STAT1 and/or PI3K-signaling because activity of these signaling pathways is characteristic for M2 macrophages (98, 204).

Production of the immunosuppressive cytokine IL-10 is characteristic for TAM. Although underlying molecular pathways remain unclear, it is known that S1P can provoke secretion of IL-10 from T-cells and dendritic cells, which was furthermore correlated to a diminished pro-inflammatory activity in these cells (196, 197). IL-10 formation may require PI3K signaling, a pathway that is activated downstream of S1PRs (179). Furthermore, PI3K may negatively regulate TLR-signaling during inflammation, thus down-regulating NF-κB signaling (205) and has been proposed as a potential target to circumvent immunosuppression in cancer (206). In this respect, knockout of Src homology2-containing inositol-5'-phosphatase (SHIP), a potent negative regulator of PI3K, induced on itself a M2-like phenotype in mouse macrophages, which was strikingly associated with impaired NO-production and enhanced tumor growth (204). Moreover, phosphorylation-dependent inhibition of glycogen synthase kinase 3 (GSK3)-β, a downstream target of PI3K, reduced TNF-α and IL-12 but increased IL-10 release from monocytic cells (207) thereby adding evidence for a immune regulatory role of PI3K.

As stated above, IL-10 was previously related to defective IL-12 production in TAM, which was furthermore explained by defective NF-κB signaling (164). IL-10 was produced in co-cultures with MCF-7 cells, even after tumor cells were killed. Therefore, co-culture primed macrophages should produce less IL-12-p70, which indeed was the case. IL-12-p70 and TNF-α production in macrophages from co-cultures were equally affected. Therefore I did not investigate the release of IL-12-p70 in further experiments. However, I

observed that S1P reduced NF-κB DNA-binding. Since NF-κB is the principal pro-inflammatory transcription factor, it is likely to attenuate generation of IL-12-p70 as well (205).

Enhanced production of IL-8 in macrophages derived from MCF-7 co-cultures is not immediately apparent considering the attenuated activity of NF-κB, a prominent inducer of IL-8 (208). Under conditions of S1P release, other transcriptional activators of IL-8 such as C/EBPβ, AP-1, or STAT1 may substitute for NF-κB and it will be interesting in the future to define how S1P enhances IL-8 production.

Despite uncertainties in IL-8 regulation, its production may explain how S1P contributes to tumor angiogenesis, since IL-8 expression was related to TAM-dependent angiogenesis and poor prognosis in uterine cancer (209). As mentioned in the introduction, recent *in vivo* studies refer to a role of S1P in tumor vascularization (125, 126). Forced S1P receptor desensitization with FTY720 abrogated S1P- and VEGF-induced angiogenesis and attenuated metastatic tumor growth (126). Moreover, the use of a monoclonal S1P antibody reduced tumor growth via inhibition of tumor angiogenesis and survival (125). These observations support a direct connection between S1P production and tumorigenesis, although the source of S1P in human tumors is undefined.

Considering that high levels of SphK1 in glioblastoma correlated with low patient survival (210), it seems attractive to assume gain of expression regulation as an underlying mechanism. My studies identified SphK2 activity in close association with tumor cell apoptosis induced by macrophages as another possible S1P origin. The release of S1P from apoptotic, but not viable tumor cells induced macrophage polarization towards an alternatively activated phenotype, characterized by a change in cytokine production, reduced tumor cytotoxicity and an attenuated NF-κB response (Figure 33).

As mentioned, other factors such as TGF-β or PS may account for phenotype alterations in macrophages after interaction with AC (10, 83). Since suppression of S1P release via SphK2 knock-down did not restore TNF-α completely, these molecules might also be involved in triggering the macrophage phenotype. Nevertheless, one has to keep in mind that S1P production during apoptosis is also dependent on PS exposure. Furthermore,

S1P was shown to mimic the anti-inflammatory signaling properties of TGF-β by cross-activating the TGF-βII receptor (211). Therefore, functional responses depending on these two molecular signals may depend on a crosstalk with S1P signaling.
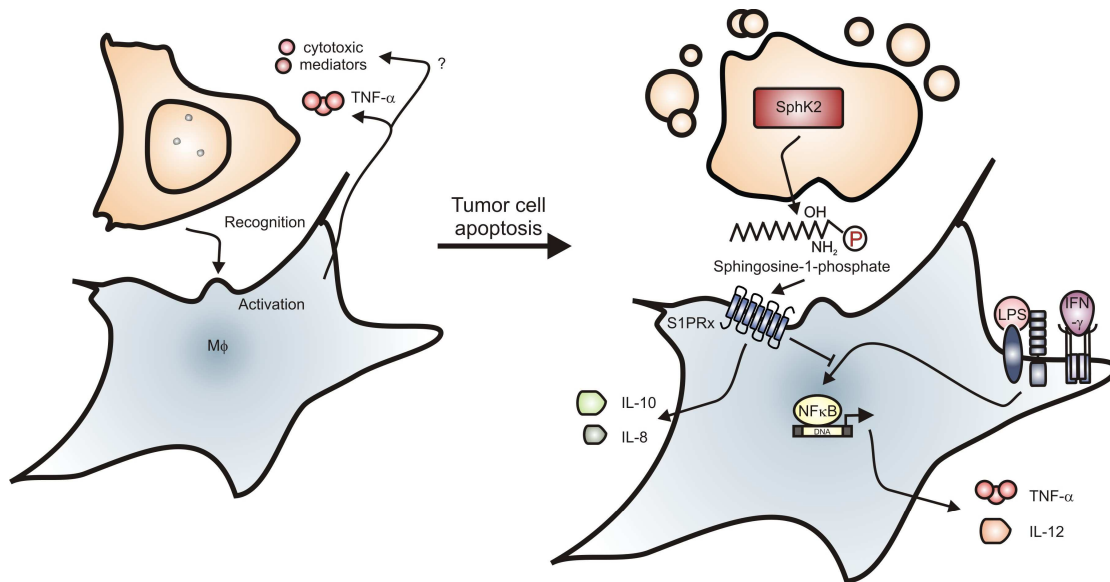


Figure 33: Tumor cell apoptosis polarizes macrophages. Macrophages produce tumor necrosis factor (TNF)-α, and potentially other cytotoxic mediators, upon recognition of tumor cells. Tumor cells undergo apoptosis, whereupon they produce Sphingosine kinase (SphK) 2-derived sphingosine-1-phosphate (S1P). S1P most likely binds to its receptors (S1PRx) on the macrophage surface. S1P suppresses lipopolysacharide (LPS)/interferon (IFN)-γ-induced TNF-α and interleukin (IL)-12 release from macrophages, probably via inhibition of NF-κB DNA binding. Furthermore, S1P mediates the production of IL-10 and IL-8.

Taken together, my results suggest that induction of tumor cell apoptosis by invading macrophages may account as an additional process to explain the existence of TAM. This may be true at least in early stages of tumor formation, where the tumor has not yet acquired full resistance against apoptosis via a series of beneficial mutations.

## 6.4   *In vivo* evidence for SphK2 implication in cancer development

Being aware of the co-culture system's limitations in proving a role of S1P produced by apoptotic tumor cells via SphK2 in cancer development, I started the tumor xenograft model in nude mice. It could be argued that the nude mouse model is limited as well for the study of immunity-dependent aspects of tumor development, since nude mice are devoid of thymus-derived T cells. However, this model might be considered as straightforward for studying the role of macrophage polarization in this context, because nude mouse macrophages tend to exhibit a basal M1 phenotype even without respective stimulation (212). This would fit well to the hypothesis that emerged from my previous observations: Macrophages would then induce tumor cell death upon which they would develop a TAM-like phenotype, promoting growth, survival and sustentation (via blood vessel infiltration) of remaining tumor cells (Figure 34).

The first results that emerged from the nude mouse xenograft model were encouraging. I noticed markedly reduced growth of MCF-siSphK2- compared to MCF-7 xenografts. This was accompanied by reduced angiogenesis in MCF-7-siSphK2 tumors. Importantly, the number of infiltrating macrophages was not decreased in MCF-siSphK2 tumors in comparison to control tumors. Indeed, rather the reverse was observed. Because Lin *et. al.* provided strong evidence that macrophage are essential in promoting the angiogenic switch, at least in this model of breast cancer, it can be concluded that rather macrophage polarization than their simple presence is crucial.

I must admit, that although the current data could be interpreted in that way, the persuasiveness is weak at present. It could simply be argued that SphK2 knock-down in tumor cells interferes heavily with total sphingolipid metabolism since production of ceramide species during apoptosis may depend on the action of SphK2 (108), thereby producing macrophage-independent side effects. However, following this objection consequently, it is more likely that SphK2 depletion would foster tumor progression by reducing pro-apoptotic ceramide levels. Contrarily, my data clearly show tumor growth suppression by SphK2 depletion.
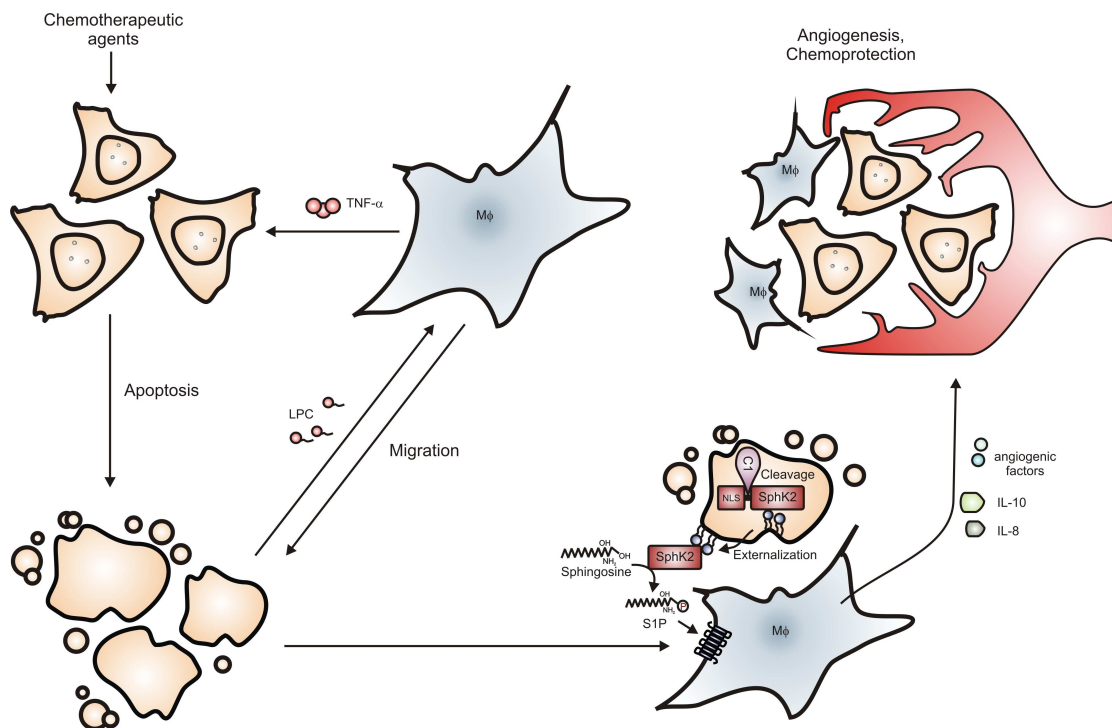
Figure 34: A role of tumor cell death-derived S1P in tumor development. During early stages of tumor progression, macrophages may induce tumor cell death, e.g. via tumor necrosis factor (TNF)-α. Induction of tumor cell death is furthermore a major aim in chemotherapy. Apoptotic tumor cells produce lysophosphatidylcholine (LPC), which attracts macrophages. Moreover, sphingosine kinase (SphK) 2 may be released from apoptotic tumor cells after binding to phosphatidylserine (PS) on the intracellular plasma membrane surface, followed by caspase-1 (C1)-mediated N-terminal cleavage and subsequent release into the intracellular space, due to PS binding. SphK2 catalyzes the conversion of sphingosine to sphingosine-1-phosphate, which induces an alternatively activated phenotype (M2) in macrophages. The M2 macrophages release cytoprotective and/or pro-angiogenic factors such as interleukin (IL)-10 and IL-8, which provokes protection of tumor cells against cell death and to enhanced tumor angiogenesis.

Another possible demur against my hypothesis is the missing experimental evidence for tumor cell death induction in the nude mouse model. One approach to solve this problem could be the use of Bcl-2-overexpressing MCF-7-siSphK2 cells for the xenograft model. These cells should be protected from apoptosis (5.3.2) and, in concordance with the hypothesis, should produce well growing tumors.

Conclusively, SphK2 seems to be important for tumor growth *in vivo*. Whether this is macrophage-dependent or not will be studied in further experiments.

Therefore, macrophages will be isolated from MCF-7-siSphK2- and MCF-7 xenografts and analyzed for cytokine production, both under basal conditions and after stimulation with M1 phenotype-inducing agonists. If the hypothesis proves to be correct, extracellular SphK2 should be considered as a target for tumor therapy, at least in breast cancer.

## 6.5   Concluding remarks

Recognition of AC by macrophages, which provokes a macrophage phenotype shift towards M2, is crucial for the termination of inflammation and plays a role in human pathologies that are associated with inflammation and/or apoptosis. Many aspects of AC-dependent macrophage polarization where attributed to specific recognition of PS and/or subsequent release of TGF-β, acting in an autocrine manner to reprogram macrophages (3.3.2). I could show that AC-derived S1P considerably contributes in shaping alternative macrophage polarization. Interestingly, this was also dependent on PS. Therefore, S1P production by AC could be considered as another feature of 'specific recognition', besides e.g. PS recognition by VnR or identification of CD31 modification, which in this case is binding of S1P to its specific receptors (most likely S1PR1) on the macrophage surface. Furthermore, S1P might be important to support the effects of TGF-β, via cross-activation of TGF-β receptor-dependent signaling pathways (211). Moreover, S1P may account for additional characteristic features of macrophage polarization that are induced by AC. It may induce expression of COX-2, thereby eliciting $PGE_2$ production (213), which was indeed recently observed in our laboratory (Johann *et. al.*, The Journal of Immunology, in revision). My studies irradiate a new aspect of AC-dependent macrophage polarization. What exactly are the contributions of S1P and SphK2, compared to other mediators, regarding regulation of inflammation and tumor development might well be of value to understand the development of certain human diseases.

# 7    References

1.   Castedo, M., et al., Cell death by mitotic catastrophe: a molecular definition. Oncogene, 2004. 23(16): p. 2825-37.
2.   Festjens, N., T. Vanden Berghe, and P. Vandenabeele, Necrosis, a well-orchestrated form of cell demise: signalling cascades, important mediators and concomitant immune response. Biochim Biophys Acta, 2006. 1757(9-10): p. 1371-87.
3.   Yoshimori, T., Autophagy: paying Charon's toll. Cell, 2007. 128(5): p. 833-6.
4.   Clarke, P.G. and S. Clarke, Nineteenth century research on naturally occurring cell death and related phenomena. Anat Embryol (Berl), 1996. 193(2): p. 81-99.
5.   Lockshin, R.A. and C.M. Williams, Programmed Cell Death--I. Cytology of Degeneration in the Intersegmental Muscles of the Pernyi Silkmoth. J Insect Physiol, 1965. 11: p. 123-33.
6.   Kerr, J.F., A.H. Wyllie, and A.R. Currie, Apoptosis: a basic biological phenomenon with wide-ranging implications in tissue kinetics. Br J Cancer, 1972. 26(4): p. 239-57.
7.   Wyllie, A.H., J.F. Kerr, and A.R. Currie, Cell death: the significance of apoptosis. Int Rev Cytol, 1980. 68: p. 251-306.
8.   Savill, J.S., et al., Macrophage phagocytosis of aging neutrophils in inflammation. Programmed cell death in the neutrophil leads to its recognition by macrophages. J Clin Invest, 1989. 83(3): p. 865-75.
9.   Savill, J. and V. Fadok, Corpse clearance defines the meaning of cell death. Nature, 2000. 407(6805): p. 784-8.
10.  Savill, J., et al., A blast from the past: clearance of apoptotic cells regulates immune responses. Nat Rev Immunol, 2002. 2(12): p. 965-75.
11.  Kumar, S., Caspase function in programmed cell death. Cell Death Differ, 2007. 14(1): p. 32-43.
12.  Earnshaw, W.C., L.M. Martins, and S.H. Kaufmann, Mammalian caspases: structure, activation, substrates, and functions during apoptosis. Annu Rev Biochem, 1999. 68: p. 383-424.
13.  Cikala, M., et al., Identification of caspases and apoptosis in the simple metazoan Hydra. Curr Biol, 1999. 9(17): p. 959-62.
14.  Ogura, Y., F.S. Sutterwala, and R.A. Flavell, The inflammasome: first line of the immune response to cell stress. Cell, 2006. 126(4): p. 659-62.
15.  Martinon, F. and J. Tschopp, Inflammatory caspases and inflammasomes: master switches of inflammation. Cell Death Differ, 2007. 14(1): p. 10-22.
16.  Thornberry, N.A., The caspase family of cysteine proteases. Br Med Bull, 1997. 53(3): p. 478-90.
17.  Hengartner, M.O., The biochemistry of apoptosis. Nature, 2000. 407(6805): p. 770-6.
18.  Fuentes-Prior, P. and G.S. Salvesen, The protein structures that shape caspase activity, specificity, activation and inhibition. Biochem J, 2004. 384(Pt 2): p. 201-32.
19.  Muzio, M., et al., FLICE, a novel FADD-homologous ICE/CED-3-like protease, is recruited to the CD95 (Fas/APO-1) death--inducing signaling complex. Cell, 1996. 85(6): p. 817-27.
20.  Varfolomeev, E.E., et al., Targeted disruption of the mouse Caspase 8 gene ablates cell death induction by the TNF receptors, Fas/Apo1, and DR3 and is lethal prenatally. Immunity, 1998. 9(2): p. 267-76.
21.  Kroemer, G. and J.C. Reed, Mitochondrial control of cell death. Nat Med, 2000. 6(5): p. 513-9.
22.  Cory, S. and J.M. Adams, The Bcl2 family: regulators of the cellular life-or-death switch. Nat Rev Cancer, 2002. 2(9): p. 647-56.
23.  Green, D.R., Apoptotic pathways: ten minutes to dead. Cell, 2005. 121(5): p. 671-4.
24.  Riedl, S.J. and G.S. Salvesen, The apoptosome: signalling platform of cell death. Nat Rev Mol Cell Biol, 2007. 8(5): p. 405-13.
25.  Kitada, S., et al., Dysregulation of apoptosis genes in hematopoietic malignancies. Oncogene, 2002. 21(21): p. 3459-74.
26.  Thompson, C.B., Apoptosis in the pathogenesis and treatment of disease. Science, 1995. 267(5203): p. 1456-62.

27. Lane, D.P., Cancer. p53, guardian of the genome. Nature, 1992. 358(6381): p. 15-6.
28. Soussi, T., p53 alterations in human cancer: more questions than answers. Oncogene, 2007. 26(15): p. 2145-56.
29. Varbanov, M., L. Espert, and M. Biard-Piechaczyk, Mechanisms of CD4 T-cell depletion triggered by HIV-1 viral proteins. AIDS Rev, 2006. 8(4): p. 221-36.
30. Vila, M. and S. Przedborski, Targeting programmed cell death in neurodegenerative diseases. Nat Rev Neurosci, 2003. 4(5): p. 365-75.
31. Opferman, J.T. and S.J. Korsmeyer, Apoptosis in the development and maintenance of the immune system. Nat Immunol, 2003. 4(5): p. 410-5.
32. Michlewska, S., et al., Clearance of dying cells and autoimmunity. Autoimmunity, 2007. 40(4): p. 267-73.
33. Serhan, C.N. and J. Savill, Resolution of inflammation: the beginning programs the end. Nat Immunol, 2005. 6(12): p. 1191-7.
34. Liang, C.P., et al., The macrophage at the crossroads of insulin resistance and atherosclerosis. Circ Res, 2007. 100(11): p. 1546-55.
35. Lauber, K., et al., Apoptotic cells induce migration of phagocytes via caspase-3-mediated release of a lipid attraction signal. Cell, 2003. 113(6): p. 717-30.
36. Wakasugi, K. and P. Schimmel, Two distinct cytokines released from a human aminoacyl-tRNA synthetase. Science, 1999. 284(5411): p. 147-51.
37. Atsumi, G., et al., Distinct roles of two intracellular phospholipase A2s in fatty acid release in the cell death pathway. Proteolytic fragment of type IVA cytosolic phospholipase A2alpha inhibits stimulus-induced arachidonate release, whereas that of type VI Ca2+-independent phospholipase A2 augments spontaneous fatty acid release. J Biol Chem, 2000. 275(24): p. 18248-58.
38. Mueller, R.B., et al., Attraction of phagocytes by apoptotic cells is mediated by lysophosphatidylcholine. Autoimmunity, 2007. 40(4): p. 342-4.
39. Kougias, P., et al., Lysophosphatidylcholine and secretory phospholipase A2 in vascular disease: mediators of endothelial dysfunction and atherosclerosis. Med Sci Monit, 2006. 12(1): p. RA5-16.
40. Stuart, L.M. and R.A. Ezekowitz, Phagocytosis: elegant complexity. Immunity, 2005. 22(5): p. 539-50.
41. Martin, S.J., et al., Early redistribution of plasma membrane phosphatidylserine is a general feature of apoptosis regardless of the initiating stimulus: inhibition by overexpression of Bcl-2 and Abl. J Exp Med, 1995. 182(5): p. 1545-56.
42. Verhoven, B., R.A. Schlegel, and P. Williamson, Mechanisms of phosphatidylserine exposure, a phagocyte recognition signal, on apoptotic T lymphocytes. J Exp Med, 1995. 182(5): p. 1597-601.
43. Bratton, D.L., et al., Appearance of phosphatidylserine on apoptotic cells requires calcium-mediated nonspecific flip-flop and is enhanced by loss of the aminophospholipid translocase. J Biol Chem, 1997. 272(42): p. 26159-65.
44. Frasch, S.C., et al., Regulation of phospholipid scramblase activity during apoptosis and cell activation by protein kinase Cdelta. J Biol Chem, 2000. 275(30): p. 23065-73.
45. Kagan, V.E., et al., Appetizing rancidity of apoptotic cells for macrophages: oxidation, externalization, and recognition of phosphatidylserine. Am J Physiol Lung Cell Mol Physiol, 2003. 285(1): p. L1-17.
46. Brouckaert, G., et al., Phagocytosis of necrotic cells by macrophages is phosphatidylserine dependent and does not induce inflammatory cytokine production. Mol Biol Cell, 2004. 15(3): p. 1089-100.
47. Cocca, B.A., et al., Structural basis for autoantibody recognition of phosphatidylserine-beta 2 glycoprotein I and apoptotic cells. Proc Natl Acad Sci U S A, 2001. 98(24): p. 13826-31.
48. Wu, Y., N. Tibrewal, and R.B. Birge, Phosphatidylserine recognition by phagocytes: a view to a kill. Trends Cell Biol, 2006. 16(4): p. 189-97.
49. Fadok, V.A., et al., A receptor for phosphatidylserine-specific clearance of apoptotic cells. Nature, 2000. 405(6782): p. 85-90.
50. Mitchell, J.E., et al., The presumptive phosphatidylserine receptor is dispensable for innate anti-inflammatory recognition and clearance of apoptotic cells. J Biol Chem, 2006. 281(9): p. 5718-25.
51. Ren, Y., et al., CD36 gene transfer confers capacity for phagocytosis of cells undergoing apoptosis. J Exp Med, 1995. 181(5): p. 1857-62.

52.     Platt, N., et al., Role for the class A macrophage scavenger receptor in the phagocytosis of apoptotic thymocytes in vitro. Proc Natl Acad Sci U S A, 1996. 93(22): p. 12456-60.

53.     Murphy, J.E., et al., LOX-1 scavenger receptor mediates calcium-dependent recognition of phosphatidylserine and apoptotic cells. Biochem J, 2006. 393(Pt 1): p. 107-15.

54.     Brown, S., et al., Apoptosis disables CD31-mediated cell detachment from phagocytes promoting binding and engulfment. Nature, 2002. 418(6894): p. 200-3.

55.     Gumienny, T.L., et al., CED-12/ELMO, a novel member of the CrkII/Dock180/Rac pathway, is required for phagocytosis and cell migration. Cell, 2001. 107(1): p. 27-41.

56.     Lauber, K., et al., Clearance of apoptotic cells: getting rid of the corpses. Mol Cell, 2004. 14(3): p. 277-87.

57.     Akakura, S., et al., The opsonin MFG-E8 is a ligand for the alphavbeta5 integrin and triggers DOCK180-dependent Rac1 activation for the phagocytosis of apoptotic cells. Exp Cell Res, 2004. 292(2): p. 403-16.

58.     Gordon, S., The macrophage. Bioessays, 1995. 17(11): p. 977-86.

59.     Gordon, S., Alternative activation of macrophages. Nat Rev Immunol, 2003. 3(1): p. 23-35.

60.     Baker, A.J., et al., Mesangial cell apoptosis: the major mechanism for resolution of glomerular hypercellularity in experimental mesangial proliferative nephritis. J Clin Invest, 1994. 94(5): p. 2105-16.

61.     Duffield, J.S., The inflammatory macrophage: a story of Jekyll and Hyde. Clin Sci (Lond), 2003. 104(1): p. 27-38.

62.     Mosser, D.M., The many faces of macrophage activation. J Leukoc Biol, 2003. 73(2): p. 209-12.

63.     Mantovani, A., A. Sica, and M. Locati, Macrophage polarization comes of age. Immunity, 2005. 23(4): p. 344-6.

64.     Voll, R.E., et al., Immunosuppressive effects of apoptotic cells. Nature, 1997. 390(6658): p. 350-1.

65.     Fadok, V.A., et al., Macrophages that have ingested apoptotic cells in vitro inhibit proinflammatory cytokine production through autocrine/paracrine mechanisms involving TGF-beta, PGE2, and PAF. J Clin Invest, 1998. 101(4): p. 890-8.

66.     Devitt, A., et al., Persistence of apoptotic cells without autoimmune disease or inflammation in CD14-/- mice. J Cell Biol, 2004. 167(6): p. 1161-70.

67.     Li, M.O., et al., Phosphatidylserine receptor is required for clearance of apoptotic cells. Science, 2003. 302(5650): p. 1560-3.

68.     Kunisaki, Y., et al., Defective fetal liver erythropoiesis and T lymphopoiesis in mice lacking the phosphatidylserine receptor. Blood, 2004. 103(9): p. 3362-4.

69.     Bose, J., et al., The phosphatidylserine receptor has essential functions during embryogenesis but not in apoptotic cell removal. J Biol, 2004. 3(4): p. 15.

70.     Cikala, M., et al., The phosphatidylserine receptor from Hydra is a nuclear protein with potential Fe(II) dependent oxygenase activity. BMC Cell Biol, 2004. 5: p. 26.

71.     Scott, R.S., et al., Phagocytosis and clearance of apoptotic cells is mediated by MER. Nature, 2001. 411(6834): p. 207-11.

72.     Duncan, J.L., et al., Inherited retinal dystrophy in Mer knockout mice. Adv Exp Med Biol, 2003. 533: p. 165-72.

73.     Camenisch, T.D., et al., A novel receptor tyrosine kinase, Mer, inhibits TNF-alpha production and lipopolysaccharide-induced endotoxic shock. J Immunol, 1999. 162(6): p. 3498-503.

74.     Asano, K., et al., Masking of phosphatidylserine inhibits apoptotic cell engulfment and induces autoantibody production in mice. J Exp Med, 2004. 200(4): p. 459-67.

75.     Freire-de-Lima, C.G., et al., Uptake of apoptotic cells drives the growth of a pathogenic trypanosome in macrophages. Nature, 2000. 403(6766): p. 199-203.

76.     Serinkan, B.F., et al., Apoptotic cells quench reactive oxygen and nitrogen species and modulate TNF-alpha/TGF-beta1 balance in activated macrophages: involvement of phosphatidylserine-dependent and -independent pathways. Cell Death Differ, 2005. 12(8): p. 1141-4.

77.     Johann, A.M., et al., Recognition of apoptotic cells by macrophages activates the peroxisome proliferator-activated receptor-gamma and attenuates the oxidative burst. Cell Death Differ, 2006. 13(9): p. 1533-40.

78. Bailey, S.T. and S. Ghosh, 'PPAR'ting ways with inflammation. Nat Immunol, 2005. 6(10): p. 966-7.

79. Cvetanovic, M. and D.S. Ucker, Innate immune discrimination of apoptotic cells: repression of proinflammatory macrophage transcription is coupled directly to specific recognition. J Immunol, 2004. 172(2): p. 880-9.

80. Lawrence, T., et al., IKKalpha limits macrophage NF-kappaB activation and contributes to the resolution of inflammation. Nature, 2005. 434(7037): p. 1138-43.

81. Cvetanovic, M., et al., Specific recognition of apoptotic cells reveals a ubiquitous and unconventional innate immunity. J Biol Chem, 2006.

82. Daynes, R.A. and D.C. Jones, Emerging roles of PPARs in inflammation and immunity. Nat Rev Immunol, 2002. 2(10): p. 748-59.

83. Chen, W., et al., TGF-beta released by apoptotic T cells contributes to an immunosuppressive milieu. Immunity, 2001. 14(6): p. 715-25.

84. Tomimori, Y., Y. Ikawa, and N. Oyaizu, Ultraviolet-irradiated apoptotic lymphocytes produce interleukin-10 by themselves. Immunol Lett, 2000. 71(1): p. 49-54.

85. Hodge, S., et al., Up-regulation of production of TGF-beta and IL-4 and down-regulation of IL-6 by apoptotic human bronchial epithelial cells. Immunol Cell Biol, 2002. 80(6): p. 537-43.

86. Turner, C., et al., Macrophage-mediated clearance of cells undergoing caspase-3-independent death. Cell Death Differ, 2003. 10(3): p. 302-12.

87. Mantovani, A., et al., Macrophage polarization: tumor-associated macrophages as a paradigm for polarized M2 mononuclear phagocytes. Trends Immunol, 2002. 23(11): p. 549-55.

88. Murdoch, C., A. Giannoudis, and C.E. Lewis, Mechanisms regulating the recruitment of macrophages into hypoxic areas of tumors and other ischemic tissues. Blood, 2004. 104(8): p. 2224-34.

89. Bingle, L., N.J. Brown, and C.E. Lewis, The role of tumor-associated macrophages in tumor progression: implications for new anticancer therapies. J Pathol, 2002. 196(3): p. 254-65.

90. Lewis, C.E. and J.W. Pollard, Distinct role of macrophages in different tumor microenvironments. Cancer Res, 2006. 66(2): p. 605-12.

91. Mantovani, A., P. Allavena, and A. Sica, Tumor-associated macrophages as a prototypic type II polarised phagocyte population: role in tumor progression. Eur J Cancer, 2004. 40(11): p. 1660-7.

92. Pollard, J.W., Tumor-educated macrophages promote tumor progression and metastasis. Nat Rev Cancer, 2004. 4(1): p. 71-8.

93. Lin, E.Y., et al., Macrophages regulate the angiogenic switch in a mouse model of breast cancer. Cancer Res, 2006. 66(23): p. 11238-46.

94. Yu, J.L. and J.W. Rak, Host microenvironment in breast cancer development: inflammatory and immune cells in tumor angiogenesis and arteriogenesis. Breast Cancer Res, 2003. 5(2): p. 83-8.

95. Mantovani, A., et al., The chemokine system in diverse forms of macrophage activation and polarization. Trends Immunol, 2004. 25(12): p. 677-86.

96. Reiter, I., B. Krammer, and G. Schwamberger, Cutting edge: differential effect of apoptotic versus necrotic tumor cells on macrophage antitumor activities. J Immunol, 1999. 163(4): p. 1730-2.

97. Bondanza, A., et al., Inhibition of phosphatidylserine recognition heightens the immunogenicity of irradiated lymphoma cells in vivo. J Exp Med, 2004. 200(9): p. 1157-65.

98. Biswas, S.K., et al., A distinct and unique transcriptional program expressed by tumor-associated macrophages (defective NF-kappaB and enhanced IRF-3/STAT1 activation). Blood, 2006. 107(5): p. 2112-22.

99. Le Stunff, H., S. Milstien, and S. Spiegel, Generation and metabolism of bioactive sphingosine-1-phosphate. J Cell Biochem, 2004. 92(5): p. 882-99.

100. Shu, X., et al., Sphingosine kinase mediates vascular endothelial growth factor-induced activation of ras and mitogen-activated protein kinases. Mol Cell Biol, 2002. 22(22): p. 7758-68.

101. Xia, P., et al., Sphingosine kinase interacts with TRAF2 and dissects tumor necrosis factor-alpha signaling. J Biol Chem, 2002. 277(10): p. 7996-8003.

102. Hla, T., et al., Lysophospholipids--receptor revelations. Science, 2001. 294(5548): p. 1875-8.
103. Spiegel, S. and S. Milstien, Sphingosine-1-phosphate: an enigmatic signalling lipid. Nat Rev Mol Cell Biol, 2003. 4(5): p. 397-407.
104. Sanna, M.G., et al., Sphingosine 1-phosphate (S1P) receptor subtypes S1P1 and S1P3, respectively, regulate lymphocyte recirculation and heart rate. J Biol Chem, 2004. 279(14): p. 13839-48.
105. Mitra, P., et al., Role of ABCC1 in export of sphingosine-1-phosphate from mast cells. Proc Natl Acad Sci U S A, 2006. 103(44): p. 16394-9.
106. Kobayashi, N., et al., Sphingosine 1-phosphate is released from the cytosol of rat platelets in a carrier-mediated manner. J Lipid Res, 2006. 47(3): p. 614-21.
107. Venkataraman, K., et al., Extracellular export of sphingosine kinase-1a contributes to the vascular S1P gradient. Biochem J, 2006. 397(3): p. 461-71.
108. Maceyka, M., et al., SphK1 and SphK2, sphingosine kinase isoenzymes with opposing functions in sphingolipid metabolism. J Biol Chem, 2005. 280(44): p. 37118-29.
109. Taha, T.A., Y.A. Hannun, and L.M. Obeid, Sphingosine kinase: biochemical and cellular regulation and role in disease. J Biochem Mol Biol, 2006. 39(2): p. 113-31.
110. Billich, A., et al., Phosphorylation of the immunomodulatory drug FTY720 by sphingosine kinases. J Biol Chem, 2003. 278(48): p. 47408-15.
111. Okada, T., et al., Involvement of N-terminal-extended form of sphingosine kinase 2 in serum-dependent regulation of cell proliferation and apoptosis. J Biol Chem, 2005. 280(43): p. 36318-25.
112. Mizugishi, K., et al., Essential role for sphingosine kinases in neural and vascular development. Mol Cell Biol, 2005. 25(24): p. 11113-21.
113. Alemany, R., et al., Regulation and functional roles of sphingosine kinases. Naunyn Schmiedebergs Arch Pharmacol, 2007. 374(5-6): p. 413-28.
114. Sanchez, T., et al., Phosphorylation and action of the immunomodulator FTY720 inhibits vascular endothelial cell growth factor-induced vascular permeability. J Biol Chem, 2003. 278(47): p. 47281-90.
115. Zemann, B., et al., Sphingosine kinase type 2 is essential for lymphopenia induced by the immunomodulatory drug FTY720. Blood, 2006. 107(4): p. 1454-8.
116. Graler, M.H. and E.J. Goetzl, The immunosuppressant FTY720 down-regulates sphingosine 1-phosphate G-protein-coupled receptors. Faseb J, 2004. 18(3): p. 551-3.
117. Liu, H., et al., Molecular cloning and functional characterization of a novel mammalian sphingosine kinase type 2 isoform. J Biol Chem, 2000. 275(26): p. 19513-20.
118. Olivera, A., et al., Sphingosine kinase expression increases intracellular sphingosine-1-phosphate and promotes cell growth and survival. J Cell Biol, 1999. 147(3): p. 545-58.
119. Taha, T.A., et al., Down-regulation of sphingosine kinase-1 by DNA damage: dependence on proteases and p53. J Biol Chem, 2004. 279(19): p. 20546-54.
120. Igarashi, N., et al., Sphingosine kinase 2 is a nuclear protein and inhibits DNA synthesis. J Biol Chem, 2003. 278(47): p. 46832-9.
121. Liu, H., et al., Sphingosine kinase type 2 is a putative BH3-only protein that induces apoptosis. J Biol Chem, 2003. 278(41): p. 40330-6.
122. Sabbadini, R.A., Targeting sphingosine-1-phosphate for cancer therapy. Br J Cancer, 2006. 95(9): p. 1131-5.
123. Hait, N.C., et al., Role of sphingosine kinase 2 in cell migration toward epidermal growth factor. J Biol Chem, 2005. 280(33): p. 29462-9.
124. Sarkar, S., et al., Sphingosine kinase 1 is required for migration, proliferation and survival of MCF-7 human breast cancer cells. FEBS Lett, 2005. 579(24): p. 5313-7.
125. Visentin, B., et al., Validation of an anti-sphingosine-1-phosphate antibody as a potential therapeutic in reducing growth, invasion, and angiogenesis in multiple tumor lineages. Cancer Cell, 2006. 9(3): p. 225-38.
126. LaMontagne, K., et al., Antagonism of sphingosine-1-phosphate receptors by FTY720 inhibits angiogenesis and tumor vascularization. Cancer Res, 2006. 66(1): p. 221-31.
127. Peng, H.B., P. Libby, and J.K. Liao, Induction and stabilization of I kappa B alpha by nitric oxide mediates inhibition of NF-kappa B. J Biol Chem, 1995. 270(23): p. 14214-9.

128. Messmer, U.K., U.K. Reed, and B. Brune, Bcl-2 protects macrophages from nitric oxide-induced apoptosis. J Biol Chem, 1996. 271(33): p. 20192-7.

129. Schneider, U., H.U. Schwenk, and G. Bornkamm, Characterization of EBV-genome negative "null" and "T" cell lines derived from children with acute lymphoblastic leukemia and leukemic transformed non-Hodgkin lymphoma. Int J Cancer, 1977. 19(5): p. 621-6.

130. Graham, F.L., et al., Characteristics of a human cell line transformed by DNA from human adenovirus type 5. J Gen Virol, 1977. 36(1): p. 59-74.

131. Soule, H.D., et al., A human cell line from a pleural effusion derived from a breast carcinoma. J Natl Cancer Inst, 1973. 51(5): p. 1409-16.

132. Tsuchiya, S., et al., Establishment and characterization of a human acute monocytic leukemia cell line (THP-1). Int J Cancer, 1980. 26(2): p. 171-6.

133. Brattain, M.G., et al., Heterogeneity of human colon carcinoma. Cancer Metastasis Rev, 1984. 3(3): p. 177-91.

134. Raschke, W.C., et al., Functional macrophage cell lines transformed by Abelson leukemia virus. Cell, 1978. 15(1): p. 261-7.

135. Semple, T.U., et al., Tumor and lymphoid cell lines from a patient with carcinoma of the colon for a cytotoxicity model. Cancer Res, 1978. 38(5): p. 1345-55.

136. Knowles, B.B., C.C. Howe, and D.P. Aden, Human hepatocellular carcinoma cell lines secrete the major plasma proteins and hepatitis B surface antigen. Science, 1980. 209(4455): p. 497-9.

137. Jainchill, J.L., S.A. Aaronson, and G.J. Todaro, Murine sarcoma and leukemia viruses: assay using clonal lines of contact-inhibited mouse cells. J Virol, 1969. 4(5): p. 549-53.

138. Rabson, A.S., et al., Production of human chorionic gonadotropin in vitro by a cell line derived from a carcinoma of the lung. J Natl Cancer Inst, 1973. 50(3): p. 669-74.

139. Pretlow, T.P., G.L. Glover, and T.G. Pretlow, 2nd, Purification of malignant cells and lymphocytes from a rat transplantable mucinous adenocarcinoma of the colon by isokinetic sedimentation in gradients of Ficoll. J Natl Cancer Inst, 1977. 59(3): p. 981-7.

140. Von Knethen, A.A. and B. Brune, Delayed activation of PPARgamma by LPS and IFN-gamma attenuates the oxidative burst in macrophages. Faseb J, 2001. 15(2): p. 535-44.

141. von Knethen, A., A. Lotero, and B. Brune, Etoposide and cisplatin induced apoptosis in activated RAW 264.7 macrophages is attenuated by cAMP-induced gene expression. Oncogene, 1998. 17(3): p. 387-94.

142. Segundo, C., et al., Surface molecule loss and bleb formation by human germinal center B cells undergoing apoptosis: role of apoptotic blebs in monocyte chemotaxis. Blood, 1999. 94(3): p. 1012-20.

143. Anelli, V., et al., Extracellular release of newly synthesized sphingosine-1-phosphate by cerebellar granule cells and astrocytes. J Neurochem, 2005. 92(5): p. 1204-15.

144. Popi, A.F., J.D. Lopes, and M. Mariano, Interleukin-10 secreted by B-1 cells modulates the phagocytic activity of murine macrophages in vitro. Immunology, 2004. 113(3): p. 348-54.

145. Albee, L., B. Shi, and H. Perlman, Aspartic protease and caspase 3/7 activation are central for macrophage apoptosis following infection with Escherichia coli. J Leukoc Biol, 2007. 81(1): p. 229-37.

146. Salvioli, S., et al., JC-1, but not DiOC6(3) or rhodamine 123, is a reliable fluorescent probe to assess delta psi changes in intact cells: implications for studies on mitochondrial functionality during apoptosis. FEBS Lett, 1997. 411(1): p. 77-82.

147. Sandau, K.B., D. Callsen, and B. Brune, Protection against nitric oxide-induced apoptosis in rat mesangial cells demands mitogen-activated protein kinases and reduced glutathione. Mol Pharmacol, 1999. 56(4): p. 744-51.

148. Lowry, O.H., et al., Protein measurement with the Folin phenol reagent. J Biol Chem, 1951. 193(1): p. 265-75.

149. Camandola, S., et al., Nuclear factor kB is activated by arachidonic acid but not by eicosapentaenoic acid. Biochem Biophys Res Commun, 1996. 229(2): p. 643-7.

150. He, B., et al., Lymphoma B cells evade apoptosis through the TNF family members BAFF/BLyS and APRIL. J Immunol, 2004. 172(5): p. 3268-79.

151.    Schmidt, H., R. Schmidt, and G. Geisslinger, LC-MS/MS-analysis of sphingosine-1-phosphate and related compounds in plasma samples. Prostaglandins Other Lipid Mediat, 2006. 81(3-4): p. 162-70.

152.    Billich, A. and P. Ettmayer, Fluorescence-based assay of sphingosine kinases. Anal Biochem, 2004. 326(1): p. 114-9.

153.    Walker, P.R., et al., Topoisomerase II-reactive chemotherapeutic drugs induce apoptosis in thymocytes. Cancer Res, 1991. 51(4): p. 1078-85.

154.    van Deurs, B., et al., Destabilization of plasma membrane structure by prevention of actin polymerization. Microtubule-dependent tubulation of the plasma membrane. J Cell Sci, 1996. 109 ( Pt 7): p. 1655-65.

155.    Liu, H., et al., Serine phosphorylation of STAT3 is essential for Mcl-1 expression and macrophage survival. Blood, 2003. 102(1): p. 344-52.

156.    Gomez-Munoz, A., et al., Sphingosine-1-phosphate inhibits acid sphingomyelinase and blocks apoptosis in macrophages. FEBS Lett, 2003. 539(1-3): p. 56-60.

157.    Duong, C.Q., et al., Expression of the lysophospholipid receptor family and investigation of lysophospholipid-mediated responses in human macrophages. Biochim Biophys Acta, 2004. 1682(1-3): p. 112-9.

158.    Fueller, M., et al., Activation of human monocytic cells by lysophosphatidic acid and sphingosine-1-phosphate. Cell Signal, 2003. 15(4): p. 367-75.

159.    Horton, P., et al., WoLF PSORT: protein localization predictor. Nucleic Acids Res, 2007. 35(Web Server issue): p. W585-7.

160.    Gregory, C.D. and A. Devitt, The macrophage and the apoptotic cell: an innate immune interaction viewed simplistically? Immunology, 2004. 113(1): p. 1-14.

161.    Stahelin, R.V., et al., The mechanism of membrane targeting of human sphingosine kinase 1. J Biol Chem, 2005. 280(52): p. 43030-8.

162.    Tyurina, Y.Y., et al., Lipid antioxidant, etoposide, inhibits phosphatidylserine externalization and macrophage clearance of apoptotic cells by preventing phosphatidylserine oxidation. J Biol Chem, 2004. 279(7): p. 6056-64.

163.    Balasubramanian, K., B. Mirnikjoo, and A.J. Schroit, Regulated Externalization of Phosphatidylserine at the Cell Surface: IMPLICATIONS FOR APOPTOSIS. J Biol Chem, 2007. 282(25): p. 18357-64.

164.    Sica, A., et al., Autocrine production of IL-10 mediates defective IL-12 production and NF-kappa B activation in tumor-associated macrophages. J Immunol, 2000. 164(2): p. 762-7.

165.    Draffin, J.E., et al., CD44 potentiates the adherence of metastatic prostate and breast cancer cells to bone marrow endothelial cells. Cancer Res, 2004. 64(16): p. 5702-11.

166.    Tegeder, I., et al., G protein-independent G1 cell cycle block and apoptosis with morphine in adenocarcinoma cells: involvement of p53 phosphorylation. Cancer Res, 2003. 63(8): p. 1846-52.

167.    Zeisberger, S.M., et al., Clodronate-liposome-mediated depletion of tumor-associated macrophages: a new and highly effective antiangiogenic therapy approach. Br J Cancer, 2006. 95(3): p. 272-81.

168.    Robertson, F.M., et al., Cyclooxygenase-2 directly induces MCF-7 breast tumor cells to develop into exponentially growing, highly angiogenic and regionally invasive human ductal carcinoma xenografts. Anticancer Res, 2007. 27(2): p. 719-27.

169.    Sica, A., et al., Tumor-associated macrophages are a distinct M2 polarised population promoting tumor progression: potential targets of anti-cancer therapy. Eur J Cancer, 2006. 42(6): p. 717-27.

170.    Erwig, L.P., et al., Initial cytokine exposure determines function of macrophages and renders them unresponsive to other cytokines. J Immunol, 1998. 161(4): p. 1983-8.

171.    Duffield, J.S., et al., Suppression by apoptotic cells defines tumor necrosis factor-mediated induction of glomerular mesangial cell apoptosis by activated macrophages. Am J Pathol, 2001. 159(4): p. 1397-404.

172.    Gordon, S. and P.R. Taylor, Monocyte and macrophage heterogeneity. Nat Rev Immunol, 2005. 5(12): p. 953-64.

173.    Reddy, S.M., et al., Phagocytosis of apoptotic cells by macrophages induces novel signaling events leading to cytokine-independent survival and inhibition of proliferation: activation of Akt and inhibition of extracellular signal-regulated kinases 1 and 2. J Immunol, 2002. 169(2): p. 702-13.

174. Oka, T., M. Hori, and H. Ozaki, Microtubule disruption suppresses allergic response through the inhibition of calcium influx in the mast cell degranulation pathway. J Immunol, 2005. 174(8): p. 4584-9.

175. Golpon, H.A., et al., Life after corpse engulfment: phagocytosis of apoptotic cells leads to VEGF secretion and cell growth. Faseb J, 2004. 18(14): p. 1716-8.

176. Gerber, H.P., V. Dixit, and N. Ferrara, Vascular endothelial growth factor induces expression of the antiapoptotic proteins Bcl-2 and A1 in vascular endothelial cells. J Biol Chem, 1998. 273(21): p. 13313-6.

177. Gerber, H.P., et al., Vascular endothelial growth factor regulates endothelial cell survival through the phosphatidylinositol 3'-kinase/Akt signal transduction pathway. Requirement for Flk-1/KDR activation. J Biol Chem, 1998. 273(46): p. 30336-43.

178. Ishii, I., et al., Lysophospholipid receptors: signaling and biology. Annu Rev Biochem, 2004. 73: p. 321-54.

179. Taha, T.A., K.M. Argraves, and L.M. Obeid, Sphingosine-1-phosphate receptors: receptor specificity versus functional redundancy. Biochim Biophys Acta, 2004. 1682(1-3): p. 48-55.

180. Downward, J., PI 3-kinase, Akt and cell survival. Semin Cell Dev Biol, 2004. 15(2): p. 177-82.

181. Hundal, R.S., et al., Oxidized low density lipoprotein inhibits macrophage apoptosis through activation of the PI 3-kinase/PKB pathway. J Lipid Res, 2001. 42(9): p. 1483-91.

182. Bhatt, N.Y., et al., Macrophage-colony-stimulating factor-induced activation of extracellular-regulated kinase involves phosphatidylinositol 3-kinase and reactive oxygen species in human monocytes. J Immunol, 2002. 169(11): p. 6427-34.

183. Chin, B.Y., et al., Transforming growth factor beta1 rescues serum deprivation-induced apoptosis via the mitogen-activated protein kinase (MAPK) pathway in macrophages. J Biol Chem, 1999. 274(16): p. 11362-8.

184. Rizzuto, R., et al., Calcium and apoptosis: facts and hypotheses. Oncogene, 2003. 22(53): p. 8619-27.

185. Yano, S., H. Tokumitsu, and T.R. Soderling, Calcium promotes cell survival through CaM-K kinase activation of the protein-kinase-B pathway. Nature, 1998. 396(6711): p. 584-7.

186. Maceyka, M., et al., SphK1 and SphK2: Sphingosine kinase isoenzymes with opposing functions in sphingolipid metabolism. J Biol Chem, 2005.

187. Kabarowski, J.H., et al., Lysophosphatidylcholine as a ligand for the immunoregulatory receptor G2A. Science, 2001. 293(5530): p. 702-5.

188. Atsumi, G., et al., Fas-induced arachidonic acid release is mediated by Ca2+-independent phospholipase A2 but not cytosolic phospholipase A2, which undergoes proteolytic inactivation. J Biol Chem, 1998. 273(22): p. 13870-7.

189. Tani, M., M. Ito, and Y. Igarashi, Ceramide/sphingosine/sphingosine 1-phosphate metabolism on the cell surface and in the extracellular space. Cell Signal, 2007. 19(2): p. 229-37.

190. Mao, P.L., et al., Activation of caspase-1 in the nucleus requires nuclear translocation of pro-caspase-1 mediated by its prodomain. J Biol Chem, 1998. 273(37): p. 23621-4.

191. Ding, G., et al., Protein kinase D-mediated phosphorylation and nuclear export of sphingosine kinase 2. J Biol Chem, 2007.

192. Franz, S., et al., After shrinkage apoptotic cells expose internal membrane-derived epitopes on their plasma membranes. Cell Death Differ, 2007. 14(4): p. 733-42.

193. Mambula, S.S. and S.K. Calderwood, Heat shock protein 70 is secreted from tumor cells by a nonclassical pathway involving lysosomal endosomes. J Immunol, 2006. 177(11): p. 7849-57.

194. Peterson, E.A., et al., Thrombin induces endothelial cell-surface exposure of the plasminogen receptor annexin 2. J Cell Sci, 2003. 116(Pt 12): p. 2399-408.

195. Wang, X., et al., C. elegans mitochondrial factor WAH-1 promotes phosphatidylserine externalization in apoptotic cells through phospholipid scramblase SCRM-1. Nat Cell Biol, 2007. 9(5): p. 541-9.

196. Idzko, M., et al., Sphingosine 1-phosphate induces chemotaxis of immature and modulates cytokine-release in mature human dendritic cells for emergence of Th2 immune responses. Faseb J, 2002. 16(6): p. 625-7.

197. Wang, W., M.H. Graeler, and E.J. Goetzl, Type 4 sphingosine 1-phosphate G protein-coupled receptor (S1P4) transduces S1P effects on T cell proliferation and cytokine secretion without signaling migration. Faseb J, 2005. 19(12): p. 1731-3.

198. Kim, R., et al., Tumor-driven evolution of immunosuppressive networks during malignant progression. Cancer Res, 2006. 66(11): p. 5527-36.

199. Burow, M.E., et al., Differences in susceptibility to tumor necrosis factor alpha-induced apoptosis among MCF-7 breast cancer cell variants. Cancer Res, 1998. 58(21): p. 4940-6.

200. Siehler, S., et al., Sphingosine 1-phosphate activates nuclear factor-kappa B through Edg receptors. Activation through Edg-3 and Edg-5, but not Edg-1, in human embryonic kidney 293 cells. J Biol Chem, 2001. 276(52): p. 48733-9.

201. Kimura, T., et al., Sphingosine 1-phosphate receptors mediate stimulatory and inhibitory signalings for expression of adhesion molecules in endothelial cells. Cell Signal, 2006. 18(6): p. 841-50.

202. Man, K., et al., FTY720 attenuates hepatic ischemia-reperfusion injury in normal and cirrhotic livers. Am J Transplant, 2005. 5(1): p. 40-9.

203. Mauro, C., et al., ABIN-1 Binds to NEMO/IKK{gamma} and Co-operates with A20 in Inhibiting NF-{kappa}B. J Biol Chem, 2006. 281(27): p. 18482-8.

204. Rauh, M.J., et al., SHIP represses the generation of alternatively activated macrophages. Immunity, 2005. 23(4): p. 361-74.

205. Polumuri, S.K., V.Y. Toshchakov, and S.N. Vogel, Role of phosphatidylinositol-3 kinase in transcriptional regulation of TLR-induced IL-12 and IL-10 by Fc gamma receptor ligation in murine macrophages. J Immunol, 2007. 179(1): p. 236-46.

206. Fukao, T. and S. Koyasu, PI3K and negative regulation of TLR signaling. Trends Immunol, 2003. 24(7): p. 358-63.

207. Martin, M., et al., Toll-like receptor-mediated cytokine production is differentially regulated by glycogen synthase kinase 3. Nat Immunol, 2005. 6(8): p. 777-84.

208. Hoffmann, E., et al., Multiple control of interleukin-8 gene expression. J Leukoc Biol, 2002. 72(5): p. 847-55.

209. Fujimoto, J., et al., Clinical implications of expression of interleukin-8 related to myometrial invasion with angiogenesis in uterine endometrial cancers. Ann Oncol, 2002. 13(3): p. 430-4.

210. Van Brocklyn, J.R., et al., Sphingosine kinase-1 expression correlates with poor survival of patients with glioblastoma multiforme: roles of sphingosine kinase isoforms in growth of glioblastoma cell lines. J Neuropathol Exp Neurol, 2005. 64(8): p. 695-705.

211. Xin, C., et al., Sphingosine 1-phosphate cross-activates the Smad signaling cascade and mimics transforming growth factor-beta-induced cell responses. J Biol Chem, 2004. 279(34): p. 35255-62.

212. Mills, C.D., et al., M-1/M-2 macrophages and the Th1/Th2 paradigm. J Immunol, 2000. 164(12): p. 6166-73.

213. Pettus, B.J., et al., The coordination of prostaglandin E2 production by sphingosine-1-phosphate and ceramide-1-phosphate. Mol Pharmacol, 2005. 68(2): p. 330-5.

# 8    Publications

## Papers

**Weigert, A.**, Johann, A.M., von Knethen, A., Schmidt, H., Geisslinger, G., and Brüne, B., Apoptotic cells promote macrophage survival by releasing the antiapoptotic mediator sphingosine-1-phosphate. Blood, 2006. 108(5): p. 1635-42.

von Knethen, A., Soller, M., Tzieply, N., **Weigert, A.**, Johann, A.M., Jennewein, C., Köhl, R., and Brüne, B., PPARgamma1 attenuates cytosol to membrane translocation of PKCalpha to desensitize monocytes/macrophages. J Cell Biol, 2007. 176(5): p. 681-94.

**Weigert, A.**, Tzieply, N., von Knethen, A., Johann, A.M., Schmidt, H., Geisslinger, G., and Brüne, B., Tumor Cell Apoptosis Polarizes Macrophages - Role of Sphingosine-1-Phosphate. Mol Biol Cell, 2007. 18(10): 3810-9.

Johann, A.M., Barra, V., Kuhn, A.M., **Weigert, A.**, von Knethen, A., and Brüne, B., Apoptotic cells induce arginase II in macrophages, thereby attenuating NO production. Faseb J, 2007. 21(11): p. 2704-12.

Johann, A.M., **Weigert, A.**, Eberhardt, W., Kuhn, A.M., Barra, V., von Knethen, A., Pfeilschifter J.M., and Brüne, B., Apoptotic cell-derived S1P promotes HuR-dependent COX-2 mRNA stabilization and protein expression. J Immunol. *in revision*.

**Weigert, A.**, von Knethen, A., and Brüne, B., Cleavage of sphingosine kinase 2 by caspase-1 provokes its release from apoptotic cells. *in submission*.

## Books

Brüne, B., **Weigert, A.**, and Johann, A.M. (2007): Signaling of apoptotic cells towards alternative macrophage activation. In: Cell apoptotic signaling pathways, Pickens, C.O., ed. (Hauppauge, USA: Nova Science Publishers Inc), pp. 115-132.

## Meeting abstracts

**Weigert, A.**, Johann, A.M., von Knethen, A., and Brüne, B., Apoptotic cells release sphingosine-1-phosphate and polarize macrophages. Keystone Symposia on Molecular and Cellular Biology: Bioactive Lipids in the Lipidomics Era (2007), Abstract book, p. 57.

# 9    Acknowledgements

After more than three years of highly interesting and exiting, but also difficult and often frustrating work, I would like to thank many people that contributed in various ways to the successful finishing of my thesis:

Prof. Dr. Bernhard Brüne for giving me the opportunity to perform my PH.D. thesis in his labs in Kaiserslautern and Frankfurt, for excellent discussions, intensive mentoring and for scientific as well as financial support.

Dr. Andreas von Knethen for strong scientific support, and for creating a highly encouraging working and social atmosphere.

My parents and my brothers, who always supported my career and all other aspects of my life, and who provided a home for mental and physical recreation.

All members of the lab for having a good time, both in scientific and private affairs and for the numerous recreational activities e.g. on the balcony.

My friends, especially my brothers in song from the "Collegium vocalis", Kim for the "Ensemble Barockhaus" and for bashing the stress out of my head with a small rubber ball, and last but not least Salomé for pure inspiration.

# 10 Curriculum Vitae

| | |
|---|---|
| Name: | Andreas Mathias Weigert |
| Geburtsdatum: | 17.05.1979 |
| Geburtsort: | Worms |
| Nationalität: | Deutsch |
| Familienstand: | Ledig |
| Adresse: | Cranachstrasse 15 |
| | 60596 Frankfurt/Main |
| | Tel: 069-47890830 |
| | Mail: weigert@zbc.kgu.de |

**Ausbildung und beruflicher Werdegang:**

| | |
|---|---|
| 1986-1989: | Grundschule Ellerstadt |
| 1989-1998: | Integrierte Gesamtschule Ernst Bloch Ludwigshafen-Oggersheim |
| 1998: | Abschluss: Allgemeine Hochschulreife |
| 1998-1999: | Zivildienst beim Malteser Hilfsdienst Speyer als Sanitäter und Erste-Hilfe-Ausbilder |
| 1999-2004: | Studium der Biologie an der Universität Kaiserslautern |
| 2004: | Diplom im Fach Biologie am Institut für Molekulare Zellbiologie der Universität Kaiserslautern mit dem Thema: „Identifikation von anti-apoptotischen Genen mit einer Rescue-Library." |
| 2004-2005: | Promotion am Institut für Molekulare Zellbiologie (Prof. Bernhard Brüne) der Technischen Universität Kaiserslautern |
| 2004: | wissenschaftlicher Austausch am *Centro Nacional de Investigaciones Cardiovasculares* (CNIC, Prof. Lisardo Bosca), Madrid, Spanien |
| seit 2006: | Promotion am Institut für Biochemie I (Prof. Bernhard Brüne), Klinikum der Johann Wolfgang Goethe-Universität, Frankfurt am Main |
| Dezember 2007: | Voraussichtliches Ende der Promotion |

Frankfurt am Main, den

# Ehrenwörtliche Erklärung

Ich erkläre ehrenwörtlich, dass ich die dem Fachbereich Medizin der Johann Wolfgang Goethe-Universität Frankfurt am Main zur Promotionsprüfung eingereichte Arbeit mit dem Titel

**"Generation of sphingosine-1-phosphate by apoptotic cells and its impact on macrophage polarization in cancer development"**

Im Institut für Biochemie I – Pathobiochemie unter Betreuung und Anleitung von Prof. Dr. Bernhard Brüne ohne sonstige Hilfe selbst durchgeführt und bei der Abfassung der Arbeit keine anderen als die in der Dissertation angeführten Hilfsmittel benutzt habe.

Ich habe bisher an keiner in- oder ausländischen Universität ein Gesuch um Zulassung zur Promotion eingereicht. Die vorliegende Arbeit wurde bisher nicht als Dissertation eingereicht.

Teile der vorliegenden Arbeit wurden in den folgenden Publikationsorganen veröffentlicht:

Blood, 2006. 108(5): p. 1635-42.
Molecular Biology of the Cell, 2007. 18(10): 3810-9.


Frankfurt am Main, den